Circadian Rhythms as Novel Chemotherapeutic Strategies for Breast Cancer

by
Megan Irvette Mitchell

Thesis presented in fulfilment of the requirements for the degree of Master of Science in the Faculty of Science at Stellenbosch University

Supervisor: Prof. Anna-Mart Engelbrecht

December 2014

Financial assistance by the National Research Foundation

Declaration

By submitting this thesis electronically, I declare that the entirety of the work contained therein is my own, original work, that I am the sole author thereof (save to the extent explicitly otherwise stated), that reproduction and publication thereof by Stellenbosch University will not infringe any third party rights and that I have not previously in its entirety or in part submitted it for obtaining any qualification.

Megan Irvette Mitchell

December 2014

Abstract

Introduction: Mammalian circadian rhythms form an integral physiological system allowing for the synchronisation of all metabolic processes to daily light/dark cycles, thereby optimising their efficacy. Circadian disruptions have been implicated in the onset and progression of different types of cancers, including those arising in the breast. Several links between the circadian protein Per2 and DNA damage responses exist. Aberrant Per2 expression results in potent downstream effects to both cell cycle and apoptotic targets, suggestive of a tumour suppressive role for Per2. Due to the severe dose limiting side effects associated with current chemotherapeutic strategies, including the use of doxorubicin, a need for more effective adjuvant therapies to increase cancer cell susceptibility has arisen. We therefore hypothesize, that the manipulation of the circadian Per2 protein in conjunction with doxorubicin may provide a more effective chemotherapeutic strategy for the treatment of breast cancer. The aims of this project were thus to: (i) Characterize the role of Per2 in normal breast epithelial cells as well as in ER+ and ER- breast cancer cells; (ii) to determine the role of Per2 in doxorubicin-induced cell death, (iii) to determine the role of Per2 in autophagy and finally (iv) to assess whether the pharmacological inhibition of Per2 with metformin, can sensitize chemo-resistant MDA-MB-231 breast cancer cells to doxorubicin-induced cell death.

Methods: An *in vitro* model of breast cancer was employed using the normal MCF-12A breast epithelial, estrogen receptor positive (ER^+) MCF-7 and estrogen receptor negative (ER^-) MDA-MB-231 breast adenocarcinoma cell lines. Circadian rhythmicity of Per2 protein expression was determined using western blotting, and Per2 cellular localization was assessed using fluorescent confocal microscopy. Per2 was then silenced by means of an endoribonuclease-prepared siRNA, and silencing efficiency was determined with

the use of western blotting. The roles of Per2 in doxorubicin-induced cell death and autophagy were assessed by treating MDA-MB-231 breast cancer cells under the following conditions (1) Control, (2) 2.5 µM doxorubicin or 10 nM bafilomycin A1 (3) 30 nM esiPer2 and (4) 30 nM esiPer2 in combination with 2.5 µM doxorubicin or 10 nM bafilomycin A1. Following treatments cell viability was assessed using the MTT assay, western blotting for markers of apoptosis including p-MDM2 (Ser^{166}), p-p53 (Ser^{15}), cleaved caspase-3 and –PARP as well as markers of autophagy (AMPKα, mTOR and LC3). Furthermore, cell cycle analysis, G2/M transition and cell death (Hoechst 33342 and propidium iodide staining) were assessed by means of flow cytometry. The pharmacological inhibition of Per2 was achieved by treating MDA-MB-231 cells with 40 mM metformin as well as in combination with 2.5 µM doxorubicin. MTT cell viability assays, cell cycle analysis (flow cytometry) and western blotting for apoptosis (Per2, p-AMPKα (Thr^{172}), p53, caspase-3 and PARP) were assessed.

Results and discussion: A circadian pattern of Per2 protein expression was observed in the normal MCF-12A and MDA-MB-231 cancer cells with protein levels peaking at ±700% and ±500% of baseline was observed. However, no rhythmic expression was observed in the MCF-7 cancer cells. Immunostaining for Per2 showed localization OF Per2 in the cytoplasm as well as in the nucleus of both the MCF-12A and MDA-MB-231 cells. Concentration curves showed a significant reduction in cell viability following 2.5 µM doxorubicin treatment for 24 hours. Per2 protein expression was significantly reduced with both esiPer2 and metformin treatment. Silencing of Per2 in combination with doxorubicin treatment resulted in cell cycle arrest with a significant increase in apoptosis, indicating that Per2 silencing effectively sensitized the MDA-MB-231 cancer cells to the anti-carcinogenic properties of doxorubicin. Modulation of Per2 protein expression was effectively achieved with the use metformin although this decrease occurred independently of AMPKα phosphorylation. A significant increase in apoptosis

was observed following treatment with metformin in combination with doxorubicin treatment. However, no changes in cell cycle regulation were observed. Per2 appears to be involved in the regulation of autophagy as a significant increase in autophagy flux was observed when Per2 was silenced. Additionally, this increase in autophagic flux resulted in a significant increase in MDA-MB-231 cancer cell death which was enhanced further when autophagy was inhibited with bafilomycin A1 subsequent to Per2 silencing.

Conclusions: Per2 **protein** expression was shown to display a 24 hour circadian rhythm in the MCF-12A cells, and to a lesser extent in the MDA-MB-231 cells. However, the MCF-7 cells failed to show rhythmic changes in Per2 protein expression. Per2 was shown to be located predominantly in the cytoplasm, with nuclear localization observed when cytoplasmic fluorescent intensity was lower. Per2 silencing effectively sensitized the chemo-resistant MDA-MB-231 breast cancer cells to both doxorubicin-induced cell death and autophagic inhibition.

Uittreksel

Inleiding: Sirkadiese ritmes vorm ‘n integrale fisiologiese sisteem wat die sinkronisasie van alle metaboliese prosesse asook lig/donker siklusse se effektiwiteit optimaliseer. Onderbreking van hierdie sirkadiese ritmes word geïmpliseer in die ontstaan en bevordering van verskillende kankertipes, insluitend borskanker. Verskeie raakpunte bestaan tussen die sirkadiese proteïen, Per2, en die DNA skade-respons. Abnormale Per2 uitdrukking veroorsaak afstroom effekte op beide die selsiklus en apoptotiese teikens wat moontlik aanduidend van ‘n tumor-onderdrukkende rol vir Per2 kan wees. Daar bestaan ‘n groot nood vir meer effektiewe adjuvante terapieë om kankersel vatbaarheid vir chemoterapie te verhoog as gevolg van dosis-beperkende newe-effekte wat geassosieer word met huidige chemoterapeutiese strategieë, insluitende dié van doxorubicin. Ons hipotese is dus dat die manipulering van die sirkadiese Per2 proteïen tesame met doxorubicin ‘n meer effektiewe chemoterapeutiese strategie vir die behandeling van borskanker sal wees. Die doelwitte van hierdie projek was dus om: (i) Die rol van Per2 in normale borsepiteelselle sowel as in ER^+ en ER^- borsepiteel kankerselle te karakteriseer; (ii) die rol van Per2 in doxorubicin-geïnduseerde seldood te bepaal; (iii) te bepaal of Per2 ‘n rol in autofagie speel en laastens (iv) te bepaal of die farmakologiese inhibisie van Per2 met metformin chemo-weerstandbiedende MDA-MB-231 kankerselle kan sensitiseer vir doxorubicin-geïnduseerde seldood.

Metodes: ‘n *In vitro* model vir borskanker is gebruik wat normale MCF-12A borsepiteelselle, estrogeen reseptor positiewe (ER^+) MCF-7 en estrogeen reseptor negatiewe (ER^-) MDA-MB-231 bors adenokarsenoomselle insluit. Sirkadiese ritmisiteit van Per2 proteïen uitdrukking is deur middel van die westelike kladtegniek bepaal en die sellulêre ligging van Per2 deur middel van fluoresensie mikroskopie. siPer2 is voorberei

deur middel van endoribonuklease-siRNA en die effektiwiteit daarvan is deur middel van westelike kladtegniek getoon. Die rol van Per2 in doxorubicin-geinduseerde seldood en autofagie is bepaal deur MDA-MB-231 borskankerselle onder die volgende omstandighede te toets: (1) Kontrole, (2) 2.5 µM doxorubicin of 10 nM bafilomycin A1 (3) 30 nM esiPer2 en (4) 30 nM esiPer2 in kombinasie met 2.5 µM doxorubicin of 10 nM bafilomycin A1. Na die behandeling, is sellewensvatbaarheid bepaal deur gebruik te maak van ‘n MTT toets; westelike kladtegniek is gebruik om vir merkers van apoptose soos p-MDM2 (Ser^{166}), p-p53 (Ser^{15}), gekliefde caspase-3 en -PARP asook vir merkers van autofagie (AMPKα, mTOR en LC3) te toets. Die selsiklus, G2/M oorgang en seldood (Hoechst 33342 en propidium iodide kleuring) is deur middel van vloeisitometrie bepaal. Per2 is ook farmakologies geïnhibeer deur MDA-MB-231 selle met 40 mM metformin asook in kombinasie met 2.5 µM doxorubicin te behandel. Daarna is sellewensvatbaarheid (MTT) sowel as die selsiklus (vloeisitometrie) en apoptose (westelike kladtegniek vir Per2, p-AMPKα (Thr^{172}), p53, caspase-3 and PARP) gemeet.

Resultate en bespreking: ‘n Sirkadiese patroon vir Per2 proteïen uitdrukking is in die normale MCF-12A selle asook in die MDA-MB-231 kankerselle waargeneem met proteïenvlakke wat hul piek by ±700% and ±500% onderskeidelik in vergelyking met basislyn bereik het. Geen ritmiese patroon van Per2 proteïen uitdrukking is egter in die MCF-7 kankerselle waargeneem nie. Immunokleuring om Per2 ligging te bepaal het getoon dat Per2 in the sitoplasma sowel as in die nukleus in beide MCF-12A en MDA-MB-231 selle voorgekom het. Konsentrasie kurwes het aangetoon dat daar ‘n insiggewende vermindering in sellewensvatbaarheid voorgekom het na die behandeling van die selle met 2.5 µM doxorubicin vir 24 uur. Per2 proteïen uitdrukking is insiggewend verlaag met beide esiPer2 en metformin behandeling van die selle. esiPer2 aleen of in kombinasie met doxorubicin behandeling het selsiklus staking tot gevolg gehad asook ‘n beduidende toename in apoptose veroorsaak wat dus aangedui het dat

esiPer2 effektief was om MDA-MB-231 kankerselle te sensitiseer vir die anti-karsinogeniese doxorubicin behandeling. Modulering van Per2 proteïen uitdrukking was effektief met metformin behandeling, alhoewel die afname onafhanklik van AMPKα fosforilasie plaasgevind het. ‘n Insiggewende toename in apoptose is waargeneem na metformin behandeling in kombinasie met doxorubicin. Geen veranderinge in die selsiklus is egter onder hierdie omstandighede waargeneem nie. Per2 blyk betrokke te wees in die regulering van autofagie aangesien ‘n insiggewende verhoging in autofagie omsetting waargeneem is na esiPer2 behandeling. Die toename in autofagie omsetting is geassosieer met ‘n insiggewende toename in seldood in MDA-MB-231 kankerselle wat verder verhoog is wanneer autofagie met bafilomycin A1 (autofagie inhibitor) in kombinasie met esiPer2 behandel is.

Gevolgtrekkings: Per2 **proteïen** uitdrukking het ‘n 24 uur sirkadiese ritme in die MCF-12A normale selle, en tot ‘n mindere mate in die MDA-MB-231 selle getoon. Die MCF-7 selle het egter geen ritmiese patroon van Per2 proteïen uitdrukking getoon nie. Per2 kom hoofsaaklik in die sitoplasma voor en het slegs in die nukleus voorgekom wanneer die sitoplasmiese fluoresensie intensiteit laer was. esiPer2 was dus effektief om die chemo-weerstandbiedende MDA-MB-231 borskankerselle te sensitiseer vir doxorubicin-geïnduseerde seldood.

Acknowledgements

I would like to sincerely thank the following people:

My dearest mama, thank you for being the rock that has gotten me through the years, your unending love and support has gotten me through this degree, and the others before this.

My supervisor Prof. Anna-Mart Engelbrecht, thank you from the bottom of my heart for all the support and guidance you provided throughout this study. Thank you for always being willing to listen and for the countless hours you devoted in helping me structure this thesis. You truly are amazing and I will be forever grateful to have you as my supervisor.

Dr Ben Loos and Dr Balindiwe Sishi, for always providing excellent support and advice in making this project better.

The DSG group, thank you all for providing such amazing support and an enjoyable atmosphere in which to work.

CAF lab, Lize, Dumisile and Rozanne for all the help provided in obtaining the confocal and flow cytometry data.

My Godmother and –sister, thank you for all the support you have provided and for being so willing to listen to my explanations of the work I have done.

Special thanks to the NRF foundation for the financial support that has allowed me to carry out this study.

Table of Contents

List of Figures

Chapter 1

Chapter 2

Chapter 3

Chapter 5

List of Tables

Chapter 2

Chapter 3

List of Abbreviations

4E-BP1	eIF4E-binding protein

A

ABC	ATP-binding cassette
Akt	Protein kinase B
AMPK	5' AMP-activated protein kinase
ANOVA	One-way analysis of variance
Apaf-1	Apoptotic protease-activating factor-1
APC	Allophycocyanin
APE1	Human apurinic/apyrimidinic (AP) endonuclease
ASR	Age-standardised rate
ATG	Autophagy-specific genes
ATP	Adenosine triphosphate

B

Bax	Bcl-2–associated X protein
Bcl-2	B-cell lymphoma-2 homology
Bcl-XL	B-cell lymphoma-extra-large protein
BECN1	Beclin-1
BER	Base excision repair
BH3	Bcl-2 homology domain 3
Bid	BH3 interacting domain death agonist

C

C/EBPβ	CCAAT/enhancer binding protein
CAD	Caspase-activated deoxyribonuclease
CaMKKβ	Calcium/calmodulin-dependent protein kinase kinase β

Caspase	Cysteine aspartate-specific protease
CCGs	Clock-controlled genes
CCND1	Cyclin D1
CDK	Cyclin-dependent kinases
c-FLIP	Cellular flice (fadd-like il-1β-converting enzyme)-inhibitory protein
CK1ε	Casein kinase 1 ε
CO_2	Carbon dioxide
CRY	Cryptochrome
Cyt *c*	Cytochrome *c*

D

DAPI	4',6-diamidino-2-phenylindole
DED	Death effector domain
DIABLO	Direct IAP binding protein with low Pi
DISC	Death-inducing signalling complex
DMEM	Dulbecco's Modified Eagles Medium
DMSO	Dimethyl sulfoxide
DNA	Deoxyribonucleic acid
Dox	Doxorubicin
DR	Death receptors
DSB	Double strand breakage

E

EGF	Epidermal Growth Factor
eGFP	Enhanced green fluorescent protein
ERα	Estrogen receptor α
esiRNA	Endoribonuclease-prepared small interfering ribonucleic acid

F

FADD	Fas associated death domain
FasL/FasR	Fatty acid synthase Ligand/ Fatty acid synthase Receptor
FASPS	Familial advanced sleep phase syndrome
FBS	Fetal bovine serum
FBXL3	F-box and leucine-rich repeat protein 3
FITC	Fluorescein isothiocyanate

G

GCS	Glycosylceramide synthase

H

HAT	Histone acetyl-transferase
HR	Homologous recombination

I

IAP	Inhibitors of apoptosis
IARC	International Agency for Research on Cancer

L

LC3	Microtubule-associated protein light chain-3
LKB1	Liver kinase B1

M

MBC	Metastatic breast cancer
Mdm2	Mouse double minute 2
MDR1	Multidrug resistance gene
MPT	Mitochondrial permeability transition
mRNA	Messenger ribonucleic acid
mTOR	mammalian Target of Rapamycin

MTT	3-(4,5-dimethylthiazol-2-yl)-2,5-diphenyltetrazolium bromide

N

NAD^+	Nicotinamide adenine dinucleotide
NCR	National Cancer Registry
NHEJ	Non-homologous end joining
NHR	Orphan nuclear hormone receptor

P

p21/CIP1	CDK-interacting protein 1
p53	Tumour protein 53
p62/SQSTM1	Poly-ubiquitin protein 62/Sequestome 1
PARP	Poly (ADP-ribose) polymerase
PAS	Basic helix-loop-helix PER-ARNT-SIM
PBS	Phosphate buffered saline
PenStrep	Penicillin/Streptomycin
PER	Period
P-gp	P-glycoprotein
PI	Propidium iodide
PI3K	Phosphatidylinositol 3-kinase
PMSF	Phenylmethylsulfonyl fluoride
PTEN	Phosphatase and tensin homolog
PVDF	Polyvinylidine fluoride

R

RIP	Receptor interacting protein
RIPA	Radio immunoprecipitation assay
RNA	Ribonucleic acid
ROS	Reactive oxygen species
RT	Room temperature

Rorα	Retinoic acid-related orphan receptor α

S

SCN	Suprachiasmatic nuclei
SDS-PAGE	Sodium dodecyl sulphate polyacrylamide gel electrophoresis
SEM	Standard error of the mean
Smac	Second mitochondrial activator of caspase

T

TBS-T	Tris Buffered Saline-Tween20
TNF	Tumour necrosis factor
TNF-α/TNFR1	Tumour necrosis factor alpha/ tumour necrosis factor receptor 1
TOP2A	DNA topoisomerase II
TRADD	TNFR-associated death domain
TSC1/2	Tuberous sclerosis 1 / 2

U

Ulk1	Unc-51-like kinase

V

vs	Versus

W

WHO	World Health Organization

Units of Measurement

%	percentage
µg/ml	microgram per millilitre
µl	microlitre
µm	micrometre
µM	micromolar
g	gravitational acceleration
Hz	hertz
kD	kilodalton
l/L	litre
M	molar
mA	milli-ampere
mg	miligram
mg/ml	milligram per millilitre
min	minutes
ml	millilitres
mM	millimolar
ng/ml	nanogram per millilitre
nm	nanometre
nM	nanomolar
ºC	degrees Celsius
RPM	revolutions per minute
V	volts
w/v	weight per volume

Chapter 1: Literature Review

1.1. Introduction

In the early 18th century many people lived a predominantly rural lifestyle, with the rising and setting of the sun governing their activity and rest periods. However, due to increased urbanization as well as the perfection of the light bulb by Thomas Edison in 1879, more and more people have become exposed to increasing lengths and intensities of light deep into the night time period. As a result of this rapid urbanization, our intrinsic biological clocks, which rely on consistent light/dark cycles, are unable to keep up. Thus increased exposure to wavelength appropriate light at night has resulted in a wide range of physiological disturbances, including that of sleep deprivation, nightly melatonin suppression as well as circadian rhythm disruption (Reiter *et al.,* 2009). It is therefore reasonable to assume that constant perturbations in these intrinsic biological rhythms will result in the onset of pathophysiological diseases, such as that of coronary heart disease, Alzheimer's and cancer.

1.2. Breast Cancer

Cancer has become a global concern as both the prevalence and burden of this disease is rapidly on the rise in both developed and developing countries. According to the latest world health organization (WHO) press release, the global cancer burden has risen to an alarming 14.1 million new cases with 8.2 million cancer associated deaths compared to the estimated 12.7 million and 7.6 million respective cases occurring in 2008 (Jemal *et al.*, 2011). The most commonly diagnosed cancers are reported to be those of the lung

(13%) and breast (11.9%). This rapid increase in the prevalence of cancer in developing countries, including South Africa is largely attributed to an increase in population age and size. However, increasing evidence suggests that the adoption of more "westernized" cancer associated lifestyles play a critical role in the prevalence of cancer.

A sharp increase in the global prevalence of breast cancer is seen with the incidence rate increasing by an alarming 20% and mortality rates rising by 14%, since 2008 estimates. Currently an estimated 6.3 million women, diagnosed within the last 5 years, and an additional 1.7 million women diagnosed in 2012, are living with this disease. According to the South African National Cancer Registry (NCR) an estimated average of 1 in 29 women were newly diagnosed with breast cancer, in 2004 alone (National Cancer Registry., 2004). More recently, Globocan, a WHO project used to assess the prevalence and morality of major cancer types in 184 countries, reported that breast cancer in South Africa has escalated to an incidence rate of 41.53 per 100 000 with a mortality rate of 16.51 per 100 000 women (**Figure 1.1**) (Globocan, 2012).

According to the WHOs' International Agency for Research on Cancer (IARC) a wide range of human epidemiologic evidence suggests that circadian disruption brought on by shift work is most likely carcinogenic to humans (IARC classification – Group 2A) (Straif *et al*., 2007). In fact, various epidemiological studies have demonstrated a significant increase in the prevalence of breast cancer in women working night shift (Sahar *et al.*, 2009, Wang *et al.*, 2011). A cohort study looking at breast cancer incidence in 121 701 female nurses between the ages of 30 – 55 at the start of the study demonstrated a 36% increased breast cancer risk as well as an astonishing 79% increase in lifetime risk with prolonged periods of rotating night shift (Schernhammer *et al*., 2001 and Innominato *et al.,* 2010). Additionally, patients who slept ≤6 hours per night had an increased risk for

the development of breast cancer compared to those who slept 9 hours, indicative of an inverse correlation existing between sleep deprivation and increased risk / progression of breast cancer (Stevens, 2009).

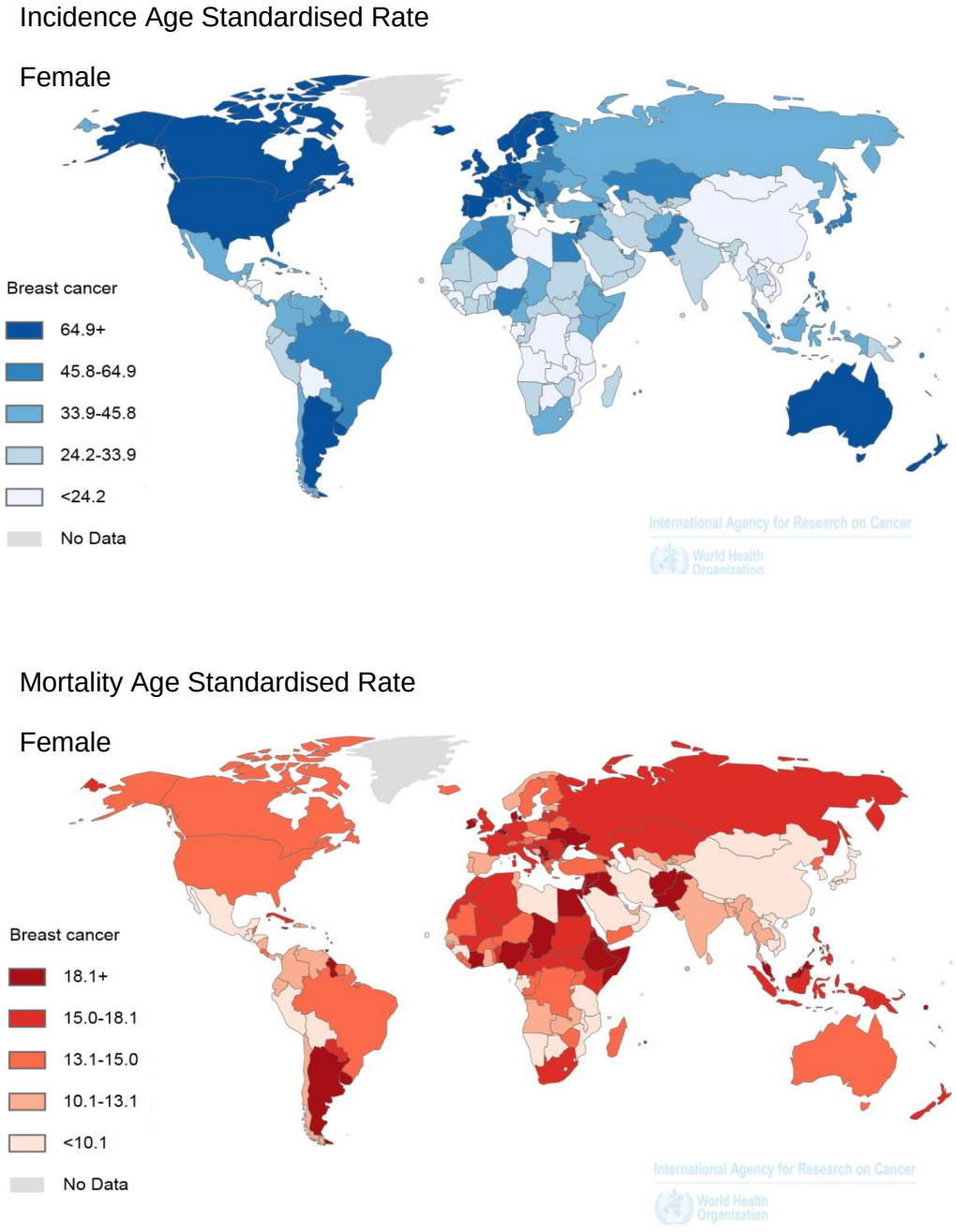

Figure 1.1: Age standardised rates (ASR) of global female breast cancer incidence and mortality (2012). Breast cancer has become a global concern and in South Africa the burden of this disease is rapidly on the rise. In 2012 an incidence rate of 41.53 per 100 000 with a mortality rate of 16.51 per 100 000 women was reported to have occurred. Adapted from: Globocan 2012.

The carcinogenic process is fundamentally complex and highly variable, with no single genetic alteration giving rise to cancer. However, the initiation of cancer development encompasses a series of stages beginning with an initial driver mutation responsible for tumourigenesis where they accumulate additional genetic mutations that confer proliferative and survival advantages (Fernald *et al.*, 2013). Cancer cells have thus developed a variety of exquisite mechanisms to evade cell death (Hanahan *et al*, 2000).

As such, current anticancer strategies involve the use of either radiation or chemotherapeutic agents, like doxorubicin, for the treatment of various solid tumours. However, severe side effects, ranging from kidney and bladder damage to neuro- and cardio-toxicity, are associated with both therapeutic strategies. Thus, a critical need for new treatment approaches, that increase cancer cell susceptibility whilst minimizing damage to normal tissue, has arisen.

1.3. Doxorubicin

Since its isolation from the fungus *Streptomyces peucetius* var. *caesius* in the early 1970's (Keizer *et al.,* 1990), doxorubicin (Dox) a potent anthracycline antibiotic (**Figure 1.2**), has been extensively used for the treatment of several cancer types, including those arising in the breast, due to its potent anti-neoplastic nature (Octavia *et al*., 2012). Pharmacological interest in the use of quinone antibiotics, specifically the anthracycline class has increased due to the finding that they exhibit potent anti-tumour effects in various animal neoplasm models.

The highly effective nature of quinone antibiotics is predominantly due to the fact that they possess a wide range of molecular mechanisms as well as multiple modes of action. Naturally occurring quinone moieties are extensively abundant in nature, and are

seen in various derivatives of both vitamin K (naphthoquinone) and coenzyme Q (ubiquitous benzoquinone). Quinones are intimately associated with one electron and two-electron sequences in cell membrane electron transport chains due to their superficial redox reactions. Quinones thus act as mobile shuttles between cytochrome and flavoprotein membrane proteins, as such these bioreactive moieties are found abundantly in a range of quinone antibiotics (Lown, 1983). Due to the promising results obtained, anthracyclines are extensively used in clinical settings as effective chemotherapeutic agents as they target cellular DNA due to their high cellular sensitivity towards chemical-induced alterations (Lown, 1983).

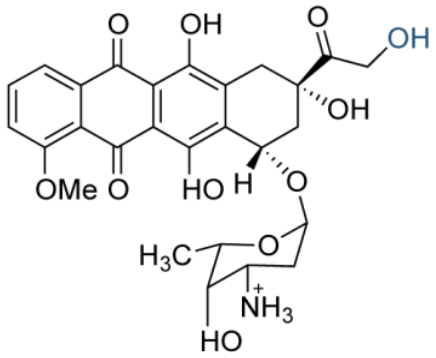

doxorubicin (adriamycin)

Figure 1.2: The molecular structure of doxorubicin (Dox). Detailed X-ray crystallographic analysis establishing the structure and conformation of doxorubicin has shown the molecule to be a glycoside consisting of a planar four-ring quinone encompassing chromophore attached at its 7-position to either one, two or three sugar moieties. The quinone ring adopts a half-chair conformation with the sugar moieties extending perpendicularly towards the plane of the chromophore.

The clinical efficacy of Dox therapy is thought to be largely attributable to the fact that Dox has the ability to intercalate between DNA base pairs (Aubel-Sadron *et al.*, 1984) thereby inhibiting the function of DNA topoisomerase II (TOP2A), thus leading to DNA strand breakage (Gewirtz, 1999). Additionally, with its intercalation into DNA, Dox has been shown to inhibit DNA and RNA polymerase, thus also inhibiting DNA replication and RNA transcription (Tacar *et al.*, 2013). A wide variety of other molecular

mechanisms behind the cytotoxic effects of Dox have been proposed, including the inhibition of macromolecule biosynthesis, as well as free radical generation thereby resulting in cell death through mitochondrial permeability transition (MPT) and its subsequent activation of apoptosis (Thorn *et al.*, 2011).

Dox displays a high binding affinity for the cytoplasmic proteasome therefore it enters the cell via diffusion across the plasma membrane. Once inside the cytoplasm, Dox binds to the 20S subunit of the proteasome where after it translocates into the nucleus. Due to its higher binding affinity for nuclear DNA, Dox dissociates from the proteasome and binds to DNA (Tacar *et al*., 2013). Additionally, the cellular uptake of Dox also involves its initial oxidation to a semiquinone free radical, which is only stable under anoxic conditions. However, in normal oxygen rich conditions, Dox is converted back to its stable state via the donation of its unpaired electron to oxygen, which results in the release of superoxide and hydrogen peroxide (Keizer *et al.*, 1990), a process known as “redox-cycling” (**Figure 1.3**). As an iron chelator doxorubicin binds to form a complex which results in the conversion of hydrogen peroxide to reactive hydroxyl radicals, adding to the effect of doxorubicin-induced oxidative stress which may result in DNA damage and cell death (Yang *et al.*, 2014).

Dox has also been shown to rapidly increase intracellular ceramide concentrations (Yang *et al*., 2014). Ceramide, a lipid molecule, mediates a range of cellular effects, including that of apoptosis and cell cycle arrest (Senchenkov *et al.*, 2001), through the down-regulation of *c-myc* expression (Liu *et al*., 2008). Cancer cells have been shown to be sensitized to Dox induced cell death by exogenous ceramide administration (Yang *et al*., 2014).

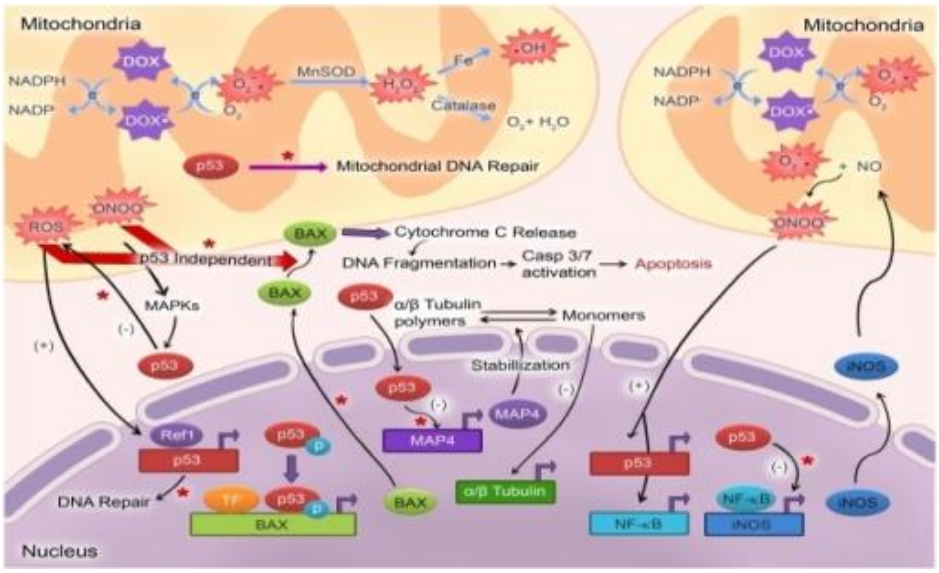

Figure 1.3: Mechanism of action of doxorubicin-induced cell death. Redox cycling of Dox by the mitochondria leads to an accumulation of superoxide, resulting in the generation of other reactive oxygen species (ROS). Accumulation of intracellular ROS leads to the increased expression of NO via the activation of NF-κB. The formation of peroxynitrite ($ONOO^-$) results in the activation of intracellular stress pathways e.g. mitogen activated protein kinases (MAPK). Intracellular ROS accumulation leads to the phosphorylation of p53 (Ser^{15}) which eventually causes the release of cytochrome c from the mitochondria, the activation of caspase-3 and ultimately results in apoptosis. The absence of p53 in certain cancers further exacerbates apoptosis induction as the negative feedback regulation of p53 on ROS production is lost. Abbreviations: Dox = Doxorubicin. Dox• = Doxorubicin semiquinone. O_2^- = superoxide. OH• = hydroxyl radical. H_2O_2 = hydrogen peroxide. Adapted from: Feridooni *et al.*, 2011.

Much research has gone into ways of minimizing anthracycline dosages given to patients due to the severe cumulative dose dependent side effects associated with Dox, the most disturbing of these side effects is that of cardiotoxicity. Cardiotoxicity can be brought on either within the initial treatment period (acute) or it may present years after (chronic).

Aside from the severe cumulative dose-dependent side effects associated with the use of anthracycline antibiotics like Dox, resistance of cancer cells to chemotherapeutic strategies (chemo-resistance) has become an ongoing complex issue faced by many cancer patients. Currently it is believed that chemo-resistance accounts for over 90% of the failure rate seen with the treatment of metastatic breast cancer (MBC) (Coley, 2008).

1.4. Chemo-Resistance

Unlike normal cells, which all respond in the same manner to drugs, cancer cells each respond differently. For example a treatment regime that works effectively for one cancer cell type may not work as effectively in another; similarly tumour cell populations are comprised of a range of heterogeneous cancer cells each with their own unique response to chemotherapeutic drugs. To date, various cellular mechanisms behind cancer cell resistance have been proposed which include (i) pharmacodynamic resistance pathways, including DNA repair processes, or (ii) pharmacokinetic resistance pathways, e.g. increased drug efflux mechanisms.

Cancer cells respond to DNA damage caused by chemotherapeutic drugs via a range of intrinsic DNA repair processes, the exact pathway chosen depends largely on the DNA adduct formed by the drug. As mentioned previously, Dox forms a covalent Dox-DNA adduct as Dox preferentially intercalates between adjacent GC base pairs stabilized by a covalent bond (Yang *et al.*, 2014), where it results in both single and double DNA strand breakages. Chemoresistance to Dox would therefore require DNA repair mechanisms specifically targeted to (i) base excision repair (BER), where base damages occur as a result of Dox induced ROS. The damaged base is removed by human apurinic/apyrimidinic (AP) endonuclease (APE1) and DNA glycosylases, the resultant site is trimmed by poly (ADP-ribose) polymerase (PARP) and polynucleotide kinase, and (ii) double strand breakage (DSB) repair, caused directly by Dox or as a result of replication from single strand breaks (Houtgraaf *et al., 2006)*. Double strand breakages (DSB) are regarded as the most severe (genotoxic) form of DNA damage and rapid repair is essential. Two main pathways exist for the repair of DSBs, which are dependent on the stage of the cell cycle. Non-homologous end joining (NHEJ) is essential in quiescent (G_o) cells or cells in G_1, as ligation of the two broken strands occurs directly in

the absence of homology, whereas, homologous recombination (HR), occurs predominantly in dividing cells (cells in S-phase or G_2) as HR requires absolute DNA homology of the sister chromatid, where missing information can be copied in without a loss of genetic information (Houtgraaf *et al*., 2006).

Certain cancer cell types have developed mechanisms whereby they effectively circumvent the toxicity of chemotherapeutic drugs through the expression of the energy-dependent drug efflux pump, P-glycoprotein (P-gp), alternatively known as the multidrug transporter. In humans P-gp, a product of the MDR1 gene, belongs to a family of ATP-binding cassette (ABC), not only responsible for the efflux of drugs but also for nutrient transportation across the plasma membrane (Gottesman, 2002). A large variety of chemotherapeutic drugs including Dox are detected and bound to P-gp as it enters the plasma membrane. The binding of Dox to P-gp results in the activation of an ATP-binding domain, and the subsequent hydrolysis of ATP. This results in a conformational change in P-gp and the release of Dox into the extracellular space. The transporter returns back to its original state upon the hydrolysis of a second ATP molecule, allowing for the cycle to be repeated (Sauna *et al.,* 2000).

As mentioned previously, Dox increases intracellular ceramide levels, which in turn results in an increase in glycosylceramide synthase (GCS) expression. Increased glycosylation of ceramide by GCS forms a positive feedback loop that is known to be anti-apoptotic. Thus, helping to confer cancer cell resistance to Dox (Tacar *et al*., 2013).

1.5. Apoptosis

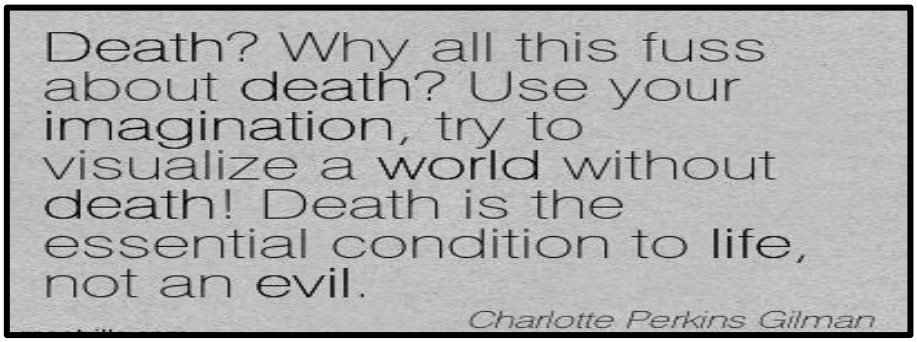

Apoptosis, adopted from the Greek word which means “falling leaves”, is a pervasive form of programmed cell death, which involves the genetic-controlled removal of cells. Apoptosis, is an essential process for the maintenance of cell populations in normal development and aging, and also acts as a defensive mechanism against damaged or infected cells.

Apoptotic cell death is an important process for a range of physiological processes including that of embryonic development, normal cell turnover, chemical induced cell death, the immune system and hormone-dependent atrophy. The inappropriate induction of apoptosis has been implicated in a wide range of human diseases, including that of autoimmune disorders, ischaemic damage, neurodegenerative diseases and several cancer types

A variety of both pathological and physiological stimuli can lead to the activation of apoptosis. However, not all cells respond to these stimuli in the same way. A classic example of this occurs in response to therapeutic strategies aimed at the eradication of cancer, where some cells react to DNA damage through the activation of a *p53*-dependent apoptotic cell death pathway (Elmore, 2007).

The onset of apoptosis occurs via a two-step process, whereby the initial commitment to cell death is followed by an execution phase, involving distinct morphological changes in cell structure (Cohen, 1997). The initial commitment to cell death involves a highly complex and sophisticated mechanism, whereby an energy-dependent cascade of molecular events are elicited. Currently two main pathways have been described: the intrinsic mitochondrial pathway, and the extrinsic death receptor pathway. Although distinct from each other, these pathways are not mutually exclusive and are intertwined as molecules from one pathway may affect the other. Both the extrinsic and intrinsic pathways converge at the same executioner pathway, which occurs via the cleavage of caspase-3 resulting in DNA damage, nuclear condensation (pyknosis) and fragmentation (karyorhexis), cytoplasmic organelle compaction, cell shrinkage, the formation of apoptotic bodies and finally phagocytosis (**Figure 1.4**) (Elmore, 2007).

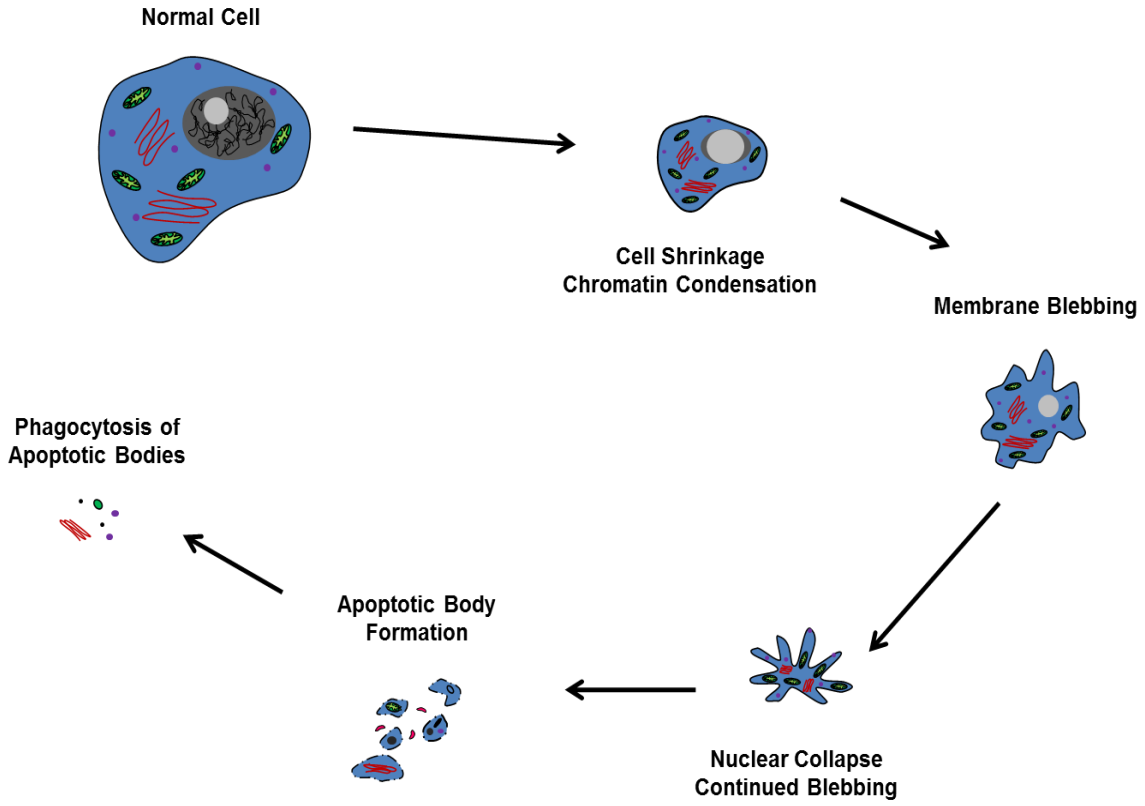

Figure 1.4: Schematic representation of the morphological changes occurring during the process of apoptotic cell death. Once a cell is committed to die via the process of apoptotic cell death, nuclear condensation (pyknosis) and fragmentation (karyorhexis) ensues, leading to cell shrinkage and the formation of apoptotic bodies. Adapted from: Kerr *et al*., 1994.

Apoptosis fundamentally differs from other modes of cell death, such as necrotic cell death, in that it is morphologically defined with the entire apoptotic process being contained within an intact plasma membrane. Thus, apoptosis does not elicit an immune response as apoptotic bodies are rapidly recognized and silently phagocytosed (Casares *et al*., 2005).

1.5.1. The Caspases

Central to the activation of apoptosis are a family of cysteine-dependent aspartate specific proteases known as the caspases (Mehmet *et al.*, 2000). Caspases are responsible for the cleavage of over 400 different proteins (Thorburn, 2008). However, they are highly specific proteases in that they only cleave after aspartic acid residues (Thornberry *et al.*, 1998).

Like many of the proteases, caspases regulate their own activation via an amplification loop, whereby an active caspase activates its own precursor either directly or indirectly. This amplification loop allows for rapid exponential activation of the caspase cascade, allowing for the rapid execution of cell death. As a result of their highly reactive nature, directly upon their synthesis, caspases are stored as inactive pro-enzymes (± 50 kDa) which are activated during the proteolytic process (Bremer *et al.*, 2006). These pro-enzymes are made up of three domains; a large subunit (± 20 kDa), a small subunit (± 10 kDa) and a NH_2 – terminal domain. Their activation involves proteolytic re-organization between domains and the formation of a tetramer between the small and large subunits with two independent catalytic sites (Thornberry *et al.*, 1998).

To date 14 mammalian caspase homologs with similarities in structure, amino acid sequences and substrate specificity have been identified (Porter *et al.*, 1999). Their

predominant function in apoptosis appears to be to cleave apoptotic substrates thereby facilitating the organized disassembly of the dying cell as well as to disable cellular repair processes. The caspase family of enzymes can be classified broadly into two main subfamilies, namely: those predominantly involved in inflammation (caspases -1, -4 and -5) and those involved in apoptosis (caspase -2, -3, -6, -7, -8, -9 and -10). The apoptotic subfamily of caspases is then further subdivided into two main groups: the initiators (caspase -2, -8, -9 and -10) and the effectors (caspase -3, -6 and -7) (Nicholson *et al.,* 1997).

1.5.2. The executioner pathway

Both the extrinsic and intrinsic apoptotic pathways converge at the same point, with the activation of caspase-3, at the start of the executioner pathway (**Figure 1.5**). Considered the most important of the executioner caspases, caspase-3 is activated by the initiator caspases (caspase-8, caspase-9 or caspase-10), and results in the activation of caspase-activated deoxyribonuclease (CAD), an endonuclease. CAD is responsible for the degradation of chromosomal DNA (Robertson *et al.*, 2000). Additionally, caspase-3 directly induces the reorganisation of the cytoskeleton and the formation of apoptotic bodies (Thornberry, 1998).

Poly (ADP-ribose) Polymerase (PARP) is a 116 kDa nuclear protein that plays a critical role in DNA damage repair mechanisms (Grasso *et al*., 2012). PARP is synthesized upon the fragmentation of DNA in the presence of nuclear poly-ADP ribosylated proteins. Its activation then occurs when PARP binds to broken DNA strands. Through the poly (ADP-ribosyl)ation of various nuclear proteins, PARP utilizes nicotinamide adenine dinucleotide (NAD^+) as a substrate. Therefore, it was originally thought that PARP contributes to apoptotic cell death via cellular depletion of NAD^+ and ATP.

However, PARP has been shown to be cleaved by caspase-3 during the initial stages of apoptosis into 24- and 89 kDa fragments respectively containing the enzymatic DNA – binding domains and active sites (Boulares *et al*, 1999). Once cleaved the smaller 24 kDa fragment binds to fragmented DNA ends, inhibiting the access of DNA repair enzymes, and thus ensuring the cells commitment to apoptosis (Grasso *et al*., 2012).

1.5.3. The extrinsic / death receptor pathway

The initiation of apoptosis via the extrinsic signalling pathway involves death receptors (DR) from the tumour necrosis factor (TNF) superfamily (Sainz *et al*., 2003). TNF receptors all share a similar “death domain” composed of a cytoplasmic domain of approximately 80 amino acids as well as cysteine-rich extracellular domains. The death domain is critical for the transmission of death signals from the cell surface to the intracellular signalling pathways.

Currently the best described mechanism for the induction of the extrinsic pathway are the Fatty acid synthase Ligand/ Fatty acid synthase Receptor (FasL/FasR) and tumour necrosis factor alpha/ tumour necrosis factor receptor 1 (TNF-α/TNFR1) models. These models involve the clustering of receptors and subsequent trimeric ligand binding. Upon the binding of ligands, cytosolic adapter proteins with corresponding death domains are recruited eliciting a cascade of responses. Binding of the Fas ligand to the Fas receptor leads to the binding of the Fas associated death domain (FADD) adapter protein. The binding of the TNF ligand to the TNF receptor leads to the binding of the adapter protein TNFR-associated death domain (TRADD) where after recruitment of FADD and receptor interacting protein (RIP) kinase occurs. Dimerization of the death effector domain (DED) occurs upon the association of FADD with procaspase-8. At this point, a death-inducing signalling complex (DISC) is formed, resulting in caspase-8s’ auto-catalytic activation,

which results in the cleavage of BH3 interacting domain death agonist (Bid) and the triggering of the executioner pathway of apoptosis. The inhibition of this death receptor-mediated pathway occurs by the binding of c-FLIP to FADD and caspase-8 resulting in a loss of function (**Figure 1.5**) (Elmore, 2007).

1.5.4. The intrinsic / mitochondrial pathway

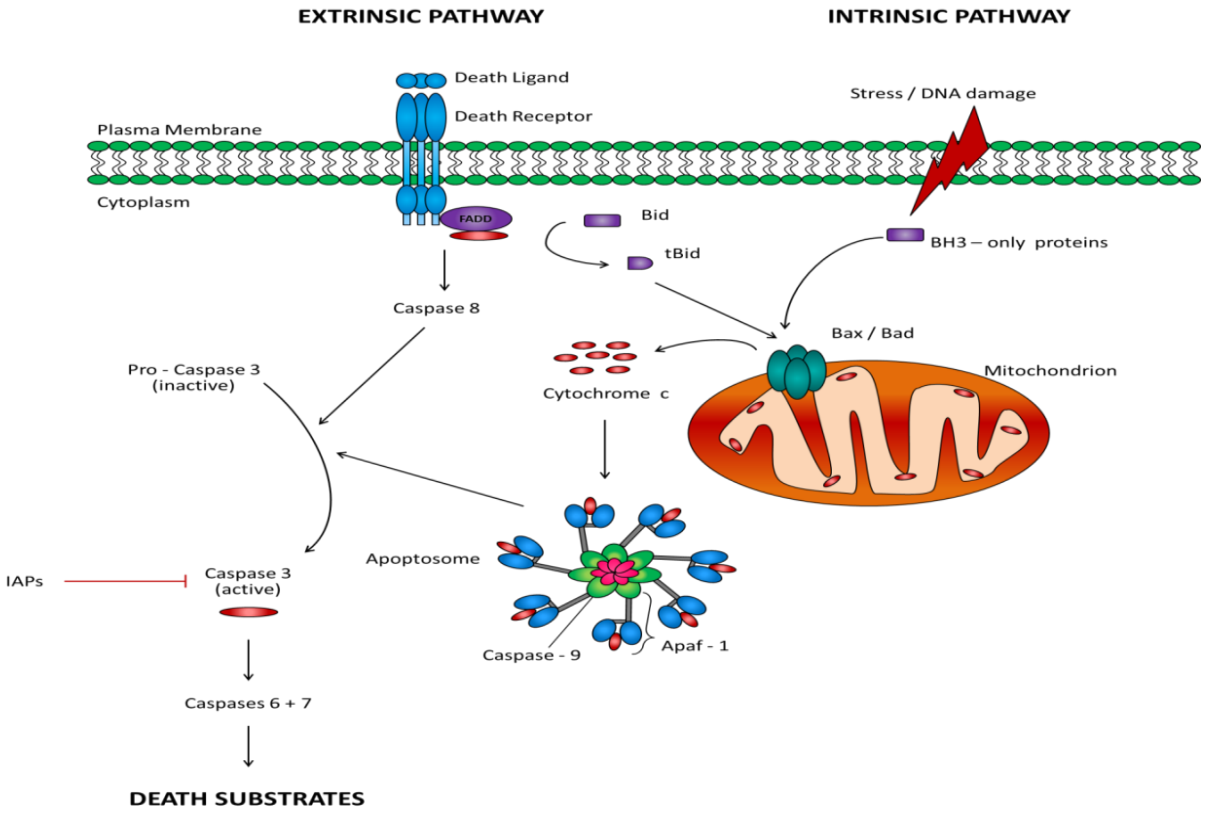

Figure 1.5: Schematic representation of the intrinsic and extrinsic pathways involved in the induction of apoptotic cell death. Adapted from: Fulda *et al.*, 2006

The intrinsic apoptotic pathway is initiated in response to a range of non-receptor mediated stressors, acting directly on intracellular targets that result in a cascade of mitochondrial driven responses. These stressors can be divided into two main groups, namely; positive signals, which include toxins, radiation and free radicals, or negative

signals, such as the withdrawal of specific hormones and growth factors that suppress apoptosis.

Mitochondria respond to these stressors through the opening of the mitochondrial permeability transition (MPT) pore, resulting in the loss of membrane potential and the subsequent release of the pro-apoptotic mediators, cytochrome *c* and second mitochondrial activator of caspase or direct IAP binding protein with low pI (Smac/DIABLO), into the cytosol. Smac/DIABLO inhibits a class of proteins known as the inhibitors of apoptosis (IAP), and thus relieves their inhibitory effect on caspase-3. Cytochrome *c* facilitates the activation of apoptosis, through its activation and association with apoptotic protease-activating factor-1 (Apaf-1) and procaspase-9 resulting in the formation an “apoptosome” and the subsequent activation of caspase-3 (**Figure 1.5**) (Elmore, 2007).

Like most physiological pathways, the extrinsic and intrinsic pathways of apoptosis cannot be mutually excluded from each other. Instead they function in concert whereby effective cell death execution occurs through the crosstalk between these two key pathways. Bid mediates this interaction, as its activation by caspase-8 results in MPT and the release of cytochrome *c* from the mitochondria (Grasso *et al*., 2012).

1.6. Apoptosis and Cancer

As mentioned previously, cancer cells have the exquisite ability to effectively circumvent apoptosis (Fernald *et al.,* 2013). This is predominantly due to the fact that within these cells, the homeostatic balance between cell death and proliferation is skewed, and as such genetic abnormalities multiply as these cells survive (Sjöström *et al.,* 2001).

One of the more common genetic aberrations associated with cancer is a loss or inactivation of the tumour suppressor p53. p53 plays an instrumental role in cellular regulatory signals, specifically those involved in cell proliferation, DNA repair and angiogenesis (Haupt *et al.*, 2003). Under normal cellular conditions p53 remains inactive, a state predominantly controlled by the p53 inhibitor mouse double minute 2 (Mdm2). Mdm2 not only inhibits p53s' transcriptional activity it also promotes its degradation via the ubiquitin proteasome system (Ashcroft *et al.*, 1999).

The activation of p53 occurs when it is stabilized though co-factor protein-protein interactions and various post-translational modifications. Once activated, p53 responds to intracellular stress such as that of hypoxia, nutrient depletion and DNA damage (Horn *et al*., 2007), by inducing apoptosis or cell cycle arrest (at G1 and/or G2 phases) (Vousden *et al.*, 2007). In this way, p53 directly prevents uncontrolled cell growth and tumour development (Bremer *et al*., 2006).The loss or dysfunction of p53 signalling is not only associated with the onset of the tumorigenic process but also with poor prognosis of patients suffering from certain cancer types (Whibley *et al.*, 2009).

Alternatively, certain cancer cell types have up-regulated expression of anti-apoptotic proteins, like BCL-2 and members of the IAP family. This ability of cancer cells to evade apoptosis makes them not only reliant on these aberrations for their survival but also for their resistance to certain chemotherapeutic drugs (Bremer *et al*., 2006).

1.7. Chemotherapeutic Drugs and Circadian Rhythms

Recent evidence suggests that synchronization of circadian rhythms may influence anti-tumour tolerability and the pharmacological efficacy of chemotherapeutic drugs (Filipski *et al.*, 2002).

Biological time is a measure of cycles ranging from milliseconds to years. The most well-known circadian rhythm in mammals is that of the sleep/wake cycle. Circadian rhythms are external manifestations of intrinsic biological time measuring cycles on a 24 hour scale (Reppert *et al.,* 2002). To date, all mammalian cell types have been shown to possess an intrinsic circadian clock, made up of self-sustained and self-perpetuating transcriptional feedback loops, responsible for keeping time within the cell (Sachdeva *et al.,* 2008).

Although the internal circadian rhythms of mammals have been known for centuries (Clairambault, 2010), the molecular nature behind these oscillations has only recently been understood (Hastings *et al.,* 2003). The crucial point of this timing system, the master clock, lies within the suprachiasmatic nuclei (SCN) of the anterior hypothalamus and is solely responsible for coordinating the circadian programme within mammalian cells (Reppert *et al.,* 2002). The SCN plays a critical role in controlling endocrine cycles and to a lesser extent metabolic rhythms. This occurs predominantly through anatomical connections that exist between the SCN and centres for sleep and wakefulness, thus controlling the timing of sleep as well as the timing of nocturnal hormonal secretion such as that of growth hormone and prolactin. Alternatively, SCN clocks are able to drive sleep-independent hormonal rhythms such as that of melatonin through connections to neuroendocrine and autonomic systems. This is evident in the continued cycling of melatonin in subjects who are prevented from sleeping (Hastings *et al.,* 2007).

Circadian clocks have been shown to play a role in cell metabolism and tissue proliferation (Clairambault, 2010). Within mammalian tissue, nutrient and energy metabolism is temporally organized in order to synchronize energy storage and utilization to daily light/dark cycles. Circulating hormones and metabolites display distinct diurnal rhythms as they peak and subside throughout the course of the day. It has been shown that the expression of various metabolic genes is limited to specific tissue types, indicating that these metabolic pathways are not only tissue specific but also limited to specific periods during the day (Ma *et al.*, 2012). This suggests that both nutrient and energy metabolism are tightly coupled to timing cues in mammalian tissue. As a result of the continuous cycling of this intrinsic circadian rhythm, rhythmic aspects of both cell proliferation and metabolism can be predicted (Mormont *et al.*, 2003).

1.8. Circadian clock genes

Similar to the negative feedback loops that are prominent in the rhythmic regulation of hormonal release, the circadian system also consists of a delayed negative feedback loop where protein products of clock genes negatively regulate their own transcription. The only difference exists in the time scale of the circadian system where events are drawn out to produce a stable cycle over a period of more or less 24 hours *(*Hastings *et al*., 2007). Central to the correct functioning of the circadian rhythm are the basic helix-loop-helix PER-ARNT-SIM (PAS) domain proteins Bmal1 and CLOCK, which heterodimerize (Xiang *et al*., 2008), and ultimately lead to the expression of their repressors: Period (Per1, Per2, and Per3) and Cryptochrome (Cry1, and Cry2) (**Figure 1.6**) (Curtis *et al.*, 2014). Upon translation Per and Cry proteins heterodimerize and associate with human casein kinase 1 ε (CK1ε). This complex translocates into the

nucleus resulting in the inhibition of CLOCK:Bmal1 mediated transcription (Sahar *et al.*, 2009).

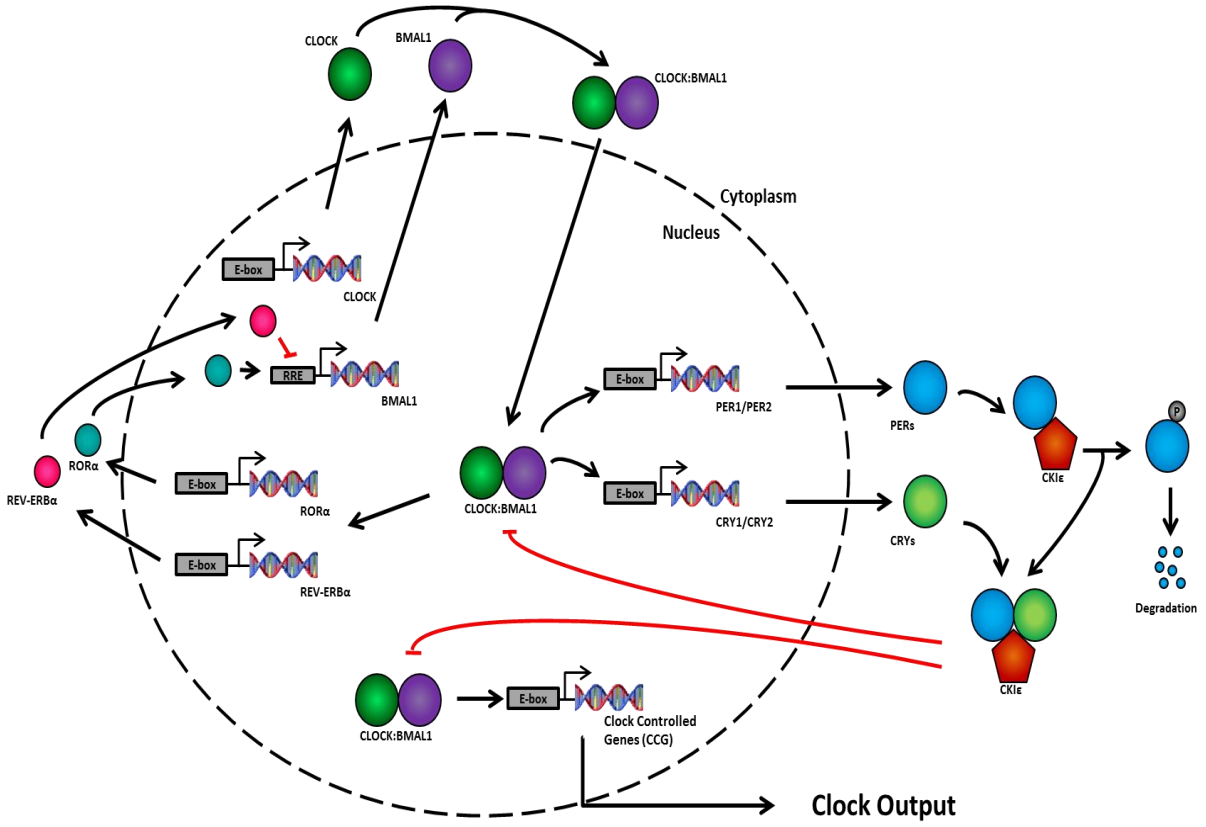

Figure 1.6: Schematic representation of the intrinsic circadian clock present in all mammalian cell types. The circadian clock system is comprised of core CLOCK and BMAL1 genes, the transcription and translation of which leads to the expression of Period and Cryptochrome genes. At the beginning of a circadian day Period and Cryptochrome proteins accumulate, dimerize to form a complex which translocates into the nucleus repressing their own transcription. This 24 hour feedback cycle is additionally stabilized through the activation of CKIε by AMPK which results in the phosphorylation and degradation of Per2, leading to a resetting of the clock system.

CLOCK is important for transactivation as it contains a glutamine rich region in its C-terminus and intrinsic histone acetyl-transferase (HAT) activity. Upon transcription of these genes SCN Per and Cry mRNA levels increase over the course of a circadian day, levels of their proteins also increase, however, they lag behind by several hours. At the end of circadian daytime the levels of Per and Cry proteins peak in the nuclei of the SCN and levels of mRNA begin to decline as a result of the negative feedback loop that

exists, specifically that of Cry proteins. Transcriptional activation and repression of Cry proteins, by the C-terminus of Bmal1, is critical for the switch mechanism between mRNA and protein synthesis.

Additionally, CLOCK and Bmal1 proteins have been shown to activate the expression of certain “clock-controlled genes” (CCGs) (**Figure 1.6**), thus allowing for circadian regulated output of cellular, metabolic and physiological processes, for example the sensitivity of cells to genotoxic stress is regulated by the functionally active CLOCK:Bmal1 complex (Sahar *et al.*, 2009).

This negative feedback loop of the circadian rhythm is additionally stabilized and enhanced through accessory pathways; the main pathway involves the two orphan nuclear hormone receptor (NHR) proteins, RevErbα and Rorα, both of which are activated in phase with Per and Cry genes via CLOCK and Bmal1 (**Figure 1.6**) (Yang *et al*., 2006). Rorα has a positive effect on Bmal1 resulting in its increased expression, whereas RevErbα is a potent suppressor of Bmal1 (Curtis *et al.*, 2014).

As RevErbα levels decline at night, its suppression of Bmal1 is lifted, resulting in Bmal1 activation. At the start of a new circadian day when the negative feedback begins to diminish; anti-phase oscillations of Bmal1 and Per mRNA’s, coupled to a surge in Bmal1 expression, results in an extra boost to initiate the new cycle of Per and Cry gene expression (Hastings *et al*., 2007).

Single gene knockouts of either Per, Cry, RevErbα or Clock do not disable the circadian clock; it may however result in alterations in the length of the circadian period. In order to stop circadian cycling entirely the deletion of both Per1 and Per2 or both Cry1 and Cry2 is essential. The only factor that appears to be indispensable in this network is Bmal1, however, mutations affecting the trans-activational role of Clock ultimately destabilize and prolong circadian periods.

The generation of this 24 hour period cycle is dependent on certain key factors; the first and most obvious is the rate at which transcription of both Per and Cry genes occurs, as they dominate within the circadian cycle. The second is the stability of the proteins that are synthesized; studies have shown that a mutation occurring in human casein kinase 1 δ (CK1δ), closely related to CK1ε, is linked to an accelerated circadian period and advanced sleep. However, a mutation affecting the phosphorylation state of human Per2 results in the manifestation of familial advanced sleep phase syndrome (FASPS) an extreme sleep disorder resulting from a similar accelerated circadian period (Hastings *et al*., 2007).

Several molecular similarities are seen to exist between the circadian clock system and the cell cycle. Both have been shown to be inherent in a wide range of cells running with a periodicity of more or less 24 hours - additionally both are reliant on chronological periods of gene transcription, translation, modifications and subsequent protein degradation (Hunt *et al.*, 2007). It is therefore feasible that CCG's involve genes dedicated to cell cycle regulation.

1.9. Cell Cycle Regulation

The human body is composed of ± 10^{13} cells, each arising from numerous cell divisions beginning from a single fertilized egg cell. Therefore, during the process of normal development the tightly controlled regulation of cell division is essential (Noatynska *et al.*, 2013). As such, the cell cycle consists of a variety of intricate mechanisms each governing specific regions in order to ensure correct cell division (Vermeulen *et al.*, 2003).

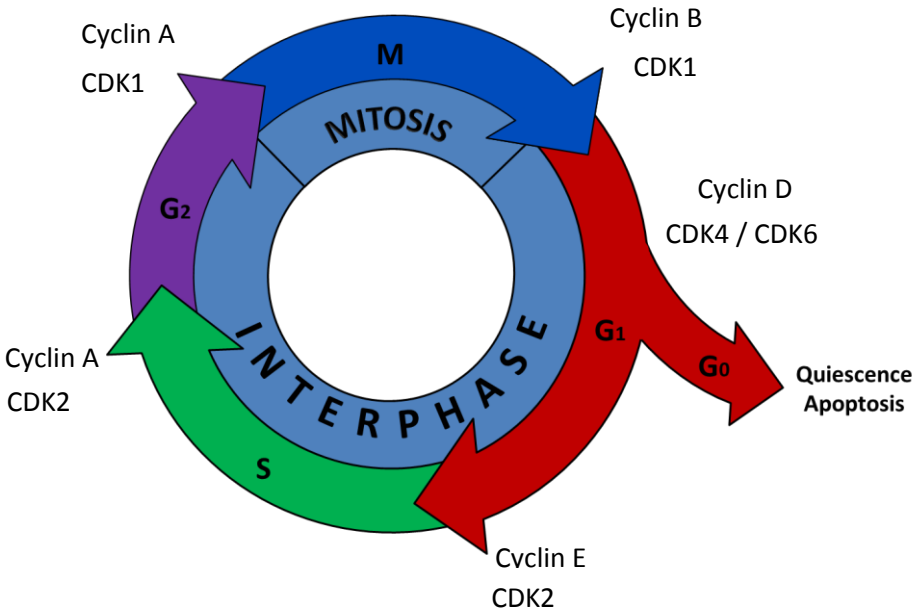

Figure 1.7: Schematic representation of the stages and regulators involved in the cell cycle. Adapted from: Vermeulen et al., 2003.

Classically cell division is characterized by the replication of DNA and its subsequent nuclear and cytoplasmic division giving rise to two daughter cells (Massague, 2004). Cell division was originally thought to consist of two main stages, namely; mitosis (M), wherein nuclear material is divided, and interphase, the period where cell growth occurs. However, due to the development of more advanced molecular techniques, interphase was shown to consist of more phases (**Figure 1.7**) characterized by a gap (G_1) where the cell prepares for DNA synthesis, DNA replication (S-phase), followed by another gap (G_2) which allows the cell to prepare for mitosis (Vermeulen *et al*., 2003).

G_1 appears to be one of the more critical phases as a variety of signals, including environmental and metabolic stress signals are integrated, influencing both cell division and development. Based on these inputs cells then decide to either proceed through to the S-phase, enter the G_0 an additional gap phase, where they become quiescent, or to exit the cycle completely and die (cell cycle arrest) (Massague, 2004). Additional

checkpoints found in the G2/M phase prevent the transition of cells with DNA damage into mitotic cell division.

Key to the highly regulated transition from one phase to another phase of the cell cycle is a family of serine-threonine protein kinases known as the cyclin-dependent kinases (CDK). Currently, five CDK proteins have been identified to play a role in the cell cycle, CDK4, CDK6 and CDK2 play a role in G_1, CDKs also plays a role in the S-phase and CDK1 plays a role in G_2 and M phases (Vermeulen *et al*., 2003). Upon their activation CDK elicit their responses through the phosphorylation of specific downstream proteins.

CDK proteins are activated by their upstream activating proteins, the cyclins. Cyclins, like CDK are required during different phases of the cell cycle. Cyclin protein levels cycle in accordance with the cell cycle, where they intermittently activate CDKs, thus ensuring their constant protein levels (Morgan, 1995). Currently three cyclins (cyclin D1, cyclin D2 and cyclin D3) are essential for the entry into G_1 as they bind to CDK4. Cyclin E associates with CDK2 and is critical for G_1 to S transition, whereas cyclin A binds to CDK2 during the S phase. During the late stages of G_2 and early mitosis, CDK1 and cyclin A form a complex that is essential for cell progression into mitosis (**Figure 1.7**) (Vermeulen *et al*., 2003).

Evidence reveals that cell cycle genes are under the regulation of circadian clocks (Kelleher *et al.,* 2014). However, circadian clocks operate accurately independent of cell cycle regulation. Additional cell cycle genes, such as *Wee1, c-myc* and *Cyclin D1* are thought to be directly regulated through the heterodimerization of CLOCK:BMAL1 (Rana *et al.*, 2010).

1.10. Circadian Rhythms and Malignancy

WEE1, a cell cycle kinase responsible for G_2-M cell cycle transition, expression increases in response to the binding of CLOCK:BMAL1 to E-boxes of the WEE1 promoter region (Masri *et al.*, 2013). Cry1 mutant mice, lacking the inhibitory effect of Cry on the CLOCK:BMAL1 heterodimer, results in the accumulation of WEE1 (Rana *et al.*, 2010). Activation of WEE1 in times of continuous DNA damage and DNA replication leads to the phosphorylation of the cell division cycle 2 (CDC2)/Cyclin B1 complex; this activation results in mitotic delay or cell cycle arrest (Hunt *et al.*, 2007). Transition between G_1 and S phases of the cell cycle is governed by *c-myc* (King *et al.*, 1998), the transcription of which plays a critical role in apoptosis and cell proliferation (Sancar *et al*., 2010). Mutant Per2 mice exhibit up-regulated *c-myc* and concomitantly down-regulated p53 transcription, an essential regulator of the G1-S checkpoint (**Figure 1.8**) (Rana *et al.*, 2010).

Under normal physiological conditions transcription of *c-myc* is inhibited by the binding of CLOCK:BMAL1 to E-boxes of *c-myc* promoter regions (Rana *et al.,* 2010). However, the up-regulation of *c-myc* transcription associated with mutations of Per2 may be attributed to the decrease seen in BMAL1 levels, as Per2 is also a potent regulator of BMAL1 gene transcription (Sancar *et al*., 2010).

Modulation of p53-mediated apoptosis plays a critical role in *c-myc* mediated oncogenic transformation, as pro-apoptotic activity needs to be overcome. Impaired p53 functioning occurs as a result of *c-myc* induced DNA damage, and is thought to occur via a reactive oxygen species (ROS) mediated mechanism. In a recent study, γ-radiation was shown to result in less proficient G1 arrest in cells overexpressing *c-myc* compared to that of normal cells, suggesting increased *c-myc* expression drives the progression of cells through the cell cycle in the presence of genomic DNA damage. Thus, γ-radiation

induced functional loss of Per2 results in diminished p53-mediated apoptosis and in turn the accumulation of DNA damaged cells. Evidence further suggests that the overexpression of *c-myc* in DNA damaged cells may still result in the proceeding of these cells through the cell cycle which may result in elevated incidences of tumour development following γ-radiation.

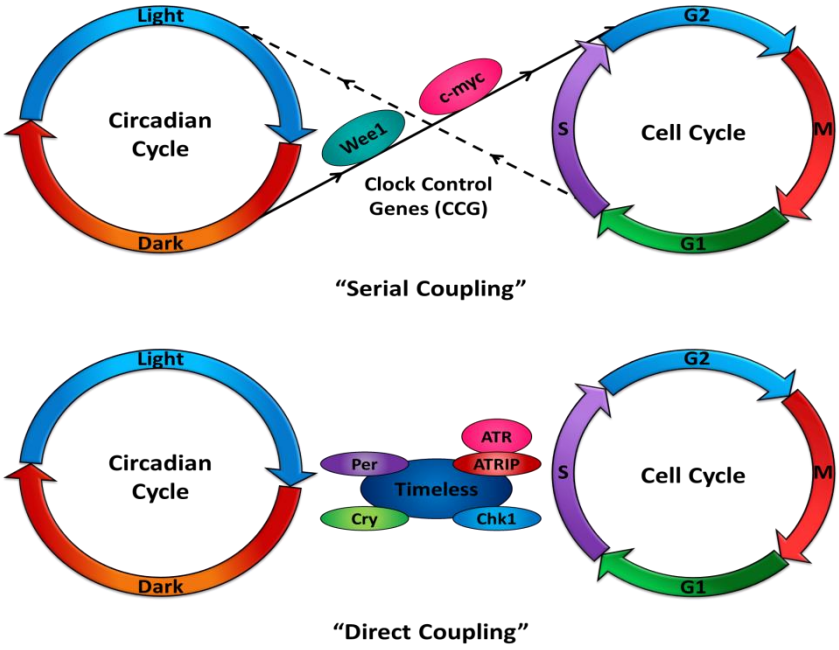

Figure 1.8: Schematic representation of the two proposed models involved in the coupling of the circadian clock system to the cell cycle. Serial coupling involves the regulation of the circadian and cell cycle via protein regulators of the other cycle. Whereas, direct coupling involves the regulation of both cycles by proteins such as timeless which play a part in the molecular machinery of both cycles. Adapted from: Ünsal-kaçmaz *et al.*, 2005.

Increasing evidence suggests that Per2 also plays a critical role in tumour suppression. A recent study, comparing a mouse mammary carcinoma (EMT6) cell line to non-tumorigenic (NIH3T3) cell line revealed diminished cellular proliferation and significantly increased apoptosis in EMT6 cells where Per2 was overexpressed. This may be explained by the fact that Per2 overexpression results in down-regulation of anti-apoptotic *c-myc*, Bcl-XL, and Bcl-2 in addition to the up-regulation of pro-apoptotic p53 and bax expression (Rana *et al.*, 2010). Although significant evidence suggests a

tumour suppressive role for Per2, further research is required to illuminate whether a specific mutation of Per2 results in oncogenic properties or if Per2 is in fact a tumour suppressor gene.

Additionally, the cell cycle gene, Cyclin D1 (CCND1), is controlled by the circadian clock system and its overexpression leads to mammary tumourigenesis. Furthermore, CCND1 overexpression in estrogen receptor α (ERα) – positive breast cancer is associated with poor patient prognosis (Rana *et al.,* 2010).

Essential cellular stress response pathways are activated in response to DNA damage; these pathways in turn result in the activation of the tumour suppressor p53, and subsequent apoptosis or cell cycle arrest. Thus, circadian proteins play a critical role in circadian controlled cellular response to DNA damage and cell proliferation. Recent evidence has also shown that human BMAL1-deficient cells activate p53 and p21 in response to DNA damage; however these cells are unable to undergo growth arrest (Antoch *et al.*, 2010).

It has also been proposed that Per1 plays a tumour suppressive role via its regulation of genes controlling cell cycle progression, as well as its ability to interact with crucial checkpoint proteins activated in response to DNA damage. Ionising radiation induced apoptosis increased in cancer cells where Per1 was overexpressed, however, apoptosis was blunted in cells where Per1 was inhibited. In addition, ionising radiation resulted in nuclear translocation of Per1 and the induction of *c-myc* expression. Thus, Per1 acts as a tumour suppressor through its ability to activate a wide range of signalling pathways including that involved in the DNA damage response.

A recent study conducted by Filipski and colleagues, showed that a severe disruption in the central circadian clock of tumour-bearing mice resulted in accelerated tumour growth, confirming known clinical results where patients with maintained 24 hour

circadian rhythms generally have an improved prognosis compared to those with disrupted circadian rhythms (Filipski *et al.*, 2006). It is evident that further investigations into the effects of circadian clock disruption on the cellular DNA damage response and cancer susceptibility are warranted, specifically with regards to elucidating the mechanisms behind this circadian clock disruption.

Mammalian circadian rhythms play a pivotal role in a wide range of physiological processes, including those involved with energy and nutrient metabolism (Green *et al.*, 2008). Based on the knowledge that peripheral circadian clocks are known to be entrained by nutrient availability, and autophagy is highly dependent on intracellular nutrient status, autophagy itself may be subject to circadian regulation in accordance with rest and activity patterns (Sachdeva *et al.*, 2008).

1.11. Autophagy

In order for physiological homeostasis to be maintained, the temporal organization of energy and nutrient metabolism (Ma *et al*., 2012) as well as a balance between cellular degradative and biosynthetic pathways is essential (Rubinsztein *et al.*, 2007). Autophagy serves as one of the predominant cellular degradative pathways, whereby faulty or redundant cellular constituents are degraded (Levine, 2007). However, unlike other degradative pathways, like the ubiquitin proteasome pathway, responsible for the degradation of sterically hindered, ubiquitin tagged proteins (Mathew *et al.*, 2011), autophagy is capable of degrading all folded proteins and protein complexes as well as whole intracellular organelles (Rubinsztein *et al*., 2007).

Autophagy, derived from the Greek “auto” meaning oneself and “phagy” to eat, is classically defined as a dynamic, evolutionary conserved degradative process occurring

within all eukaryotic cells (Kondo *et al.,* 2005). Broadly classified as several intracellular pathways that all converge with the delivery of cytoplasmic cargo into lysosomes, autophagy typically refers to chaperone-mediated, micro- and macroautophagy (Morselli *et al*., 2009). Macroautophagy (hereafter referred to as autophagy) constitutes the most abundant form of autophagy and involves the delivery of cytosolic cargo to lysosomes by means of double membrane bound vesicles, called autophagosomes (Rabinowitz *et al.*, 2010).

A low basal level of autophagy occurs under normal physiological conditions, which serves a beneficial "housekeeping" function, whereby old or redundant cellular constituents are degraded, and used as an additional energy source for various metabolic processes (Levine, 2007). Basal autophagy serves a particularly indispensable role in quiescent and terminally differentiated cells where the aggregation of defective components may become cytotoxic, as they are not diluted through the process of cell division (Rabinowitz *et al.*, 2010).

Under conditions where autophagy is activated in response to cellular stressors, such as nutrient deprivation and hypoxia, the process of autophagy becomes somewhat of a "double-edged sword" (Shintani *et al.,* 2004) as increased levels of autophagy, serve as a protective mechanism, whereby non-essential cellular constituents may be broken down to refuel essential cellular processes (Hippert *et al.*, 2006). However, unregulated autophagy in these conditions may result in the excessive "self-cannibalization" of intracellular organelles thereby resulting in cell death (Mizushima *et al.*, 2008).

The induction of autophagy occurs through the initiation of specific autophagy execution proteins eliciting a cascade of reactions that ultimately results in the formation of a phagophore, the initial isolation membrane. The newly formed phagophore then surrounds the cellular constituents to be degraded, where it matures to form a double

membrane bound vesicle called an autophagosome. Autophagosome formation is mediated by a group of autophagy-specific genes (ATG) whose products are categorized into four classes, namely; (i) an upstream autophagy regulatory complex, which responds to nutrient availability, (ii) a vesicle nucleation lipid kinase group, (iii) two ubiquitin-like protein systems, responsible for the production of modified autophagy regulatory complexes (Atg8-PE and Atg5-Atg12-Atg16) essential for autophagosome assembly and size determination (Hanada *et al*., 2007), and (iv) a group of complexes responsible for the degradation of ATG complexes (Hippert *et al*., 2006).

The autophagy receptor p62/SQSTM1 recognises and binds to proteins tagged by ubiquitin, targeting them for degradation (Komatsu *et al*., 2007). During the process of autophagosome formation, LC3 I is converted to LC3 II via a lipidation step. LC3 II is then sequestered to the inner surface of the phagophore, where it associates with p62 (Mizushima *et al*., 2008). Autophagosomal cargo is subsequently delivered to lysosomes (Rabinowitz *et al.*, 2010) where the release of lysosomal digestive enzymes into the lumen of the autophagolysosome results in the degradation of p62 as well as sequestered cellular constituents, ultimately resulting in the release of free fatty acids, amino acids, nucleotides and sugars (**Figure 1.9**) (Levine, 2007).

The pharmacological inhibition of autophagy is achieved with the use of Bafilomycin A1. Bafilomycin A1 binds to essential vacuolar ATPase subunits located on lysosomal membranes inhibiting proton translocation. This inhibition results in an elevation in lysosomal pH, and thus blocks the fusion of autophagosomes to lysosome (Rubinsztein *et al*., 2007).

As mentioned previously, autophagy undergoes diurnal (circadian) regulation based on nutrient availability. In fact, autophagy has been shown to display a robust circadian rhythm in the liver of mice (Ma *et al.,* 2011), the main site of nutrient metabolism. In

mammals, nutritional status is dependent on daily feeding/fasting periods. During the active daytime periods, where food intake is highest plasma insulin levels peak, resulting in the inhibition of autophagy via the PI3K/Akt pathway. However, during nightly rest periods where food intake is minimal, plasma glucagon levels are highest, resulting in cellular ATP depletion and AMPK- induced autophagic activation (**Figure 1.9**).

C/EBPβ has been shown to mediate the temporal orchestration of autophagy rhythms, as its rhythmic expression is tightly controlled by both nutritional status and circadian regulation. Additionally, C/EBPβ is known to be a potent activator of autophagy, through the induction of various genes involved in autophagy, such as *Ulk1,* and *LC3B*. Interestingly, an increased level of LC3 II caused by the induction of autophagy by C/EBPβ occurs independently of the protein kinase mammalian Target of Rapamycin (mTOR) activity (Ma *et al*., 2011).

mTOR the predominant regulator of the autophagic process, is a sensor of intracellular nutrient status and master regulator of cell growth. mTOR serves as a negative regulator of autophagy through its ability to phosphorylate and thus inactivate Unc-51-like kinase (ULK1) and Atg13, two of the main ULK1 components, thus inhibiting the initiation of phagophore synthesis (Mathew *et al.*, 2011). mTOR exists in two biologically functional signalling complexes namely, mTORC1 and mTORC2. Pharmacological administration of Rapamycin results in the detachment of RAPTOR from mTOR. RAPTOR acts as a scaffold for the recruitment and activation of mTOR substrates and thus the inhibition of mTORC1. Additionally, the mTORC1 substrates S6-kinase and eIF4E-binding protein (4E-BP1) interact with various mRNAs regulating the initiation of translation, and controlling protein synthesis rates (Belda-Iniesta *et al.*, 2011). Furthermore, mTORC1 governs the translation of regulators of cell growth, such as cyclin-D1, HIF1α and *c-myc*, thus promoting cellular processes such as cell cycle progression, cell growth and angiogenesis all of which become deregulated during tumourigenesis.

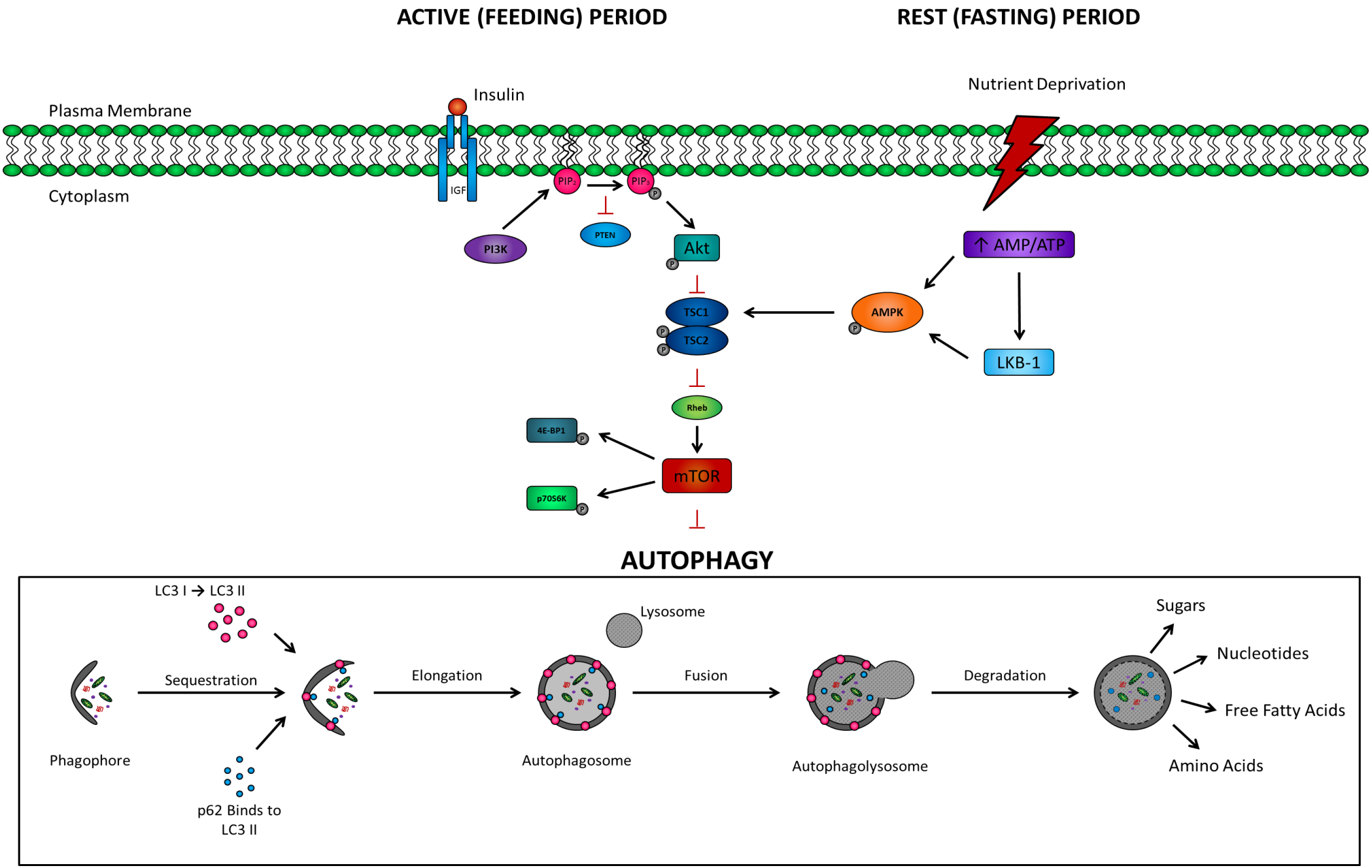

Figure 1.9: Schematic representation of the molecular pathways involved in the regulation of autophagy in mammalian cells. Adapted from: Mathew *et al.*, 2011.

1.12. The Role of Autophagy in Cancer

As stated previously, a failure in autophagy regulation has been implicated in a variety of diseases, including that of cancer (Chen *et al.*, 2010). Within the solid tumour cell microenvironment, limited angiogenesis results in a state of nutrient deprivation and hypoxia. The up-regulation of autophagy in these conditions is expected to result in an increase in tumour cell growth, whereas autophagic down-regulation may limit growth, through the rapid induction of apoptosis (Hippert *et al*., 2006).

Autophagy is known to play a paradoxical role in both cell survival and cell death in response to various intracellular stressors however, the mechanism behind this dual role in cancer cells remains to be fully elucidated. The increased signalling of the Ras pathway in certain cancer types is thought to trigger autophagy as survival mechanism within the hypoxic tumour interior until neoangiogenesis allows for revascularization (Singletary *et al.,* 2008).

Additionally, 50% of breast cancers are known to have deletions in the beclin-1 (BECN1) gene (Morselli *et al*., 2009), a mammalian homologue of the yeast autophagy-specific gene *Atg*6. BECN1 is involved in autophagosome formation (Kondo *et al*., 2005) as well as the activation of autophagy by binding to class III phosphatidylinositol 3-kinase (PI3K) (Hait *et al.*, 2006). Single allele deletions of BECN1 have been shown to result in increased tumourigenesis (Karantza-Wadsworth *et al*., 2007) whereas its overexpression results in an inhibition of tumourigenesis, suggestive of defective autophagy playing a role in cancer malignancy (Dalby *et al.*, 2010). Initially, BECN1 mutations were suggestive of autophagy being a cell death pathway, nevertheless, BECN1 null embryonic stem cells do not display any changes in sensitivity to cell death and tumours of haploinsufficient mice do not show a reduction in BECN1 protein levels.

Under normal cellular conditions the binding of BECN1 to Bcl-2 results in diminished autophagic cell death (Hippert *et al*., 2006), however, a failure in beclin-1:bcl-2 complex formation, results in excessive levels of autophagy and cell death, signifying the role of bcl-2 in the regulation of both autophagy and apoptosis (Levine *et al.*, 2008).

1.13. AMPK and Breast Cancer

AMP-activated protein kinase (AMPK), the master intracellular energy regulator, serves as a crucial mediator of metabolic signals (Lamia *et al*., 2009) where its activation in response to energy deprivation results in the stimulation of energy producing pathways concomitantly to an inhibition of energy consuming processes (Brown *et al.*, 2013).

AMPK is a heterotrimeric protein kinase (Jordan *et al.*, 2013) consisting two catalytic α-subunits, two regulatory β-subunits and three γ-subunits with multiple isoforms of each subunit existing. Various subunits of AMPK have been found to be constitutively expressed and activated in a tissue-specific manner. Expression patterns of AMPK have been extensively studied and are well characterized in animal models, however very little is currently known about its tissue distribution in humans with specific regards to human cancer cell types (Brown *et al*., 2013).

AMPK activation leads to suppression of various ATP-dependent cellular processes, including that of gluconeogenesis, fatty acid and protein synthesis as well as promoting catabolic processes such as glycolysis and fatty acid β-oxidation (Goodwin *et al.*, 2009). Additionally, AMPK activation has been also been shown to play a central role in mediating the effects of metformin.

The biguanide, metformin is a common first line pharmacological drug used in the treatment of type II diabetes. Various studies, including that conducted by Chlebowski

and colleagues, comparing incidences of breast cancer in diabetic women with that of non-diabetic women, have demonstrated a definite reduction in the incidence of breast cancer in diabetics using metformin (Chlebowski *et al*., 2013). It is also widely accepted that patients suffering from type II diabetes have an increased risk for the development of cancer as well as a reduced prognosis following the onset of breast cancer when compared to that of non-diabetic cancer patients (Belda-Iniesta *et al.*, 2011).

The molecular effects of metformin and its role in cancer malignancy has gained increased interest, as both clinical and epidemiological evidence show that insulin resistance, hyperglycaemia and diabetes results in poor breast cancer prognoses. Furthermore, metformin has been shown to influence cancer cells directly by affecting cell proliferation and apoptosis as well as indirectly via insulin-mediated signalling (Goodwin *et al.*, 2009).

Evidence suggests that metformin's mechanism of action involves increased insulin receptor mediated signalling leading to a reduction in insulin levels (Zakikhani *et al.*, 2006). However, recent evidence suggests that metformin-induced AMPK activation results in a decrease in circulating blood glucose levels through the down-regulation of hepatic gluconeogenesis and the stimulation of muscular glucose uptake (Belda-Iniesta *et al*., 2011) independently of insulin signalling (Zakikhani *et al*., 2006). This mechanism has also been shown to involve that activation of liver kinase B1 (LKB1), a serine-threonine kinase (Dowling *et al.*, 2007).

LKB1 has recently been found to act as a tumour suppressor as mutations leading to a loss of AMPK signalling and mTOR inhibition are tumorigenic. There is currently increased interest in determining whether or not AMPK agonists like metformin lead to a coupling of growth and energy signalling within cancer cells in order to inhibit their

growth. Currently evidence shows metformin inhibits the growth of breast cancer cells through the activation of AMPK (Rocha *et al*., 2011).

LKB1 and calcium/calmodulin-dependent protein kinase kinase β (CaMKKβ) act as upstream AMPK kinases that respond to depleted intracellular ATP and calcium signals respectively. However, evidence suggests that the majority of AMPK signals in the liver, and muscle are mediated via LKB1. Furthermore it is believed that LKB1 is essential in the maintenance of normal adipocyte AMPK signalling.

LKB1 loss of function is associated with the development of Peutz-Jeghers syndrome, typically characterized by the presence of by multiple gastrointestinal polyps as well as a significantly increased (>80%) risk for the development of a variety of epithelial cancers, including that of breast cancer (Zakikhani *et al.,* 2006). AMPK is a direct substrate for LKB1 and the phosphorylation of the α-subunits of AMPK at Thr^{172} results in its enhanced activity (**Figure 1.10**) (Belda-Iniesta *et al*., 2011).

AMPK has also been shown to act as a crucial regulator in many of the characteristic hallmarks of the malignant phenotype of cancer cells, including that of increased DNA and protein synthesis, proliferation, lipid production and migration, further solidifying its role in cancer (Brown *et al*., 2013).

Due to the critical role that AMPK plays in homeostatic energy control, increased interest is currently placed towards the understanding of how alterations in AMPK may be associated with increased cancer cell tumourigenicity via both direct cellular metabolic and protein synthetic effects, and indirect endocrine-mediated activities (Brown *et al*., 2013). In addition to the role that AMPK plays in energy homeostasis, it has also recently been shown to play a critical role in the regulation of p53, a potent tumour suppressor. Activation of AMPK results in the up-regulation of p53 and its subsequent

phosphorylation at Ser^{15}. Conversely, p53 activation leads to an increased expression of the β1-subunit of AMPK.

1.14. AMPK Regulation of the Circadian Clock System

Increased interest in AMPK and its effect on circadian rhythms has gained much interest due to the fact that both energy metabolism and food intake are synchronised to daily light/dark cycles. In addition, AMPK has been shown to phosphorylate Ser^{389} of casein kinase Iε, leading to the degradation of Per2 leading to a phase advance and a shortening of period length (**Figure 1.10**). Thus, AMPK is a central key regulator in energy metabolism as well as circadian length. High intracellular AMP:ATP ratio's results in the activation of AMPK by LKB1 mediated phosphorylation (Lamia *et al*., 2009).

The suprachiasmatic nucleus (SCN) is entrained by light, whereas peripheral circadian clocks are predominantly entrained by food availability, although the mechanisms behind these entrainment signals remain to a large extent a mystery. The mammalian SCN serves as the master clock, coordinating both physiological and behavioural rhythms to daily light/dark cycles. Non-light sensitive peripheral clocks are entrained by daily feeding activities, theoretically allowing for anticipation of food consumption and optimized timing of metabolic process within these peripheral tissues (Lamia *et al*., 2009)

Mammalian circadian clocks are dependent on cyclical activation and repression of transcription, wherein, CLOCK and BMAL1 result in the transcription of period and cryptochrome genes. The products of which feedback to inhibit Clock and BMAL1 thus resulting in their rhythmic expression. Posttranslational modifications, such as the ubiquitination of cryptochromes by F-box and leucine-rich repeat protein 3 (FBXL3), result in degradation and subsequent resetting of the intrinsic clock mechanism. Several

biochemical analyses suggest that modifications of Ser^{71} and Ser^{280} residues on Cry1 alter the stability of these proteins. In addition both Ser^{71} and Ser^{280} residues conform to the optimal sequence AMPK phosphorylates, where mutations in a phosphomimetic amino acid, such as aspartic acid, is sufficient to destabilize Cry1, and mutations resulting in a non-phosphorylatable amino acid, such as alanine, is sufficient to stabilize Cry1 (Lamia *et al*., 2009).

Lamia and colleagues demonstrated that AMPK is activated in response to glucose deprivation, resulting in a reduction in Cry1 stability and an increase in Clock: BMAL1 target signalling in fibroblasts (**Figure 1.10**). Furthermore, fibroblasts which stably expressed luciferase under the control of a BMAL1 promoter (BMAL1-luciferase), result in a high amplitude circadian rhythm with a periodicity of ±25.3 hours under high glucose conditions. An increase in periodicity to ±30.7 hours as well as a decrease in BMAL1-luciferase amplitude was seen after a reduction in glucose levels (Lamia *et al*., 2009).

Thus, it is therefore reasonable to assume that expression, activation and/or localization of AMPK is dependent on diurnal regulation, due to the fact that AMPK directed phosphorylation of cryptochromes regulates peripheral clock phase (Lamia *et al*., 2009).

Additionally, a wide range of evidence shows that efficient energy utilization and storage as well as the optimization of metabolic process timing are under the control of peripheral mammalian clocks. The majority of metabolism regulating receptors, enzymes and transporters display robust fluctuations throughout the course of the day (Jordan *et al.*, 2013).

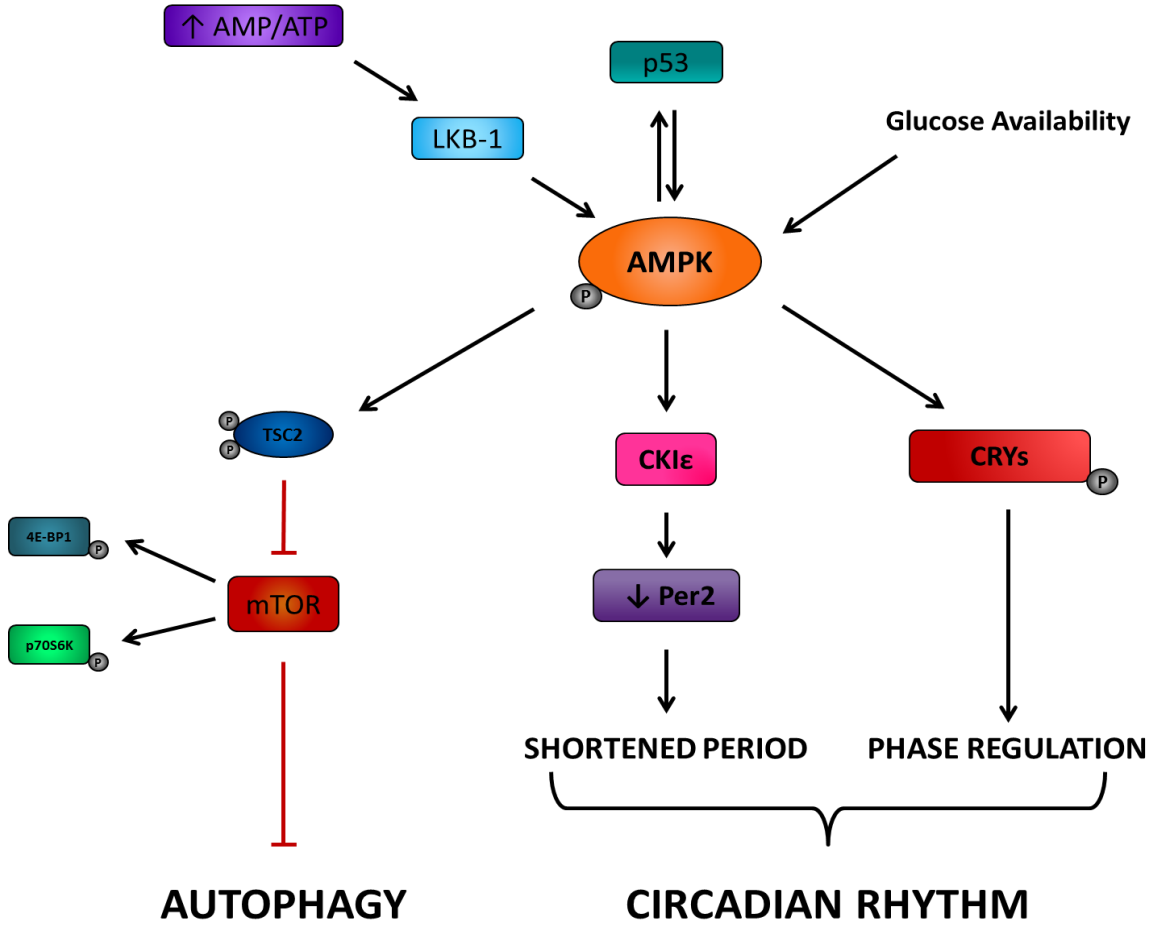

Figure 1.10: Proposed mechanism of the signalling pathways involved in the regulation of autophagy and the circadian clock system by AMPK. The activation of AMPK, either by p53, a LKB1-dependent mechanism, or alterations in glucose availability, leads to the inhibition of mTOR and the subsequent induction of the autophagy. Additionally, AMPK activation phosphorylates Cryptochrome proteins, and indirectly, via CKIε, the phosphorylation of Period 2. The phosphorylation of both Cryptochrome and Period, tags these proteins for degradation by the 26S proteasome and thus a resetting of the circadian clock system.

1.15. Problem Statement

Doxorubicin an anthracycline antibiotic is extensively used in the treatment of breast cancer. Although effective to a large extent there are severe problems associated with this line of therapy, the main one being that cancer cells have become increasingly resistant to Dox therapy. There is therefore a critical need for effective adjuvant therapies aimed at improving cancer cell susceptibility to lower doses of doxorubicin.

1.15.1. Hypothesis

We hypothesize that the manipulation of the circadian Per2 protein in conjunction with Dox may provide a more effective chemotherapeutic strategy for the treatment breast cancer.

1.15.2. Aims

1. Characterize the role of Per2 in normal breast epithelial cells as well as in ER+ and ER- breast epithelial cells
2. Determine the role of Per2 in doxorubicin-induced cell death
3. Determine the role of Per2 in autophagy
4. To evaluate the role of metformin, a modulator of Per2 expression, as a potential adjuvant chemotherapeutic agent.

Chapter 2: Materials and Methods

2.1. Cell Culture

Three different cell lines were used, namely, MCF-12A human derived breast epithelial cells, MCF-7 estrogen receptor positive (ER^+) human breast adenocarcinoma cells and MDA-MB-231 estrogen receptor negative (ER^-) human breast adenocarcinoma cells (**Figure 2.1**). Both MCF-7 and MDA-MB-231 breast cancer cells were cultured in Dulbecco's Modified Eagles Medium (DMEM) (Life Technologies) that was supplemented with 10% Foetal Calf Serum (Scientific Group) and 1% Penicillin Streptomycin (PenStrep) (Life Technologies) collectively known as growth medium. The MCF-12A non-cancerous cells were cultured in a 1:1 ratio of Dulbecco's Modified Eagles Medium (DMEM) (Life Technologies) and Ham's F-12 nutrient mixture (Life Technologies) supplemented with 10% Foetal Calf Serum and 1% Penicillin Streptomycin (PenStrep), 10 µg/ml Insulin (Humalin 30/70), 20 ng/ml Epidermal Growth Factor (EGF), 500 ng/ml Hydrocortisone and 100 ng/ml Cholera toxin (Sigma Aldrich, #C8052). Cells were cultured in T75 flasks (75 cm^2 flasks, NEST) and maintained in an incubator (C01901R, Snijders Scientific) set at an atmosphere of 37ºC and 5% CO_2 humidity. Growth media was refreshed every 2^{nd} day and were regularly sub-cultured once a confluency of 70-80% was reached. Upon reaching 80% confluency, cells were split and seeded with fresh media for experiments. Seeding was accomplished by washing the cell monolayer with warmed Phosphate Buffered Saline (PBS) before incubation in 4 ml 0.25% Trypsin EDTA (1X) (Life Technologies) until all cells loosened from the surface of the flask. Detailed step-by-step protocols for all breast epithelial cell culture procedures have been included in Appendix A (Protocol 1).

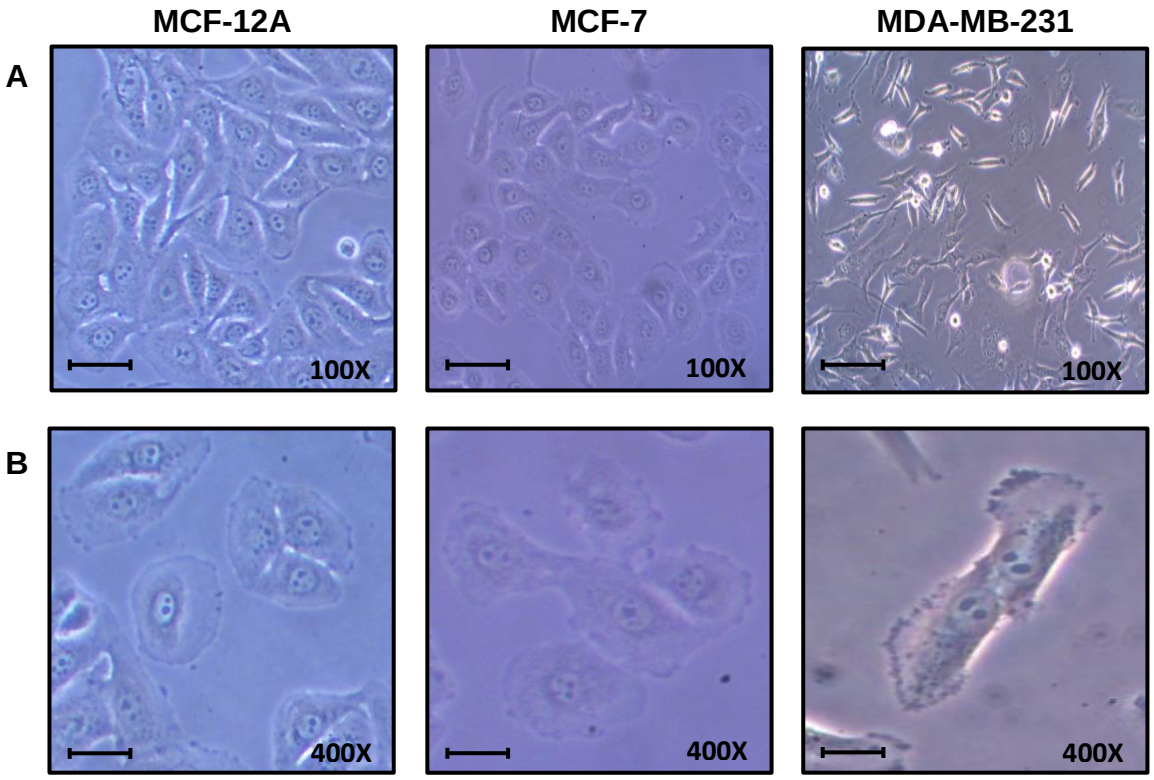

Figure 2.11: Images of the normal MCF-12A breast epithelial, the estrogen receptor negative (ER^-) MDA-MB-231 adenocarcinoma and the estrogen receptor positive (ER^+) MCF-7 adenocarcinoma cell lines obtained with an inverted microscope. (A) 100x and **(B)** 400x magnification.

2.2. Treatments

Prior to treatment, media was aspirated and cell monolayer was washed twice with warm PBS to ensure all cell debris was removed. In order to determine optimal concentrations, concentration curves were done for a treatment period of 24 hours for doxorubicin (Sigma-Aldrich, # D1515) with the following concentrations: 0.1, 1.0, 2.5, 5.0 and 10.0 µM. The selected concentration of doxorubicin based on cell viability, with the highest concentration that produces the least toxic effect in normal (MCF-12A) cells while still increasing cell death in the cancer (MDA-MB-231 and MCF-7) cells used. A concentration of Bafilomycin A1 from *Streptomyces griseus* (Sigma-Aldrich, #B1793) which is known to inhibit autophagy was chosen based on previous findings by our group (Thomas, PhD thesis, 2012. Available: http://hdl.handle.net/10019.1/19912). Once

concentrations were established, cells were arbitrarily divided into treatment groups as described in table 2.1 below. Complete treatment protocols are provided in Appendix A (Protocol 2).

Table 2.1: This study was divided into three main experiments which consist of the following groups:

Experimental Group 1	Control **(C)**	Doxorubicin **(D)**	Per2 **(P)**	Per2 + Doxorubicin **(PD)**
		2.5 µM	30 nM	30 nM + 2.5 µM
Experimental Group 2	Control **(C)**	Bafilomycin **(B)**	Per2 **(P)**	Per2 + Bafilomycin **(PB)**
		10 nM	30 nM	30 nM + 10 nM
Experimental Group 3	Control **(C)**	Doxorubicin **(D)**	Metformin **(M)**	Metformin + Doxorubicin **(MD)**
		2.5 µM	40 mM	40 mM + 2.5 µM

2.3. Per2 Silencing

Cells were transfected in 6-well plates (Whitehead Scientific, #S00023) using a forward transfection protocol (Protocol 3). 100 000 cells were plated into the culture dishes 24 hours prior to transfection. 30 nM of an endoribonuclease-prepared siRNA (esiRNA) targeted against Per2 (Sigma-Aldrich, Mission® esiRNA human Per2 (esiRNA1) #EHU070571) was diluted into 100 µl serum free growth media. 12 µl of HiPerfect

transfection reagent (Qiagen, #301705) was added to the esiRNA mixture and allowed to incubate at room temperature for 20 minutes in order for esiRNA:HiPerfect complexes to form. Antibiotic free growth media was then added to produce a final volume of 2 ml which was added drop-wise onto cells. Plates were gently swirled and incubated at an atmosphere of 37ºC and 5% CO_2 humidity for 48 hours before subsequent treatment. esiRNA against enhanced green fluorescent protein (eGFP) (Sigma-Aldrich, Mission esiRNA eGFP #EHU019931) was used as a negative control. Detailed step-by-step protocols for Per2 silencing procedures are included in Appendix A (Protocol 3).

2.4. Western Blot Analysis

In order to carry out western blot analysis cells were arbitrarily subdivided into above mentioned treatment groups (Protocol 2) and seeded accordingly into T25 flasks (25 cm^2 flasks, NEST) with 4 ml of growth media per flask. Flasks were all incubated in a 37ºC, 5% CO_2 environment for 24 hours to allow cells to attach and proliferate.

2.4.1. Protein Extraction and Quantification

Media was aspirated from T25 flasks and cells were immediately placed on ice. The cell monolayer was washed with 1 ml cold PBS, which was repeated twice more. 100 µl modified radio-immunoprecipitation assay (RIPA) buffer comprising of 2.5 mM Tris-HCL, 1 mM EDTA, 1 mM dithiothreitol, 0.1 mM phenylmethylsulfonyl fluoride (PMSF), 1 mM benzamidine, 50 mM NaF, 4 mg/ml SBTI, 10 mg/ml leupeptin, 0.1% SDS 0.5%, Na deoxycholate and 1% NP40, calibrated to pH 7.4, was added to each petri dish and allowed to stand for 5 min on ice in order to extract total cell protein. Cells were then detached from the flask surface with the use of a cell scraper which was rinsed in EtOH

between different samples. Whole cell lysates were sonicated on ice at 3 Hz for 8 seconds and centrifuged at 8000 RPM for 30 seconds. The supernatant was then decanted into eppendorf tubes and stored at -80ºC. A Bradford protein determination assay was conducted to determine the protein content of each sample. A detailed step-by-step protocol for protein extraction and determination is included in Appendix A (Protocol 4).

2.4.2. Sample Preparation

Samples used for western blots were prepared following protein determination. Aliquots were prepared containing 50 µg protein content and diluted with sample buffer. Prepared samples were then stored at -80ºC for further western blot analysis. A detailed step-by-step protocol for sample preparation is included in Appendix A (Protocol 5).

2.4.3. SDS-PAGE and Western Blot Analysis

Cell lysates were subsequently separated on 4-15% polyacrylamide precast gels (mini-PROTEAN® TGX™ Gels, Bio-Rad) by sodium dodecyl sulphate polyacrylamide gel electrophoresis (SDS-PAGE). 5 µl of a protein marker ladder (PeqGold) was loaded into the first well of each gel run; this was used for orientation of gels as well as for determination of molecular weights of separated proteins. Prepared cell lysates were heated to a temperature of 95ºC for 5 minutes in order to denature proteins and pulse centrifuged, after which 50 µg of protein was added to each lane.

Gels were run at 100 V (constant) and 400 mA for a period of ± 90 minutes (Power Pac 300, BioRad). On completion of SDS-PAGE, proteins were transferred to prepared polyvinylidine fluoride (PVDF) membranes using a semi-dry electrotransfer system (TransBlot® Turbo™ v1.02, BioRad) for 30 minutes at 25 V and 1.0 A. Membranes were placed in PoncheauS staining solution in order to visualize that proteins transferred correctly. Membranes were subsequently washed in 0.1 % Tris Buffered Saline-Tween20 (TBS-T) and blocked for 1 hour in 5 % (w/v) fat-free milk and TBS-T, whilst being gently agitated at room temperature, this prevents non-specific binding of the antibody. Membranes were then incubated at 4ºC overnight in TBS-T diluted primary antibodies (1:1000). The following day membranes were removed from the primary antibody and washed with TBS-T before being incubated in anti-rabbit IgG horseradish peroxidase conjugated secondary antibody (1:10000) (from donkey) (Cell Signalling Technologies) with gently agitation at room temperature for 1 hour. Subsequent to the incubation period membranes were washed in TBS-T before antibodies were detected with the use of an ECL western blotting substrate detection kit (Pierce®, Thermo Scientific) and protein bands visualised with the use of ImageLab 4.0 software on a Chemi-Doc™ MP (BioRad) imaging system. Exposed bands were visualized and quantification was done using densitometry with the use of QuantityOne densitometry software. Bands for each specific protein were quantified as density readings comparative to the control sample present on the same blot. A complete step by step protocol for SDS-PAGE and Western blot analysis is included in Appendix A (Protocol 6).

2.5. Immunocytochemistry – Per2 and Hoechst

MCF-12A and MDA-MB-231 cells were grown in 8-well chamber slides (Lab-Tek, Thermoscientific) at a density of 12 000 cells/well. After the treatment period, growth

medium was removed and cells were washed twice with warm PBS. Cells were fixed with ice-cold methanol and acetone (1:1) and left to incubate on ice for 10 min. The fixative mixture was then removed and cells were allowed to air-dry for 20 min. After being rinsed twice with PBS, non-specific binding was prevented by incubating cells in a 1% BSA/PBS blocking solution for 30 min at RT. After this time period, the blocking solution was drained off and a primary antibody against Per2 diluted in PBS (1:50) was added to cells and allowed to incubate overnight at 4°C. Cells were then rinsed three times with PBS and allowed to incubate with the appropriate secondary antibody for 30 min at room temperature. In this case an Alexa Fluor 488 conjugated donkey anti-rabbit secondary antibody (Life Technologies, #A-21206) was used. After incubation, Hoechst 33342 dye (1:200) was additionally added and kept in contact with cells for a further 10 min incubation period. Next, cells were rinsed and mounted with DAKO fluorescent mounting medium (DAKO Inc., CA, USA). Chambers were kept wrapped in foil at -20°C until analysis. Detailed step-by-step protocols for immunocytochemistry procedures using confocal microscopy have been included in Appendix A (Protocol 7).

2.6. MTT Assay

A MTT cell viability assay was conducted to assess the percentage of metabolically viable cells. The principle of this assay is based on the reduction of MTT to yield purple formazan crystals by various reduction enzymes present within the mitochondria. Cells from each cell line where arbitrarily divided into treatment groups (Table 2.1) and seeded at a cell density of 50 000 cells per well into 24 well plates (Cellstar, Greiner bio-one). Cells where left for 24 hours to attach and proliferate in 1 ml of growth media after which media was refreshed and treatments administered as described above. Subsequent to treatments, all media was aspirated (Mini-vac power, PeqLab biotechnologie GmbH) and

500 µl of MTT working solution (0.001 g MTT/ml PBS) was added to each well. As MTT is a light sensitive compound, this experiment was conducted in the dark and 24 well plates were covered in tin foil. After the addition of MTT working solution to wells, cells were incubated for 1.5 hours at a 37ºC, 5% CO_2 humidified environment (C01901R, Snijders Scientific). Subsequent to incubation, 500 µl Isopropanol:HCl/Triton-X-100 solution was added to each well, and the tinfoil wrapped plate was placed on a heated shaker (37ºC, 200 RPM) for a period of ±5 min until formazan crystals generated by healthy cells had dissolved. Plates were then analysed using KCjunior software on a universal micro plate reader (EL800, Bio-Tek Instruments Inc.) where absorbance values were determined at a wavelength of 595 nm. All groups were analysed in triplicate and three independent experiments were conducted. Absorbance values were all expressed as a percentage of MTT reduction versus the untreated control. Detailed step-by-step protocols for all MTT assay procedures have been included in Appendix A (Protocol 8).

2.7. Flow Cytometry – Hoechst and PI Staining

MCF-12A and MDA-MB-231 cells were grown in T25 flasks at a seeding density of 700 000 cells/flask. After the treatment period, 2 ml 0.25% Trypsin EDTA (Life Technologies) was added to each flask for 3-4 min until all cells had detached. The cell suspension was then added to 15 ml Falcon tubes (BD Biosciences) and centrifuged at 1500 RPM for 3 min. The supernatant was removed and the pellet washed with 0.1 M PBS. The cells were centrifuged again at the same specifications and the supernatant was removed. Propidium Iodide (PI) (Sigma-Aldrich) and Hoechst 33342 was added to the unfixed cells to obtain a final concentration of 1 mg/ml and incubated for 10 min where after it was analysed on the flow cytometer (BD FACSAria I). A minimum of 10 000 events were collected and analysed using a 488 nm laser and 610LP, 616/23BP

emission filters. PI inclusion signified loss in membrane integrity and cell death. Values were represented as a percentage of the control and mean percentages from three separate experiments were used to perform statistical comparisons. Detailed step-by-step protocols for cell death analysis procedures using flow cytometry have been included in Appendix A (Protocol 9).

2.8. Flow Cytometry – Cell Cycle Analysis

Cell cycle analysis was performed by flow cytometry using the CycleTEST^{TM} PLUS DNA reagent kit (Becton Dickinson, California, USA). Prior to treatments MCF-12A and MDA-MB-231 cells were seeded into T25 flasks at a density of 300 000 and 400 000 cells respectively. Media was discarded and the cell monolayer was washed twice with warm PBS where after cells were trypsinized and centrifuged at room temperature for 5 min at 300 x g. The supernatant was discarded and the pellet gently re-suspended in 1 ml of the provided buffer solution (a mixture of sodium citrate, dimethylsulfoxide (DMSO) and sucrose). This procedure was then repeated twice more. Cells were then counted using a haemocytometer using standard counting procedures and concentrations were adjusted to $1x10^6$ cells / ml using buffer solution. In order to stain prepared cells, cell suspensions were centrifuged at 400 x g for 5 min at room temperature. 250 µl of solution A (trypsin buffer) was added to each tube, and allowed to react for 10 min at room temperature. Thereafter, 200 µl of solution B (trypsin inhibitor and RNase buffer) was added to each tube and allowed to react at room temperature for 10 minutes. Finally, 200 µl of ice cold solution C (propidium iodide (PI) stain solution) was added to each tube, which was incubated for a further 10 minutes in the dark at 4ºC. Samples were analysed on the flow cytometer (BD FACSAria I) within 3 hours of adding the PI staining solution. At least 30 000 list-mode data events were acquired for each sample.

As PI has an emission spectrum of 550 – 720 nm a bandpass filter of 585/42 was employed to detect light emitted between 564 and 606 nm by stained cells. ModFit LT software (Verity software house, Inc., ME, USA) was used to determine the percentage of cells in the G0/G1, S and G2/M phases. The percentage of apoptotic cells was also determined using ModFit LT software. Mean percentages from three independent experiments were used to perform statistical comparisons. Detailed step-by-step protocols for cell cycle analysis procedures using flow cytometry have been included in Appendix A (Protocol 10).

2.9. Flow Cytometry – G2/M Analysis

MCF-12A and MDA-MB-231 cells were seeded into T25 flasks at a density of 300 000 and 400 000 cells respectively. After the treatment period, 2 ml 0.25% Trypsin EDTA (Life Technologies) was added to each flask for 3-4 min until all cells had detached. The cell suspension was then added to 15 ml Falcon tubes (BD Biosciences) and centrifuged at 1500 RPM for 3 min. The supernatant was removed and the pellet re-suspended in 1 ml PBS. Formaldehyde at a final concentration of 4% was added and cells were fixed at 37ºC for 10 min, after which cells were placed on ice. Fixative was then removed and cells were centrifuged and the supernatant removed as previously. Permeabilization was achieved by adding ice cold methanol (90%) and incubating cells on ice for 30 min. 2-3 ml incubation buffer (0.5 g BSA dissolved in 100 ml PBS) was added to cells and rinsed twice by centrifugation. Phospho-Aurora A (Thr^{288})/Aurora B (Thr^{232})/Aurora C (Thr^{198}), Alexa Fluor 488 conjugated (Cell Signalling Technologies, #8525) and Phospho-Histone H3 (Ser^{10}), Alexa Fluor 647 conjugated (Cell Signalling Technologies, #3458) primary antibodies were added to cells (1:50 dilution in incubation buffer) and incubated for 1 hour at room temperature. Cells were washed by centrifugation in incubation buffer

before being re-suspended in 0.5 ml PBS and analysed on the flow cytometer (BD FACSAria I). A minimum of 30 000 events were collected and analysed using a 488 nm laser and 502LP, 520/30BP emission filters. Mean percentages from three independent experiments were used to perform statistical comparisons. Detailed step-by-step protocols for G2/M analysis procedures using flow cytometry have been included in Appendix A (Protocol 11).

2.10. Statistical Analysis

All statistical analysis was carried out using GraphPad Prism 5. All data was assessed using mean ± SEM. One-way analysis of variance (ANOVA) with Bonferroni post hoc corrections as well as Mann-Witney U t-tests were conducted where appropriate. A p-value <0.05 was considered statistically significant.

Chapter 3: Results

3.1. Characterizing the role of Per2 in normal breast epithelial cells as well as in ER+ and ER- breast epithelial cells

3.1.1. Baseline Circadian Rhythms

To determine the presence of a circadian expression pattern in the protein levels of Per2, all three cell lines were cultured under standard cell culture conditions and protein extractions were carried out hourly for a period of 25 hours commencing at 07h00 and terminating the following day at 08h00. Western blot analysis was carried out to determine the relative Per2 protein concentrations at each time point.

MCF-12A cells show a clear circadian pattern in Per2 protein expression with a significant increase in Per2 protein levels seen at 20 hours (03h00) when compared to baseline (0 hours = 07h00) (745.9 ± 28.23% vs 100%, $p < 0.0001$). The MDA-MB-231 cells showed the same rhythmic expression pattern for Per2, with levels significantly increasing at 20 hours (03h00) when compared to baseline (0 hours = 07h00) (537.8 ± 64.91% vs 100%, $p < 0.0001$) however, to a much lesser extent than that observed in the MCF-12A cells. Although the MCF-7 cells do express the Per2 protein, they do not display a distinct rhythmic expression pattern with protein levels remaining fairly constant over time (**Figure 3.1**).

As no rhythmic pattern of Per2 protein expression was observed in the MCF-7 cancer cell line, further analyses using this cell line were terminated and only the normal MCF-12A and ER^- MDA-MB-231 cancer cells were further utilized.

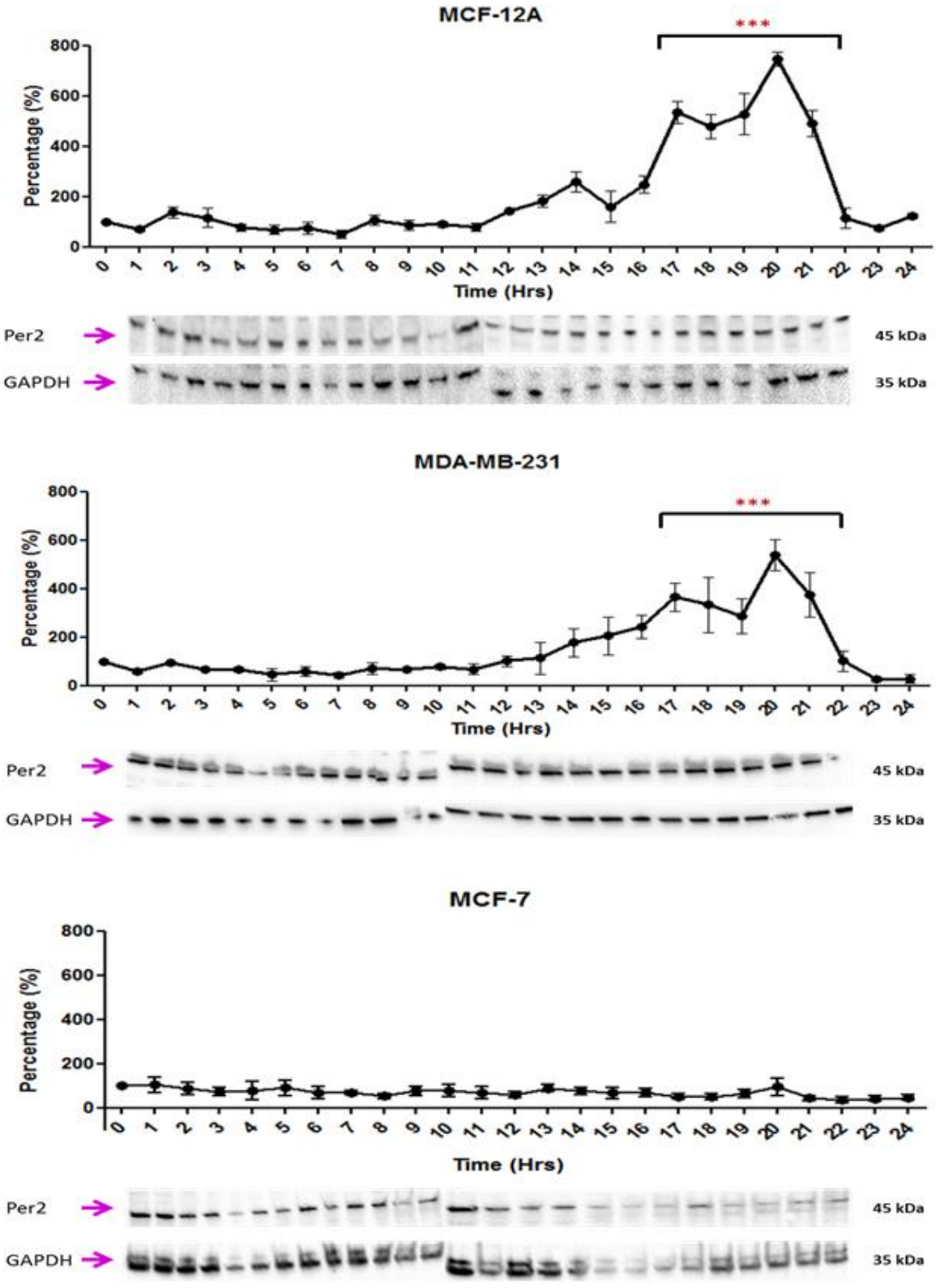

Figure 3.1: Rhythmic expression of the mammalian circadian protein period 2 (Per2) in non-tumourigenic breast epithelial MCF-12A cells (A), MDA-MB-231 estrogen receptor negative human breast adenocarcinoma cells (B) and MCF-7 estrogen receptor positive human breast adenocarcinoma cells (C). MCF-12A, MDA-MB-231 and MCF-7 cells were harvested hourly for a period of 25 hours (T0=Baseline). Western blot analysis was employed to assess relative Per2 protein levels. Values (normalized to GAPDH) are expressed as a percentage of baseline and presented as mean ± SEM (n=3). *** = P<0.0001 vs baseline.

3.1.2. Per2 Localization

In order to determine the cellular localization of Per2 both MCF-12A and MDA-MB-231 cells were cultured under standard cellular conditions until reaching confluency, after which they were immunostained with Per2:AlexaFluor 488 and Hoechst 33342 and visualized using confocal fluorescent microscopy.

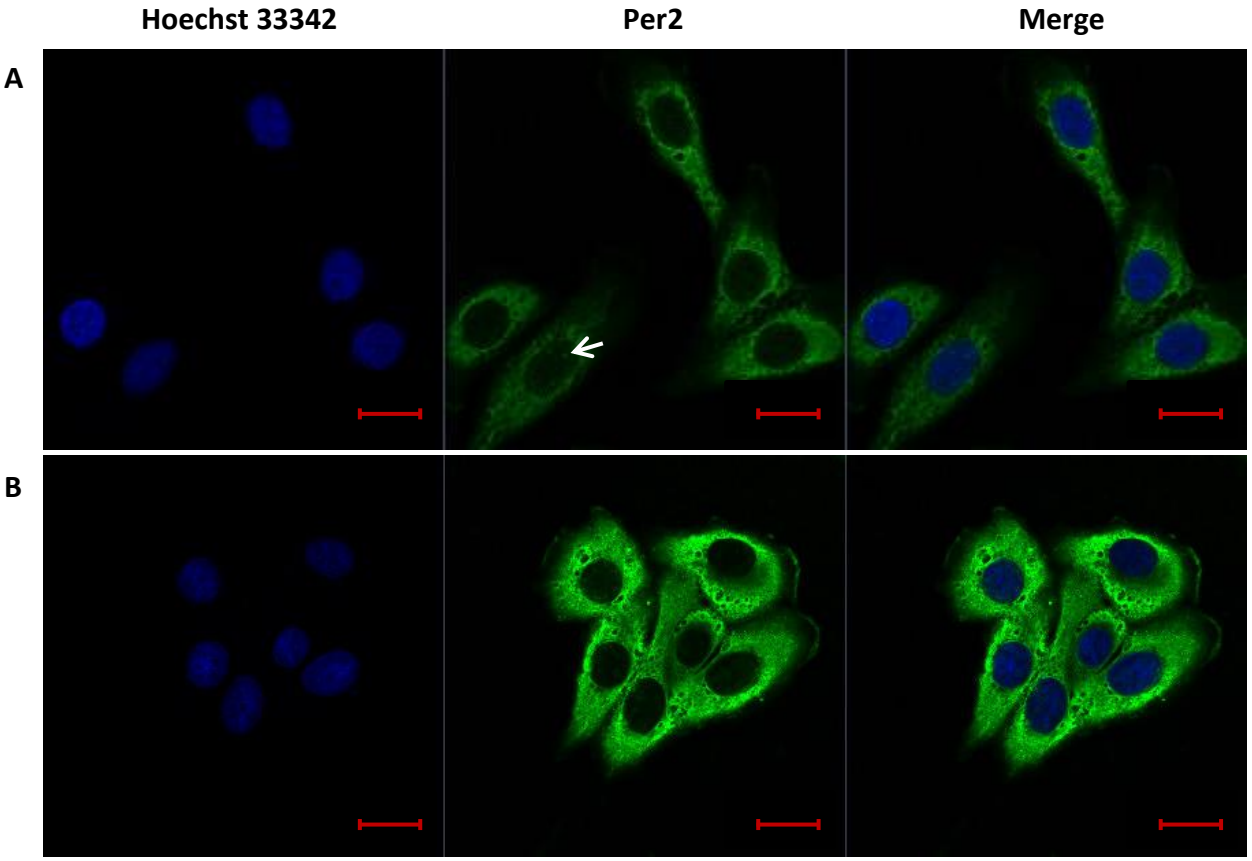

Figure 3.2: Determination of Per2 localization in MCF-12A breast epithelial cells. MCF-12A cells were cultured under standard control cellular conditions in 8-well chamber plates for a period of 24 hours. Cells were immunostained for Per2 (Green) and Hoechst 33342 (Blue) and visualized using fluorescent confocal microscopy. White arrows indicate nuclear localization of Per2. **(A)** 63x and **(B)** 63x magnification.

In the MCF-12A breast epithelial cells Per2 was seen to be localized predominantly within the cytoplasm, with only slight co-localization in the nucleus (**Figure 3.2**). In the MDA-MB-231 cancer cells Per2 also localized mainly in the cytoplasm of the cell however; nuclear co-localization was more prominent (**Figure 3.3**).

In both cell lines two distinct populations of Per2 fluorescent intense cells were seen, a dim population (**Figures 3.2A and 3.3A**) as well as a brighter more fluorescently intense population (**Figures 3.2B and 3.3B**). In both cell lines it was noted that Per2 nuclear localization was limited to the fluorescently dimmer subpopulation of cells.

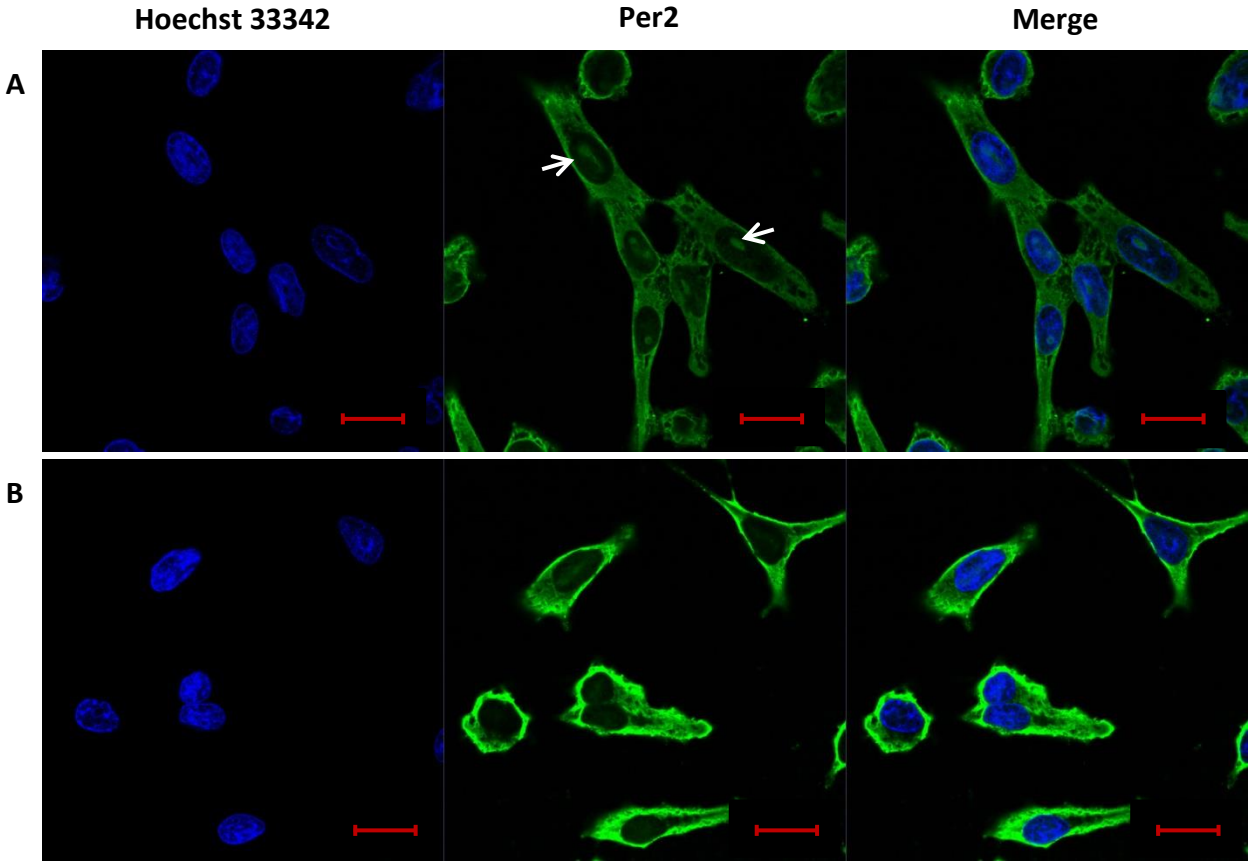

Figure 3.3: Determination of Per2 localization in MDA-MB-231 triple negative breast cancer cells. MDA-MB-231 cells were cultured under standard control cellular conditions in 8-well chamber plates or a period of 24 hours. Cells were immunostained for Per2 (Green) and Hoechst 33342 (Blue) and visualized using fluorescent confocal microscopy. White arrows indicate nuclear localization of Per2. **(A)** 63x and **(B)** 63x magnification.

3.1.3. Doxorubicin Dose Response

In order to establish a clinically relevant dose of doxorubicin that is still able to produce a significant amount of cell death in the resistant MDA-MB-231 cancer cells, both cell lines were treated with various concentrations of doxorubicin for a period of 24 hours. MTT cell viability assays were carried out to determine the relative percentage cell death in each cell line.

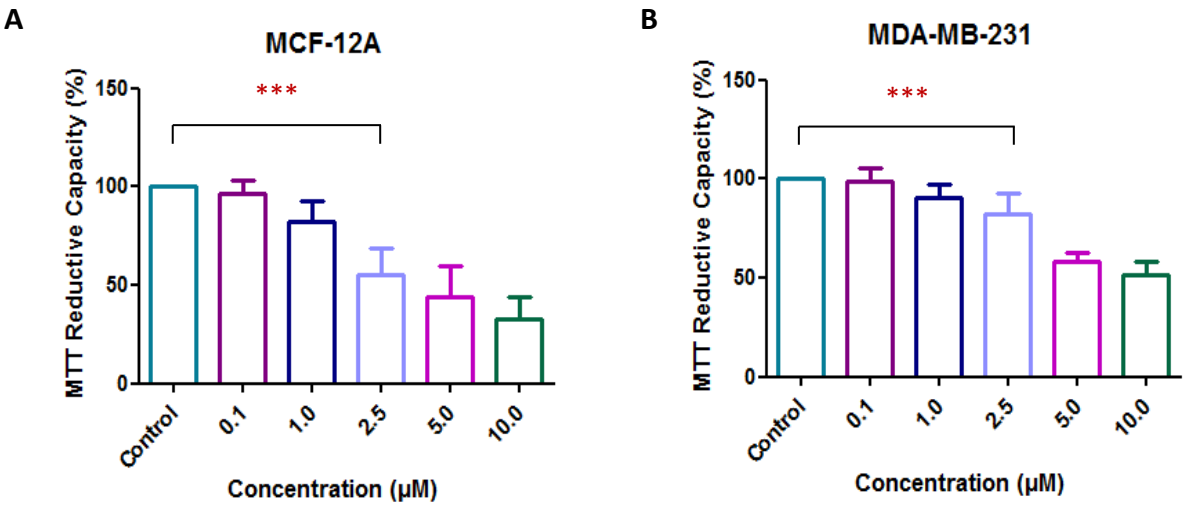

Figure 3.4: The effect of various concentrations of Doxorubicin on the viability of non-tumourigenic breast epithelial MCF-12A cells (A) and triple negative breast cancer cells MDA-MB-231 (B). MCF-12A and MDA-MB-231 cells were incubated in 0 (Control), 0.1, 2.5, 5.0 and 10.0 μM doxorubicin for 24 hours. Cell viability was assessed using the MTT assay. Values are expressed as a percentage of the control and presented as mean ± SEM (n=3). *** = P<0.0001 vs control.

When compared to control, 0.1 μM doxorubicin did not result in a decrease in the MTT reductive capacity of normal MCF-12A cells (96.14 ± 1.979% vs 100%) (**Figure 3.4A**), however when subjected to either 1.0, 2.5, 5.0, or 10.0 μM of doxorubicin for a period of 24 hours a significant reduction in MTT reductive capacity was observed when compared to control (1.0 μM: 82.38 ± 3.464% vs 100%, p<0.005. 2.5 μM: 55.41 ± 3.133% vs 100%, p<0.0001. 5.0 μM: 44.20 ± 5.302% vs 100%, p<0.0001 and 10.0 μM: 32.62 ± 3.861% vs 100%, p<0.0001).

No significant reduction in the ability of doxorubicin to reduced MTT was seen when MDA-MB-231 cancer cells were treated with either 0.1 or 1.0 μM of doxorubicin over 24 hours (**Figure 3.4B**) However, a significant decrease in MTT reductive capacity was seen in the MDA-MB-231 cancer cells following 2.5 μM doxorubicin treatment after 24 hours when compared to control (82.04 ± 2.959% vs 100%, p<0.0001). A further reduction in the MTT reductive capacity of doxorubicin in these cells was seen after treatment with 5.0 μM (58.27 ± 1.609% vs 100%, p<0.0001) and 10.0 μM (51.20 ± 2.378% vs 100%, p<0.0001) of doxorubicin when compared to control.

Clinically the administration of doxorubicin involves the intravenous bolus infusion of doses ranging between 15 and 90 mg/m^2, which results in plasma concentrations ranging from 0.3 – 5 µM (Gewirtz, 1999). Our results demonstrated that 24 hour treatment with 5 µM of doxorubicin resulted in a significant reduction in the cell viability of the chemo-resistant MDA-MB-231 cancer cells, but as this concentration falls at the extreme limit of the clinically relevant dose range, we aimed to use a lower dose which still falls within this clinically relevant range. Based on these results as well as the fact that 2.5 µM falls within the range of clinically relevant dosages for doxorubicin, for this study we used 2.5 µM for all subsequent doxorubicin treatments.

3.2. The Role of Per2 in Doxorubicin Induced Cell Death

Gene silencing with the use of small interfering RNA (siRNA) sequences has become a popular model widely used in breast cancer research, as it allows for the accurate determination of the role that specific proteins play in disease pathology. Therefore, for the initial part of this study we made use of an endoribonuclease-prepared siRNA (esiRNA) targeted specifically against Per2, to effectively silence its expression prior to treatment with doxorubicin in order to determine whether Per2 inhibition can sensitize chemo-resistant MDA-MB-231 cancer cells to doxorubicin treatment, esiRNA against Per2 was utilized in combination with doxorubicin.

3.2.1. Verification of Per2 Silencing

Per2 silencing was confirmed with the use of western blotting, after both MCF-12A and MDA-MB-231 cells were treated with 30 nM of esiRNA targeted against Per2 for a period of 48 hours.

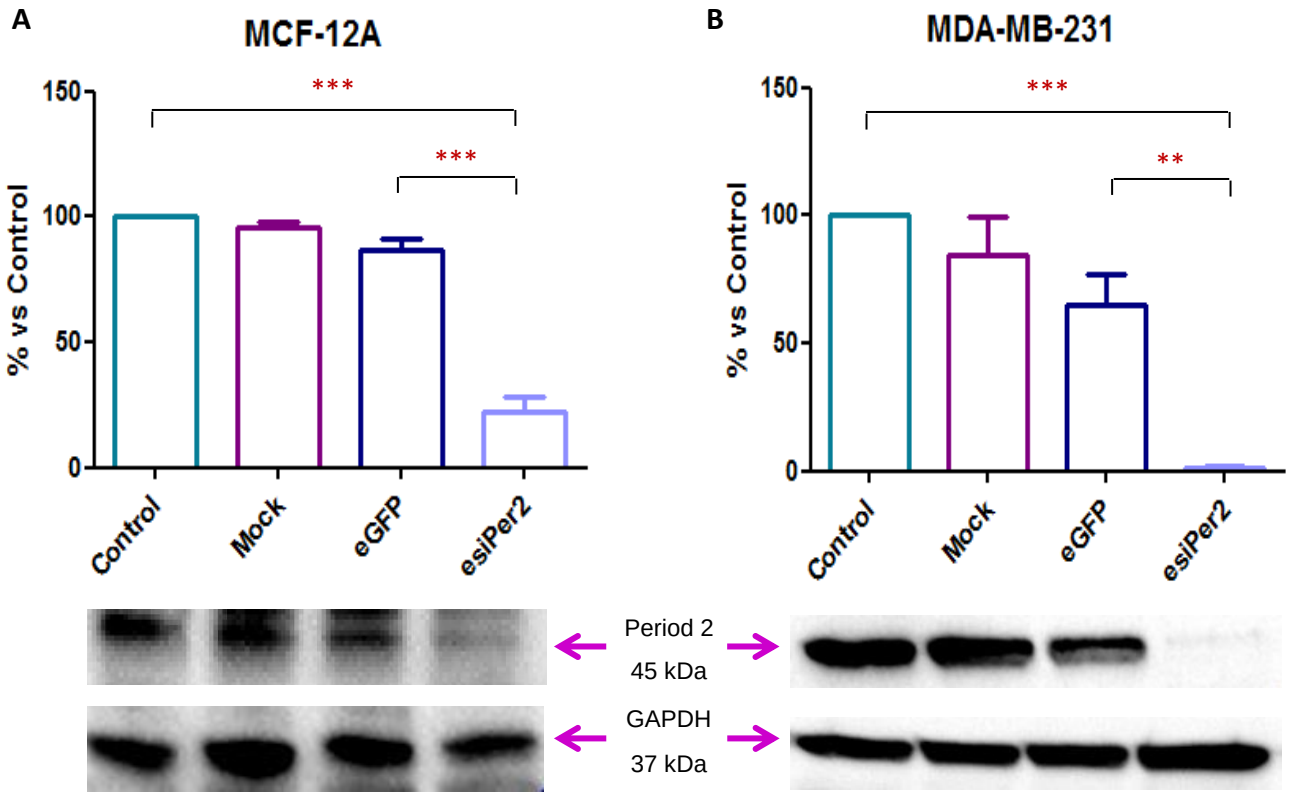

Figure 3.5: Verification of the silencing of Per2 in non-tumourigenic breast epithelial MCF-12A cells (A) and triple negative breast cancer cells MDA-MB-231 (B). MCF-12A and MDA-MB-231 cells were incubated under Control, 12 µl HiPerfect transfection reagent (Mock), 30 nM negative esiRNA control (eGFP), or 30 nM Per2 esiRNA conditions for 48 hours. Western blotting analysis was carried out to determine Per2 protein expression levels. Values are expressed as a percentage of the control and presented as mean ± SEM (n=3). *** = $p<0.0001$ vs control, ** = $p<0.001$ vs negative (eGFP) control.

The MCF-12A breast epithelial cells showed a significant reduction in Per2 protein expression levels following 48 hours of 30 nM esiRNA treatment when compared to both control (22.05 ± 6.064% vs 100%, $p<0.0001$), and the negative esiRNA control cells (22.05 ± 6.064% vs 86.68 ± 4.790%, $p<0.0001$), indicating a 77.95% silencing efficiency in the MCF-12A cells (**Figure 3.5A**). A significant reduction in Per2 protein expression was also seen following 30 nM esiRNA treatment in the MDA-MB-231 cancer cells when compared to control (1.501 ± 0.761% vs 100%, $p<0.0001$) as well as when compared to the negative eGFP control (1.501 ± 0.761% vs 64.89 ± 12.27%, $p<0.001$), indicating a 98.5% silencing efficiency in the MDA-MB-231 cancer cells (**Figure 3.5B**).

3.2.2. Cell Viability (Mitochondrial Reductive Capacity)

MTT cell viability assays were carried out to assess the effects of Per2 on doxorubicin induced cell death (**Figure 3.6**). MCF-12A cells showed a significant decrease in MTT reductive capacity following Per2 silencing when compared to control (61.58 ± 6.414% vs 100%, p<0.0001). Doxorubicin treatment alone resulted in a significant reduction in MTT reductive capacity when compared to control (55.37 ± 5.554% vs 100%, p<0.0001), which was further reduced following Per2 silencing prior to doxorubicin treatment (20.11 ± 1.898% vs 55.37 ± 5.554%, p<0.0001) in comparison to doxorubicin treatment alone.

In the MDA-MB-231 cancer cells a significant reduction in MTT reductive capacity was seen following doxorubicin treatment alone when compared to control (81.99 ± 3.212% vs 100%, p<0.0001). However, an even greater reduction was seen when Per2 was silenced prior to doxorubicin treatment (53.26 ± 3.057% vs 81.99 ± 3.212%, p<0.001) when compared to doxorubicin alone.

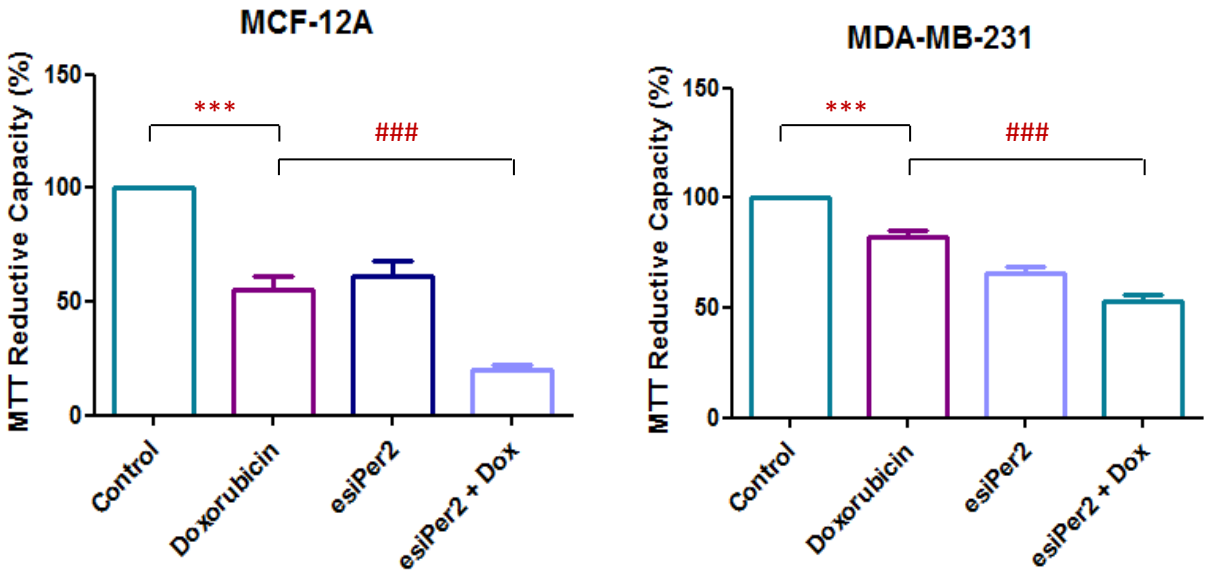

Figure 3.6: Determining the effect of Per2 silencing on the viability of non-tumorigenic breast epithelial MCF-12A cells (A) and ER$^-$ MDA-MB-231 breast cancer cells (B). MCF-12A and MDA-MB-231 cells were subjected to (1) Control conditions (C), (2) 2.5 µM Doxorubicin (D), (3) 30 nM Per2 and (P) and (4) 30 nM Per2 for 48 hours + 2.5 µM Doxorubicin for 24 hours (PD). Cell viability was assessed using the MTT assay. Values are expressed as a percentage of the control and presented as mean ± SEM (n=3). *** = p<0.0001 vs control and $^{###}$ = p<0.0001 vs doxorubicin. Abbreviations: Per2 + Dox = Period 2 + Doxorubicin.

3.2.3. Western Blot Analysis

Per2 Protein Expression

Per2 protein levels were analysed prior to western blot analysis of apoptotic markers in order to verify the effects seen are due to the silencing of Per2 (**Figure 3.7**). A significant reduction in Per2 protein expression levels was seen following Per2 silencing alone as well as in combination with doxorubicin treatment in comparison to control (Per2: 16.68 ± 5.029% vs 100%, $p<0.0001$ and Per2 + Dox: 17.76 ± 5.862% vs 100%, $p<0.0001$).

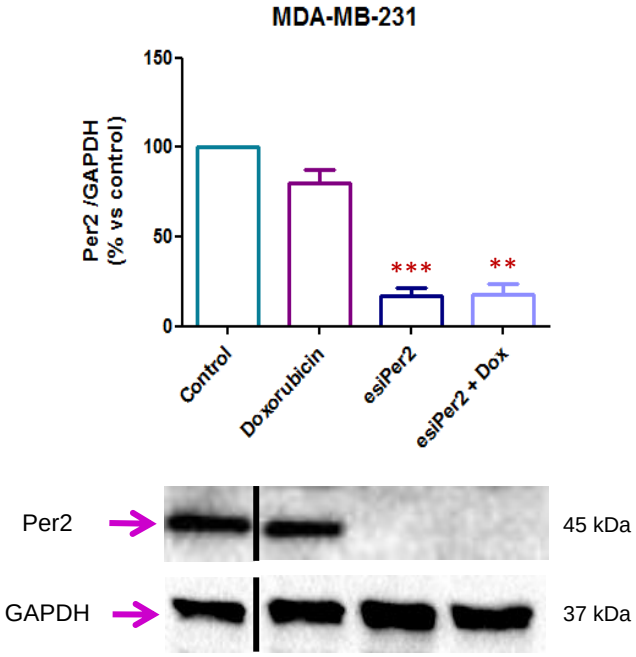

Figure 3.7: Western Blot analysis of Per2 in MDA-MB-231 breast cancer cells following Per2 silencing and doxorubicin treatment. MDA-MB-231 cells were subjected to (1) Control conditions (C), (2) 2.5 µM Doxorubicin (D), (3) 30 nM Per2 esiRNA (P) and (4) 30 nM Per2 for 48 hours + 2.5 µM Dox for 24 hours (PD). Statistical analysis: One way ANOVA with Bonferroni post hoc correction. All results are presented as mean ± SEM (n=3). ** = $p<0.001$ vs control and *** = $p<0.0001$. Abbreviations: Per2 + Dox = Period 2 + Doxorubicin.

Apoptosis was further evaluated with the use of western blotting for common markers of apoptotic cell death, namely; p-p53 (Ser^{15}) and its negative regulator p-MDM2 (Ser^{166}), cleaved Caspase-3 as well as cleaved PARP.

p-MDM2 (Ser^{166}) and p-p53 (Ser^{15}) Activity

The MDA-MB-231 breast cancer cells showed a significant increase in p-MDM2 (Ser^{166}) protein levels following Per2 silencing alone in comparison to control (1351 ± 287.5% vs 200%, p<0.05) (**Figure 3.8**). Although p-MDM2 (Ser^{166}) levels were increased following Per2 silencing in combination with doxorubicin when compared to control, they were not significant (820.6 ± 173.6% vs 200%).

A significant increase in p-p53 (Ser^{15}) protein levels was seen following doxorubicin treatment alone when compared to control (987.1 ± 92.20% vs 200%, p<0.0001) whilst Per2 silencing alone and in combination with doxorubicin had no significant effect on p-p53 (Ser^{15}) expression when compared to control (**Figure 3.8**).

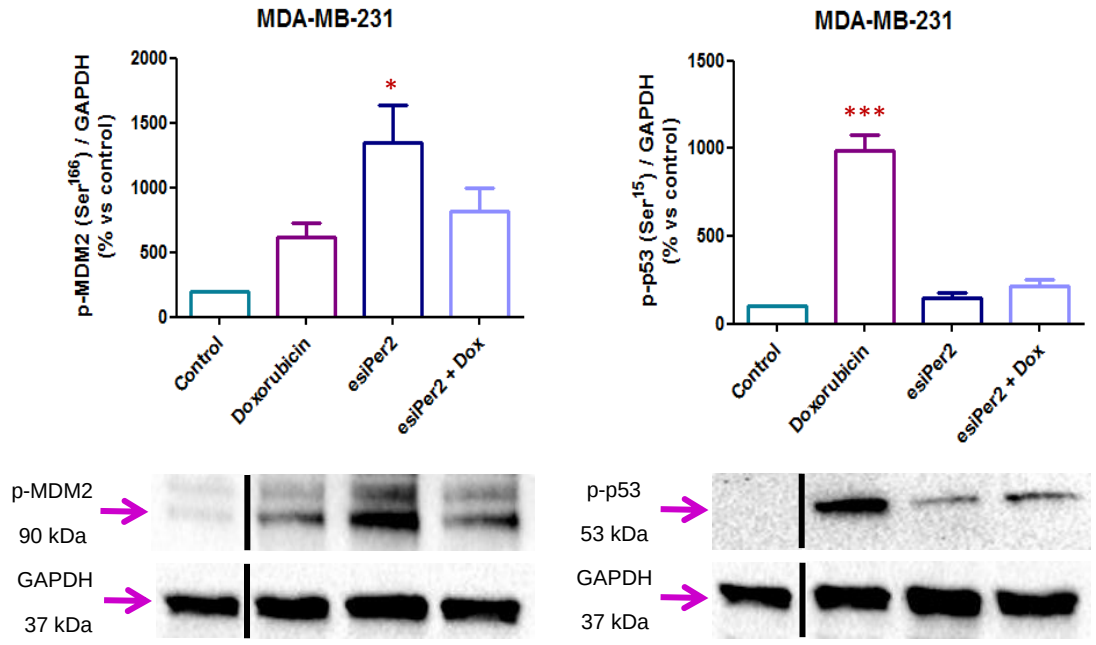

Figure 3.8: Western Blot analysis of p-MDM2 (Ser^{166}) and p-p53 (Ser^{15}) in MDA-MB-231 breast cancer cells following Per2 silencing and doxorubicin treatment. MDA-MB-231 cells were subjected to (1) Control conditions (C), (2) 2.5 µM Doxorubicin (D), (3) 30 nM Per2 esiRNA (P) and (4) 30 nM Per2 for 48 hours + 2.5 µM Dox for 24 hours (PD). Statistical analysis: One way ANOVA with Bonferroni post hoc correction. All results are presented as mean ± SEM (n=3). * = p<0.05 vs control and *** = p<0.0001 vs control. Abbreviations: Per2 + Dox = Period 2 + Doxorubicin.

Caspase-3 Cleavage

Once Caspase-3 is cleaved and activated by upstream caspases in the caspase cascade apoptotic cell death ensues. A significant increase in cleaved caspase-3 was seen following Per2 silencing alone as well as in combination with doxorubicin treatment when compared to control (Per2: 588.6 ± 105.7% vs 100%, $p<0.05$ and Per2 + Dox: 619.0 ± 111.0% vs 100%, $p<0.05$) (**Figure 3.9**).

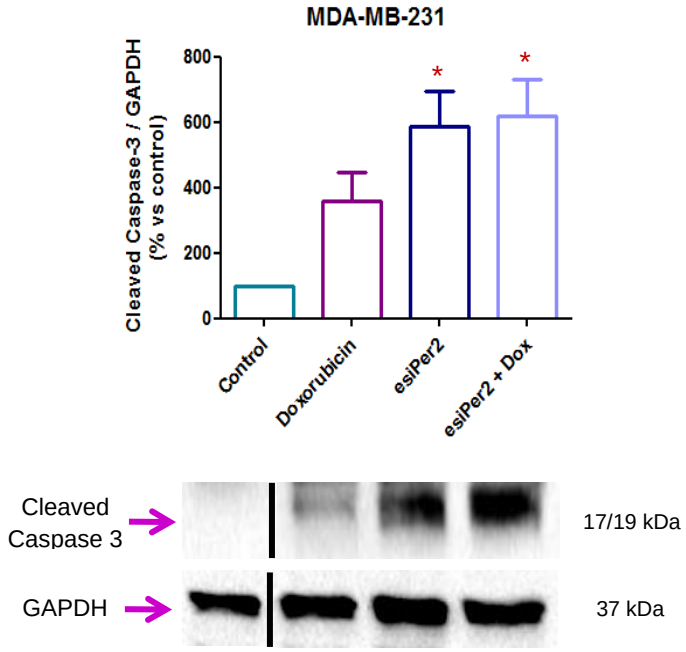

Figure 3.9: Western Blot analysis of cleaved Caspase-3 in MDA-MB-231 breast cancer cells following Per2 silencing and doxorubicin treatment. MDA-MB-231 cells were subjected to (1) Control conditions (C), (2) 2.5 µM Doxorubicin (D), (3) 30 nM Per2 esiRNA (P) and 30 nM Per2 for 48 hours + 2.5 µM Dox for 24 hours (PD). Statistical analysis: One way ANOVA with Bonferroni post hoc correction. All results are presented as mean ± SEM (n=3). * = $p<0.05$ vs control. Abbreviations: Per2 + Dox = Period 2 + Doxorubicin.

PARP - Cleavage

The MDA-MB-231 cancer cells show a significant increase in cleaved PARP levels following doxorubicin treatment (680.8 ± 43.45% vs 100%, $p<0.0001$), Per2 silencing (713.7 ± 64.57% vs 100%, $p<0.0001$), as well as the combination of Per2 silencing prior to doxorubicin treatment when compared to control (644.1 ± 39.18% vs 100%, $p<0.0001$) (**Figure 3.10**).

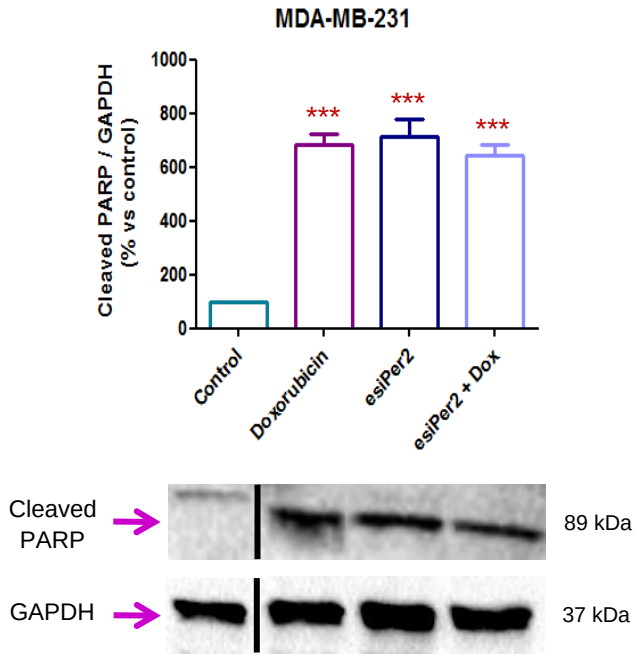

Figure 3.10: Western Blot analysis of cleaved PARP in MDA-MB-231 breast cancer cells following Per2 silencing and doxorubicin treatment. MDA-MB-231 cells were subjected to (1) Control conditions (C), (2) 2.5 µM Doxorubicin (D), (3) 30 nM Per2 esiRNA (P) and 30 nM Per2 for 48 hours + 2.5 µM Dox for 24 hours (PD). Statistical analysis: One way ANOVA with Bonferroni post hoc correction. All results are presented as mean ± SEM (n=3). *** = p<0.0001 vs control. Abbreviations: Per2 + Dox = Period 2 + Doxorubicin.

3.2.4. Flow Cytometry – Hoechst and PI

Cell death was further assessed by means of flow cytometry, in order to fully elucidate the role of Per2 in doxorubicin induced cell death in MDA-MB-231 breast cancer cells.

Doxorubicin treatment alone resulted in an increase in the percentage of cell death when compared to control (9.733 ± 0.5548% vs 7.850 ± 0.2598%, $p<0.05$) however, no significant reduction was seen in the percentage of the live cell population (**Figure 3.11**). Per2 silencing resulted in a significant reduction in the percentage of live cells (67.80 ± 7.448% vs 90.10 ± 1.484%, $p<0.05$) with a concomitant increase in the percentage of dead cells in comparison to control (31.80 ± 7.275% vs 7.850 ± 0.2598%, $p<0.05$). The combination of Per2 silencing and doxorubicin treatment resulted in a significant increase in the dead cell population (35.90 ± 0.8660% vs 7.850 ± 0.2598%, $p<0.0001$)

oand significantly decreased the live cell population when compared to control (63.70 ± 0.9238% vs 90.10 ± 1.484%, p<0.0001).

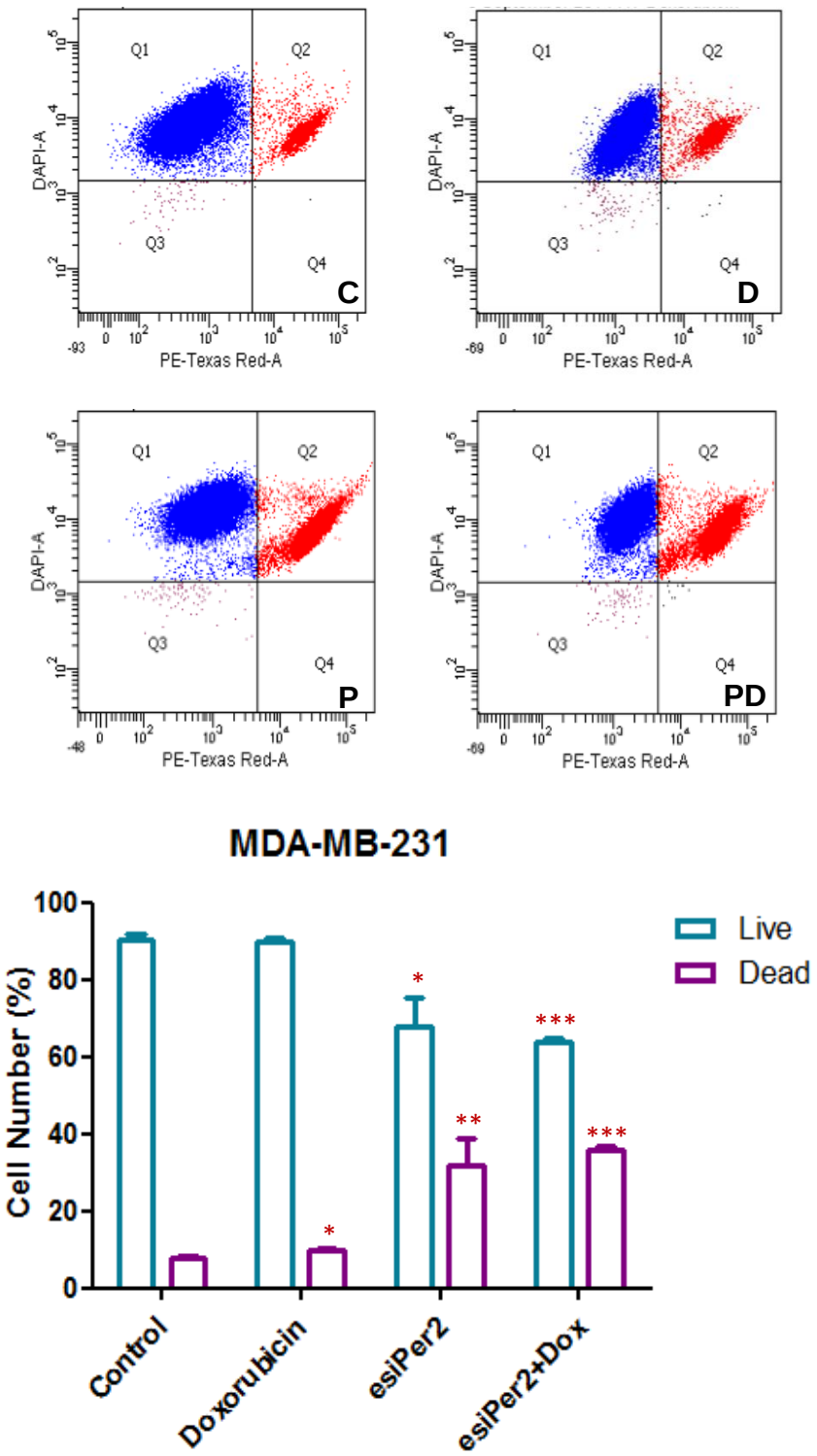

Figure 3.11: The effects of Per2 silencing in doxorubicin induced cell death of MDA-MB-231 breast cancer cells. MDA-MB-231 cells were subjected to (1) Control conditions (C), (2) 2.5 µM Doxorubicin (D) (3) 30 nM Per2 esiRNA (P) and (4) 30 nM Per2 for 48 hours + 2.5 µM Dox treatment for 24 hours (PD). G2/M transition analysis was assessed by flow cytometry. Statistical analysis: One way ANOVA with Bonferroni post hoc correction. All results are presented as mean ± SEM (n=3). * = p<0.05 vs control ** = p<0.001 vs control and *** = p<0.001 vs control. Abbreviations: Per2 + Dox = Period 2 + Doxorubicin.

3.2.5. Cell cycle progression following Per2 silencing in MDA-MB-231 breast cancer cells

As cell cycle regulation is thought to be under the control of circadian genes, cell cycle analysis using flow cytometry was assessed to determine the effects of Per2 silencing on cell cycle progression in the MDA-MB-231 cancer cells.

Silencing of Per2 in the MDA-MB-231 cancer cells resulted in a significant increase in the percentage of cells in the G0/G1 phase of the cell cycle (68.77 ± 4.901% vs 52.42 ± 0.5762%, $p<0.05$), with a concomitant decrease in the G2/M phase (5.520 ± 1.201% vs 13.88 ± 0.5505%, $p<0.001$) and significant increase in apoptosis when compared to control (16.97 ± 5.260% vs 0.070 ± 0.070%, $p<0.05$) (**Figure 3.12**). A significant increase in the percentage of cells in the G2/M phase of the cell cycle was seen following doxorubicin treatment alone in comparison to control (37.38 ± 7.341% vs 13.88 ± 0.5505%, $p<0.05$) with significantly increased levels of apoptosis (13.58 ± 4.252% vs 0.070 ± 0.070%, $p<0.05$). The combination of Per2 silencing prior to doxorubicin treatment resulted in S phase cell cycle arrest (50.84 ± 2.439% vs 33.70 ± 0.6445%, $p<0.001$), and a significant decrease in G2/M (2.200 ± 1.270% vs 13.88 ± 0.5505%, $p<0.001$). A significantly greater level of apoptosis was also seen with the silencing of Per2 prior to doxorubicin treatment when compared to control (24.68 ± 3.513% vs 0.070 ± 0.070%, $p<0.001$).

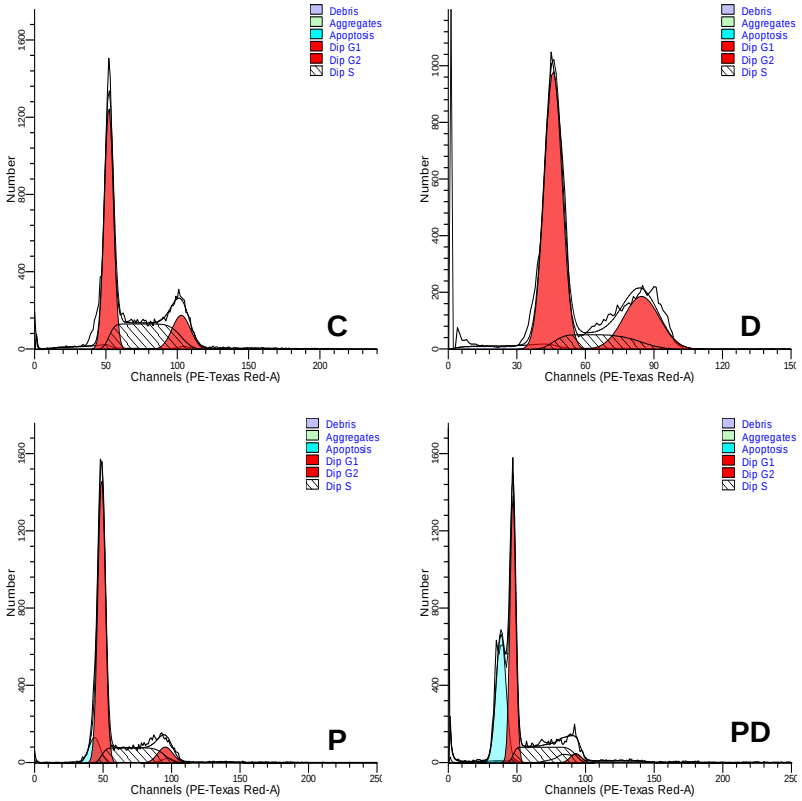

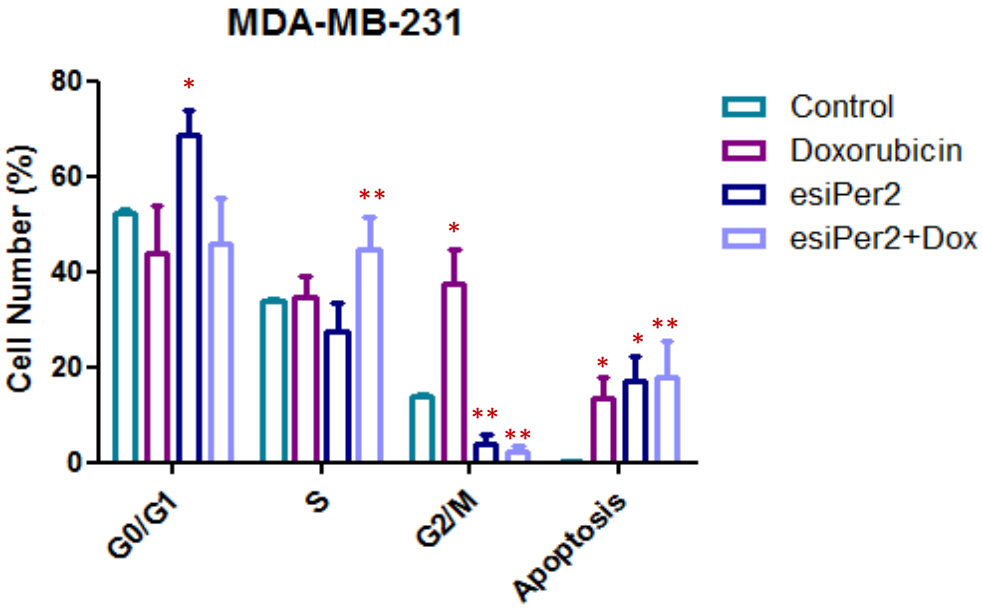

Figure 3.12: Analysis of cell cycle progression in MDA-MB-231 breast cancer cells following Per2 silencing and doxorubicin treatment. MDA-MB-231 cells were subjected to (1) Control conditions (C), (2) 2.5 µM Doxorubicin (D) (3) 30 nM Per2 esiRNA (P), and (4) 30 nM Per2 for 48 hours + 2.5 µM Dox for 24 hours (PD). Cell cycle analysis was assessed following propidium iodide staining by flow cytometry. Statistical analysis: One way ANOVA with Bonferroni post hoc correction. All results are presented as mean ± SEM (n=3). * = $p<0.05$ vs control and ** = $p<0.001$ vs control. Abbreviations: Per2 + Dox = Period 2 + Doxorubicin.

3.2.6. Modulation of G2/M cell cycle transition following Per2 silencing in MDA-MB-231 breast cancer cells

G2/M transition was analysed by means of flow cytometry using conjugated primary antibodies against phosphorylated Histone H3 (Ser^{10}) and phosphorylated Aurora A (Thr^{288}) / Aurora B (Thr^{232}) / Aurora C (Thr^{198}), in order to distinguish between cells in interphase, early mitosis and late mitosis. A significant increase in the interphase cell population was seen following doxorubicin treatment (98.70 ± 0.500% vs 36.30 ± 7.600%, $p<0.0001$), as well as a shift from mitosis as is evident from a significant decrease in p-Aurora levels in comparison to control (1.200 ± 0.400% vs 61.25 ± 6.850%, $p<0.0001$) (**Figure 3.13**). Treatment of MDA-MB-231 cells with doxorubicin resulted in a complete inhibition of the mitotic process when compared to control (0.000 ± 0.000% vs 2.350 ± 0.6500%, $p<0.001$). Per2 silencing resulted in a shift in cells from early mitosis evident by a decrease in p-Aurora (6.567 ± 2.484% vs 61.25 ± 6.850%, $p<0.0001$) and an increase in interphase when compared to control (92.77 ± 2.657% vs 36.30 ± 7.600%, $p<0.0001$). A significant decrease in mitosis was also seen following Per2 silencing in the MDA-MB-231breast cancer cells in comparison to control cells (0.3333 ± 0.2082 % vs 2.350 ± 0.6500%, $p<0.05$). The silencing of Per2 prior to doxorubicin treatment appears to have a profoundly negative effect on the MDA-MD-231 cells, as a significant reduction was seen in the both p-Aurora and mitotic cell populations in comparison to control (p-Aurora: 1.333 ± 0.5696% vs 61.25 ± 6.850%, $p<0.0001$ and mitosis: 0.0667 ± 0.0667% vs 2.350 ± 0.6500, $p<0.001$). However, a significant increase in the interphase population can be seen when compared to control (98.50 ± 0.5132% vs 36.30 ± 7.600%, $p<0.0001$).

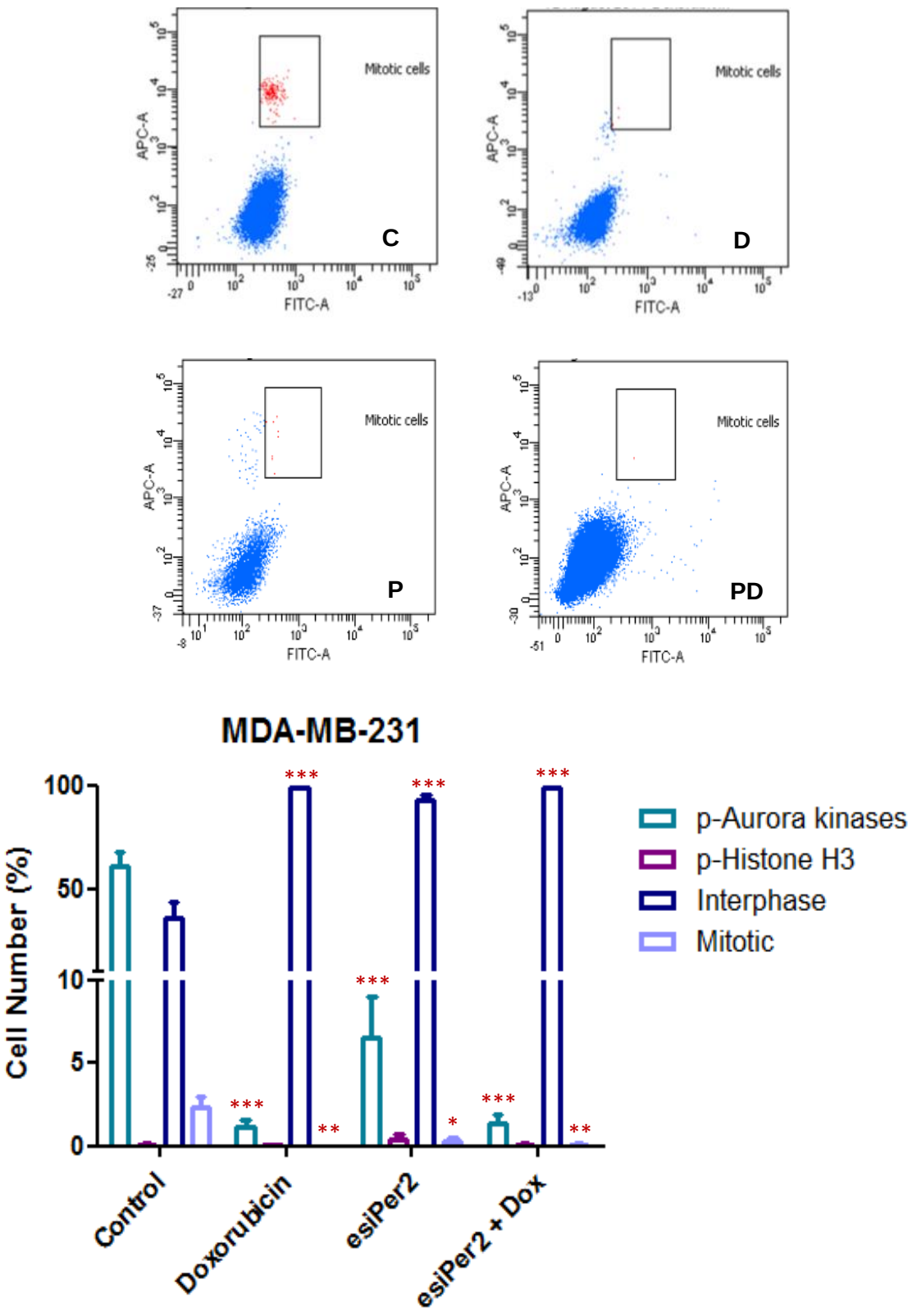

Figure 3.13: Determination of G2/M cell cycle transition in MDA-MB-231 breast cancer cells following Per2 silencing and doxorubicin treatment. MDA-MB-231 cells were subjected to (1) Control conditions (C), (2) 2.5 µM Doxorubicin (D) (3) 30 nM Per2 esiRNA (P) and (4) 30 nM Per2 for 48 hours + 2.5 µM Doxorubicin for 24 hours (PD). G2/M transition analysis was assessed by flow cytometry. Statistical analysis: One way ANOVA with Bonferroni post hoc correction. All results are presented as mean ± SEM (n=3). * = $p<0.05$ vs control ** = $p<0.001$ vs control and *** = $p<0.0001$ vs control. Abbreviations: Per2 + Dox = Period 2 + Doxorubicin.

3.3. The Role of Per2 in Autophagy

In order to determine the role of Per2 in autophagy, Per2 was silenced using an esiRNA targeted against Per2 prior to treatment with Bafilomycin A1, a known inhibitor of autophagy.

3.3.1. Cell Viability (Mitochondrial Reductive Capacity)

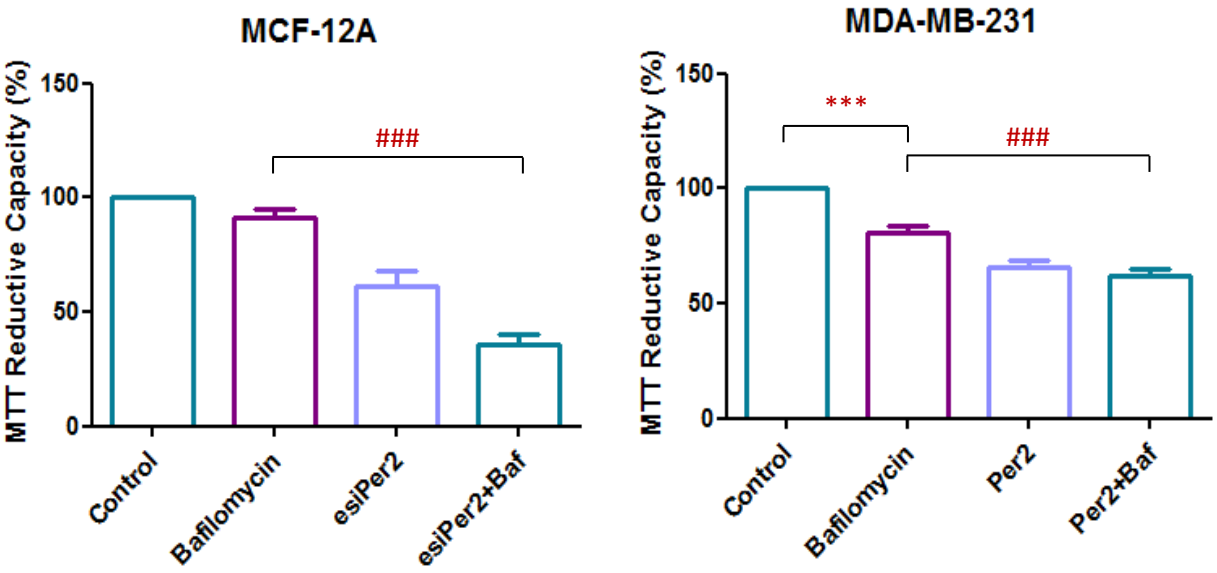

Figure 3.14: Determining the effect of Per2 silencing on the viability of non-tumorigenic breast epithelial MCF-12A cells and the ER$^-$ MDA-MB-231 breast cancer cells. MCF-12A and MDA-MB-231 cells were subjected to (1) Control conditions (C), (2) 10 nM Bafilomycin (B), (3) 30 nM Per2 esiRNA (P) and (4) 30 nM Per2 for 48 hours + 10 nM Bafilomycin for 8 hours (PB). Cell viability was assessed using the MTT assay. Values are expressed as a percentage of the control and presented as mean ± SEM (n=3). *** = p<0.0001 vs control and $^{###}$ = p<0.0001 vs Bafilomycin. Abbreviations: Per2 + Baf = Period 2 + Bafilomycin.

To gain a better understanding of Per2 and its role in cell death as well as the mechanisms involved, autophagic cell death was also assessed. MTT cell viability assays were initially carried out in order to determine the effects of Per2 silencing and bafilomycin treatment (**Figure 3.14**). MCF-12A cells showed no significant decrease in MTT reductive capacity following bafilomycin A1 treatment alone when compared to control (90.88 ± 4.121% vs 100%). Per2 silencing alone resulted in a significant reduction in MCF-12A reductive capacity (61.58 ± 6.414% vs 100%, p<0.0001), which

was further reduced with the addition of bafilomycin treatment in conjunction with Per2 silencing in comparison to bafilomycin treatment alone (35.71 ± 4.543% vs 90.88 ± 4.121%, $p<0.0001$). The MDA-MB-231 breast cancer cells showed a significant reduction in MTT reductive capacity following Per2 silencing when compared to control (65.64 ± 3.225% vs 100%, $p<0.0001$). A significant reduction in MTT reductive capacity was also seen following bafilomycin treatment alone in comparison to control cells (81.04 ± 2.645% vs 100%, $p<0.0001$). When compared to bafilomycin, a further reduction in MTT reductive capacity was seen following Per2 silencing prior to bafilomycin treatment (62.19 ± 3.098% vs 81.04 ± 2.645%, $p<0.0001$).

3.3.2. Western Blot Analysis

To provide further insight into the effect of Per2 silencing on the autophagic process, western blot analysis was carried out on MDA-MB-231 breast cancer cells using recognised markers of autophagy, namely; AMPK, mTOR and LC3.

Per2 and AMPK

Prior to the analysis of autophagic markers, Per2 silencing was again confirmed in order to ensure the effects seen are as a result of the absence of Per2 protein expression. A significant reduction in Per2 protein expression (**Figure 3.15**) was seen following Per2 silencing alone (17.77 ± 5.931% vs 100%, $p<0.0001$) as well as in combination with bafilomycin A1 treatment when compared to control (11.53 ± 5.593% vs 100%, $p<0.0001$). A significant increase in AMPKα protein expression was seen with Per2 silencing (857.5 ± 213.2% vs 100%, $p<0.001$). Although AMPKα protein expression was increased with the silencing of Per2 in combination with bafilomycin treatment, results were not statistically significant (413.8 ± 93.18% vs 100%) (**Figure 3.15**).

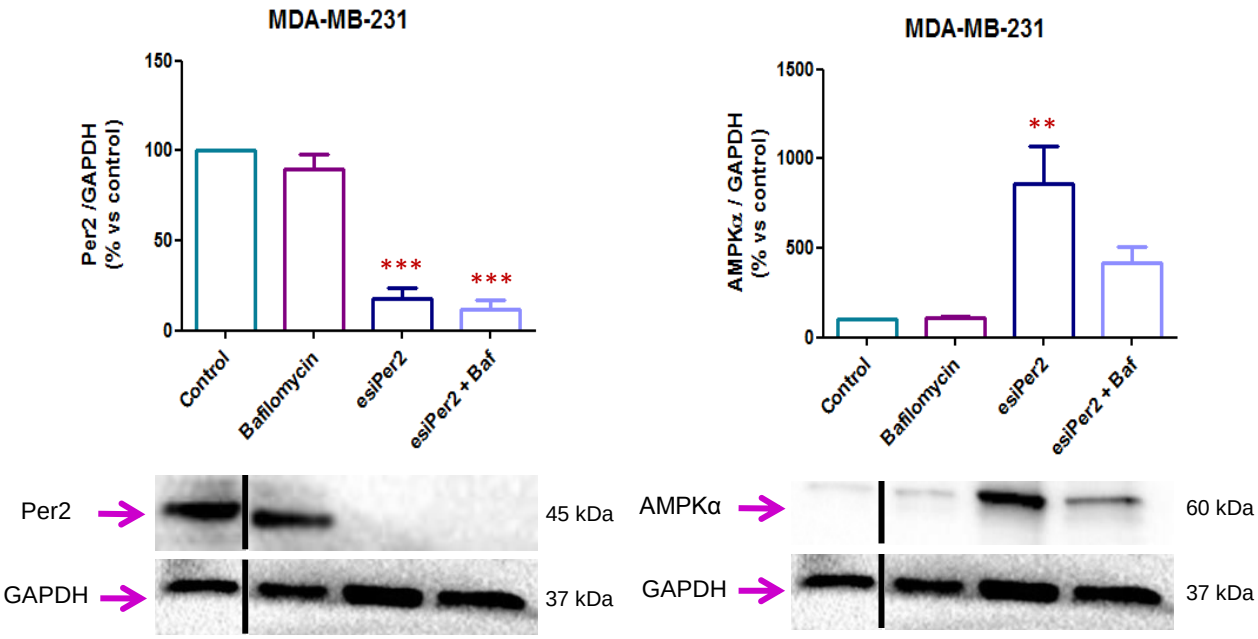

Figure 3.15: Western Blot analysis of Per2 and AMPKα in MDA-MB-231 breast cancer cells following Per2 silencing and bafilomycin A1 treatment. MDA-MB-231 cells were subjected to (1) Control conditions (C), (2) 10 nM Bafilomycin (B), (3) 30 nM Per2 esiRNA (P) and (4) 30 nM Per2 for 48 hours + 10 nM Baf for 8 hours (PB). Statistical analysis: One way ANOVA with Bonferroni post hoc correction. All results are presented as mean ± SEM (n=3). ** = $p<0.001$ vs control and *** = $p<0.0001$. Abbreviations: Per2 + Baf = Period 2 + Bafilomycin.

mTOR (Ser^{2448}) Phosphorylation

mTOR (Ser^{2448}) phosphorylation was significantly higher following Per2 silencing alone in comparison to the control (1053 ± 70.95% vs 100%, $p<0.0001$). Per2 silencing in combination with bafilomycin resulted in a significant increase in mTOR (Ser^{2448}) phosphorylation when compared to control (467.7 ± 92.66% vs 100%, $p<0.001$) however, to a much lesser extent than seen with Per2 silencing alone (**Figure 3.16**).

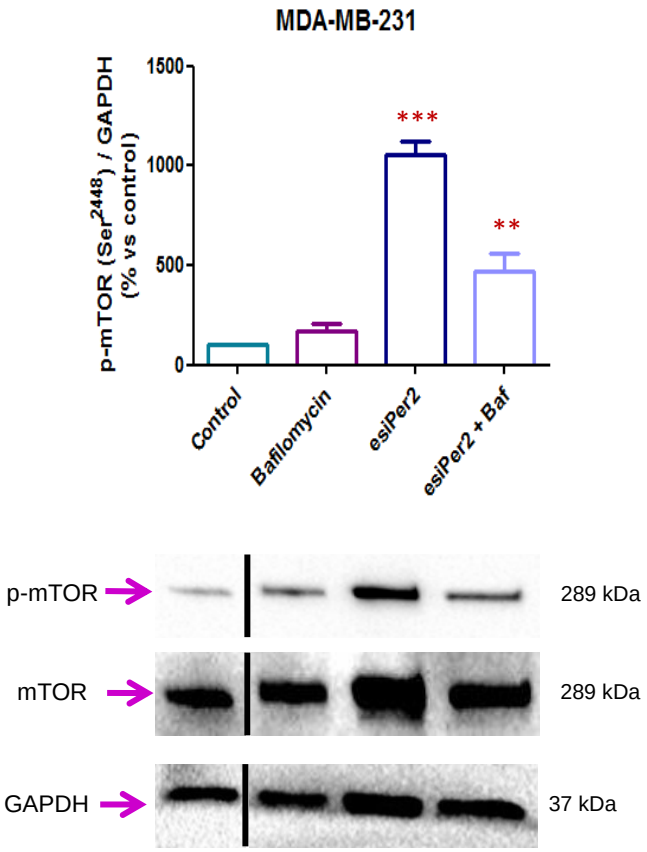

Figure 3.16: Western Blot analysis of p-mTOR (Ser^{2448}) in MDA-MB-231 breast cancer cells following Per2 silencing and bafilomycin A1 treatment. MDA-MB-231 cells were subjected to (1) Control conditions (C), (2) 10 nM Bafilomycin (B), (3) 30 nM Per2 esiRNA (P) and (4) 30 nM Per2 for 48 hours + 10 nM Baf for 8 hours (PB). Statistical analysis: One way ANOVA with Bonferroni post hoc correction. All results are presented as mean ± SEM (n=3). ** = p<0.001 vs control and *** = p<0.0001. Abbreviations: Per2 + Baf = Period 2 + Bafilomycin.

LC3

Examination of LC3 II expression revealed a significant increase in protein levels with bafilomycin treatment (1181 ± 164.4% vs 100%, p<0.05). An increase in both LC3 I and LC3 II expression was seen when Per2 was silenced however, LC3 II expression was not significant in comparison to the control (718.3 ± 83.96% vs 100%). Silencing of Per2 in combination with bafilomycin lead to a significantly greater accumulation of LC3 II in comparison to control (2164 ± 365.3% vs 100%, p<0.0001) (**Figure 3.17**).

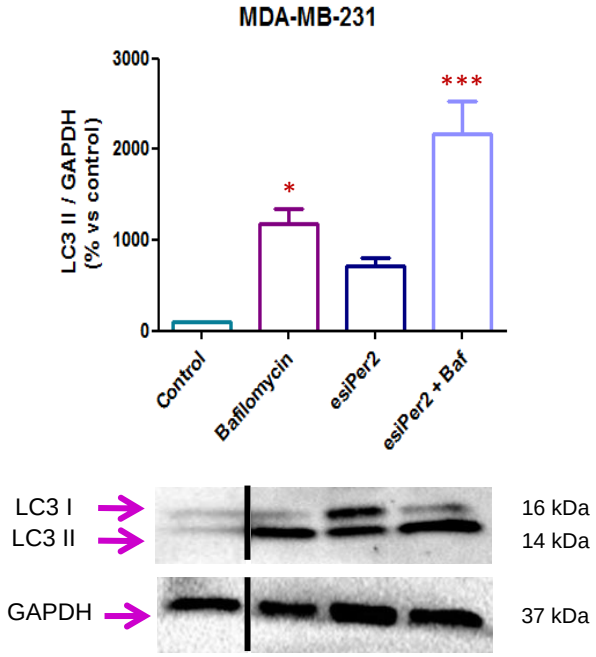

Figure 3.17: Western Blot analysis of LC3 II in MDA-MB-231 breast cancer cells following Per2 silencing and bafilomycin A1 treatment. MDA-MB-231 cells were subjected to (1) Control conditions (C), (2) 10 nM Bafilomycin (B), (3) 30 nM Per2 esiRNA (P) and (4) 30 nM Per2 for 48 hours + 10 nM Baf for 8 hours (PB). Statistical analysis: One way ANOVA with Bonferroni post hoc correction. All results are presented as mean ± SEM (n=3). * = $p<0.05$ vs control and *** = $p<0.0001$. Abbreviations: Per2 + Baf = Period 2 + Bafilomycin.

3.3.3. Flow Cytometry – Hoechst and PI

Cell death was also assessed by staining cells with Hoechst 33342 and propidium iodide analysed with flow cytometry. A significant increase in cell death (31.80 ± 7.275% vs 7.850 ± 0.2598%, $p<0.001$) and reciprocal decrease in the live cell population (67.80 ± 7.448% vs 90.10 ± 1.484%, $p<0.05$) was seen with Per2 silencing alone when compared to the control (**Figure 3.18**). The silencing of Per2 in combination with bafilomycin treatment in the MDA-MB-231 breast cancer cells resulted in an even greater percentage of cell death (60.40 ± 2.021% vs 7.850 ± 0.2598%, $p<0.0001$) and less live cells in comparison to control (39.00 ± 1.848% vs 90.10 ± 1.484%, $p<0.0001$).

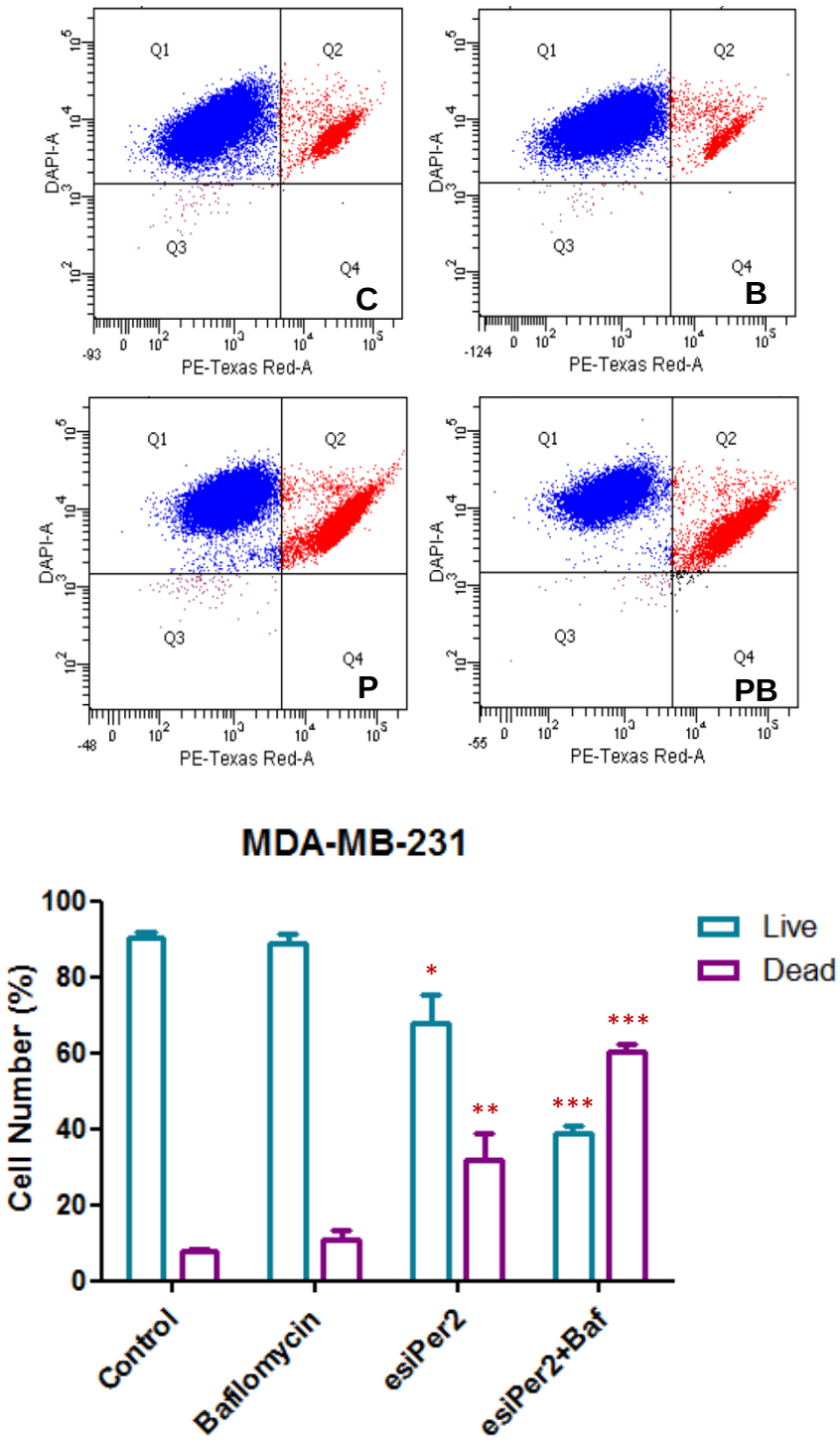

Figure 3.18: The effects of Per2 silencing on cell death in MDA-MB-231 breast cancer cells. MDA-MB-231 cells were subjected to (1) Control conditions (C), (2) 10 nM Bafilomycin (B) (3) 30 nM Per2 esiRNA (P), and (4) 30 nM Per2 for 48 hours + 10 nM Baf for 8 hours (PB). Cell death was assessed by flow cytometry. Statistical analysis: One way ANOVA with Bonferroni post hoc correction. All results are presented as mean ± SEM (n=3). * = $p<0.05$ vs control ** = $p<0.001$ vs control and *** = $p<0.001$ vs control. Abbreviations: Per2 + Dox = Period 2 + Doxorubicin.

3.3.4. Flow Cytometry – Cell Cycle Analysis

Cell cycle analysis demonstrated a significant increase in G0/G1 cell cycle arrest following individual treatments with bafilomycin and Per2 silencing as well as the combination of Per2 silencing prior to bafilomycin treatment when compared to control (baf: 72.30 ± 3.567% vs 52.42 ± 0.5762%, $p<0.001$. Per2: 68.77 ± 4.901% vs 52.42 ± 0.5762%, $p<0.05$ and Per2 + baf: 77.03 ± 5.886% vs 52.42 ± 0.5762%, $p<0.05$). A significant decrease in the G2/M cell cycle phase was seen across all treatment groups when compared to control (baf: 4.035 ± 2.042% vs 13.88 ± 0.5505%, $p<0.001$. Per2: 3.680 ± 2.197% vs 13.88 ± 0.5505%, $p<0.05$ and Per2 + baf: 3.273 ± 0.9184% vs 13.88 ± 0.5505%, $p<0.0001$). Additionally, a concomitant increase in apoptosis was seen for all treatments in comparison to control cells (baf: 20.66 ± 0.6784% vs 0.0700 ± 0.0700%, $p<0.05$. Per2: 21.43 ± 2.797% vs 0.0700 ± 0.0700%, $p<0.05$ and Per2 + baf: 23.26 ± 3.279% vs 0.0700 ± 0.0700%, $p<0.05$) (**Figure 3.19**).

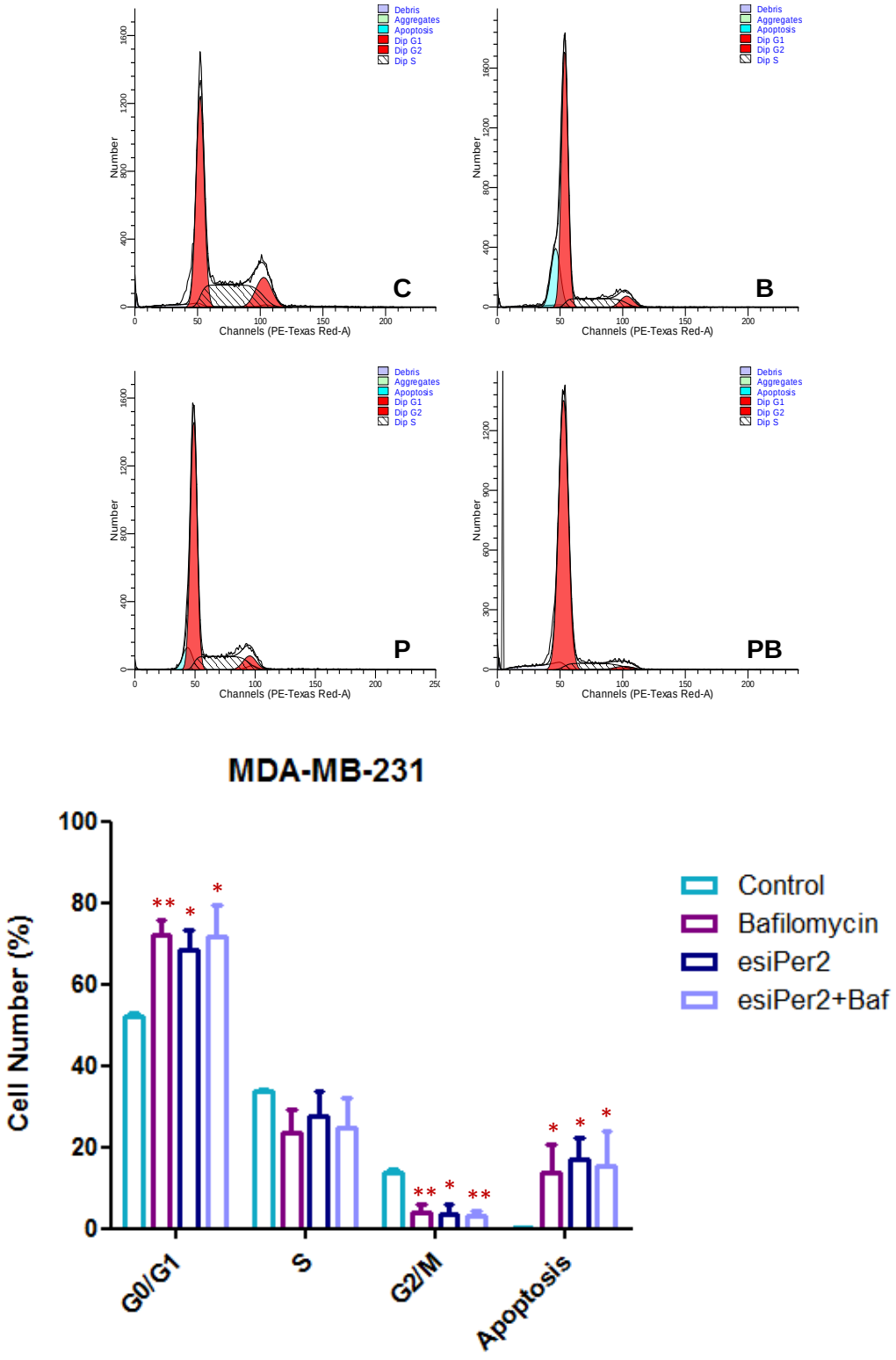

Figure 3.19: Analysis of cell cycle progression in MDA-MB-231 breast cancer cells following Per2 silencing and bafilomycin treatment. MDA-MB-231 cells were subjected to (1) Control conditions (C), (2) 10 nM Bafilomycin (B) (3) 30 nM Per2 esiRNA (P), and (4) 30 nM Per2 for 48 hours + 10 nM Baf for 8 hours (PB). Cell cycle analysis was assessed following propidium iodide staining by flow cytometry. Statistical analysis: One way ANOVA with Bonferroni post hoc correction. All results are presented as mean ± SEM (n=3). * = $p<0.05$ vs control and ** = $p<0.001$ vs control. Abbreviations: Per2 + Baf = Period 2 + Bafilomycin

3.3.5. Flow Cytometry – G2/M Analysis

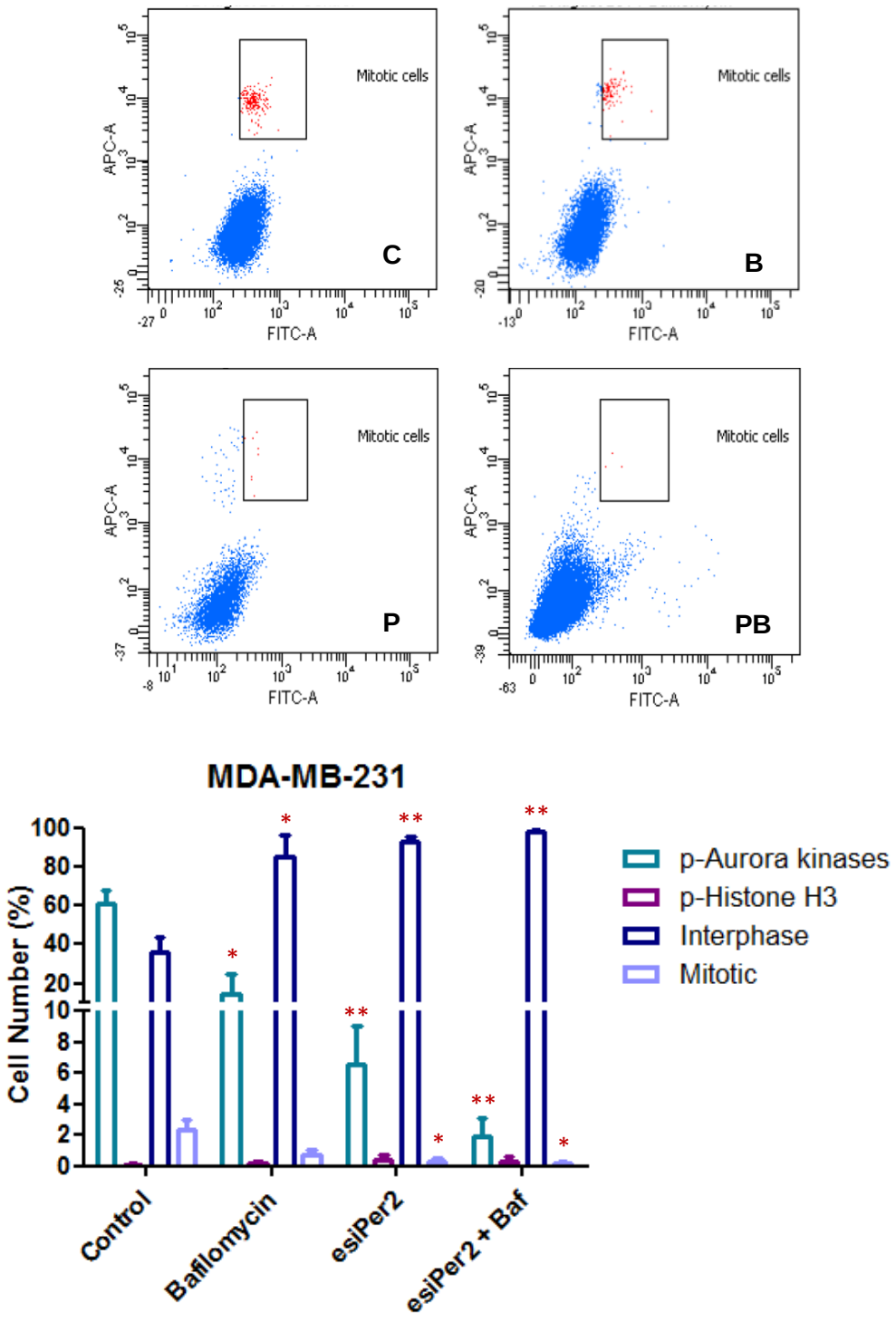

Figure 3.20: Determination of G2/M cell cycle transition in MDA-MB-231 breast cancer cells following Per2 silencing and bafilomycin treatment. MDA-MB-231 cells were subjected to (1) Control conditions (C), (2) 10 nM Bafilomycin (B), (3) 30 nM Per2 esiRNA (P), and (4) 30 nM Per2 for 48 hours + 10 nM Baf for 8 hours (PB). G2/M transition analysis was assessed by flow cytometry. Statistical analysis: One way ANOVA with Bonferroni post hoc correction. All results are presented as mean ± SEM (n=3). * = $p<0.05$ vs control and ** = $p<0.001$ vs control. Abbreviations: Per2 + Baf = Period 2 + Bafilomycin.

G2/M transition analysis of the MDA-MB-231 breast cancer cells following Per2 silencing and bafilomycin A1 treatment revealed a significant increase in the interphase cell population following bafilomycin treatment alone (85.07 ± 10.83% vs 36.30 ± 7.600%, $p<0.05$) with a shift from early mitosis seen by a decrease in p-Aurora when compared to control (14.03 ± 10.56% vs 61.25 ± 6.850%, $p<0.05$) (**Figure 3.20**). Per2 silencing alone resulted in a significant increase in interphase (92.77 ± 2.657% vs 36.30 ± 7.600%, $p<0.001$), and a decrease in p-Aurora in comparison to control (6.567 ± 2.484% vs 61.25 ± 6.850%, $p<0.001$). A significant decrease in mitosis was also seen following Per2 silencing when compared to control (0.3333 ± 0.2082 % vs 2.350 ± 0.6500%, $p<0.05$). The combination of Per2 silencing prior to bafilomycin treatment resulted in an almost complete inhibition of mitosis in comparison to control (0.133 ± 0.133% vs 2.350 ± 0.6500%, $p<0.001$) which resulted in virtually the entire population of cells in interphase (97.67 ± 1.184% vs 36.30 vs 7.600%, $p<0.001$). A significant shift from early mitosis was also seen following Per2 silencing in combination with bafilomycin treatment when compared to control (1.867 ± 1.189% vs 61.25 ± 6.850%, $p<0.001$).

3.4. Metformin - A modulator of circadian Per2 expression and a potential adjuvant chemotherapeutic agent.

3.4.1. MTT Cell Viability Assay

MTT cell viability assays were carried out to assess the cell viability of the MDA-MB-231 cancer cells following treatment with metformin and doxorubicin. The MDA-MB-231 cancer cells, which are known to be resistant to doxorubicin treatment showed a slight

although significant reduction in MTT reductive capacity when treated with 2.5 µM of doxorubicin in comparison to the control (86.82 ± 2.478% vs 100%, p<0.0001). The combination treatment of metformin and doxorubicin resulted in a statistically greater reduction in cell viability when compared to control (79.05 ± 2.398% vs 100%, p<0.0001), however when compared to doxorubicin alone only a slight reduction in cell viability was seen with the combination treatment (79.05 ± 2.398% vs 86.82 ± 2.478%, p<0.05) (**Figure 3.21**).

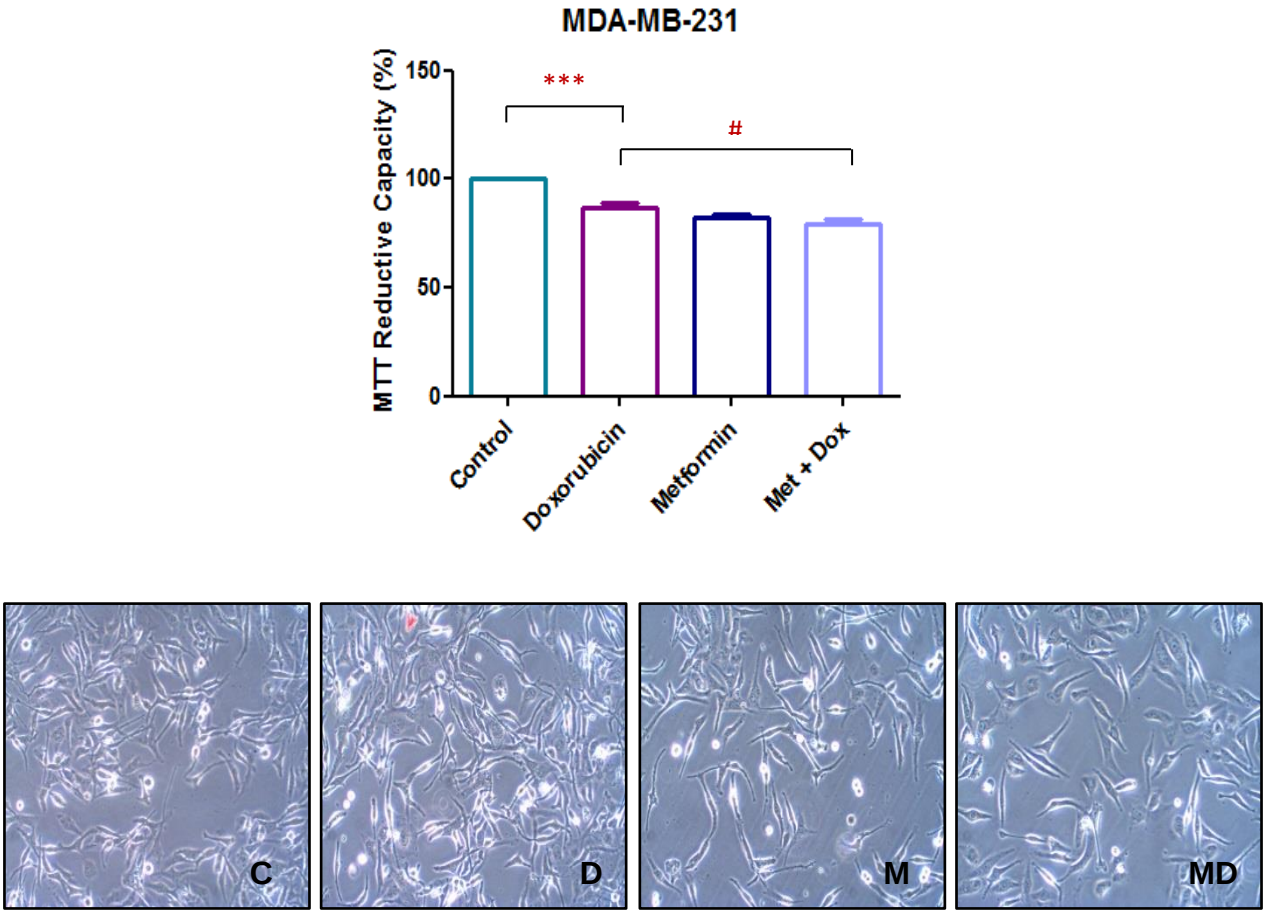

Figure 3.21: Effects of metformin on the viability and morphology of the MDA-MB-231 cancer cells. MDA-MB-231 cells were subjected to (1) Control conditions (C), (2) 2.5 µM Doxorubicin (D), (3) 40 mM Metformin (M) and (4) 2.5 µM Dox for 24 hours + 40 mM Dox for 24 hours (MD). Cell viability was assessed using the MTT assay and inverted microscope images were obtained at 100x magnification. Statistical analysis: One way ANOVA with Bonferroni post hoc correction. All results are presented as mean ± SEM (n=3). *** = p<0.0001 vs control and # = p<0.05 vs Doxorubicin. Abbreviations: C = Control, D = Doxorubicin, M = Metformin and MD = Metformin + Doxorubicin

3.4.2. Cell Cycle Analysis

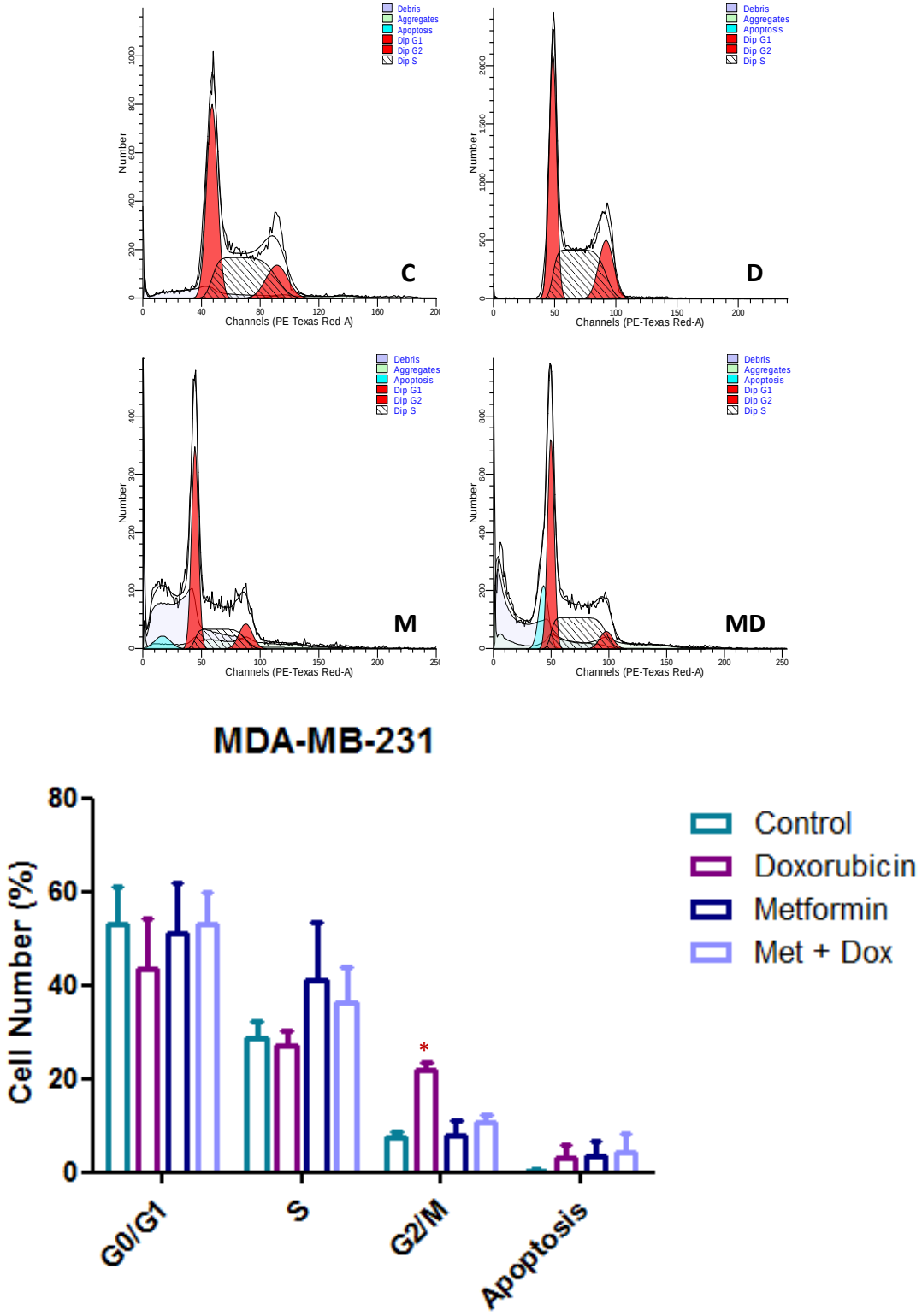

Figure 3.22: Analysis of cell cycle progression of the MDA-MB-231 cancer cells following metformin and doxorubicin treatment. MDA-MB-231 cells were subjected to (1) Control conditions (C), (2) 2.5 µM Doxorubicin (D) (3) 40 mM Metformin (M), and (4) 40 mM Metformin for 24 hours + 2.5 µM Dox for 24 hours. Cell cycle analysis was assessed following propidium iodide staining by flow cytometry. Statistical analysis: One way ANOVA with Bonferroni post hoc correction. All results are presented as mean ± SEM (n=3). * = $p<0.05$ vs control. Abbreviations: Met + Dox = Metformin + Doxorubicin.

Cell cycle regulation was assessed using flow cytometry to determine the effects of metformin on the cell cycle in the MDA-MB-231 cancer cells. The MDA-MB-231 cancer cells showed a significant increase in the percentage of cells in the G2/M phase of the cell cycle (21.91 ± 1.614% vs 7.407 ± 1.309%, p<0.001) with a slight non-significant increase in apoptosis (3.407 ± 2.656% vs 0.5233 ± 0.2621%) following doxorubicin treatment in comparison to the control. However, no significant changes were seen with either metformin treatment alone or in combination with doxorubicin when compared to the control (**Figure 3.22**).

3.4.3. Western Blot Analysis

Per2

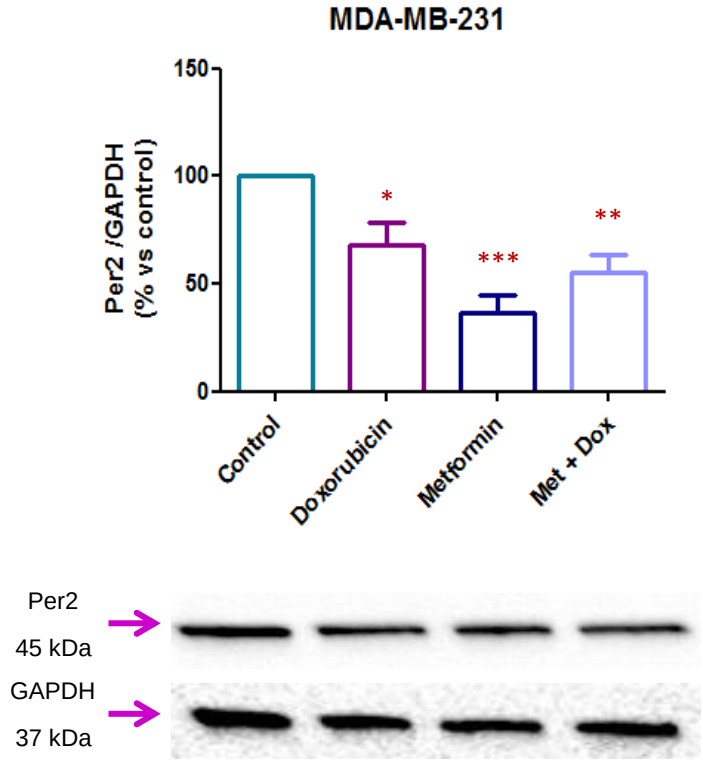

Figure 3.23: Western Blot analysis of Per2 in the MDA-MB-231 breast cancer cells following metformin and doxorubicin treatment. MDA-MB-231 cells were subjected to (1) Control conditions (C), (2) 2.5 µM Doxorubicin (D), (3) 40 mM Metformin (M) and (4) 40 mM Metformin for 24 hours + 2.5 µM Doxorubicin for 24 hours (MD). Statistical analysis: One way ANOVA with Bonferroni post hoc correction. All results are presented as mean ± SEM (n=3). * = p<0.05 vs control, ** = p<0.001 vs control and *** = p<0.0001 vs control. Abbreviations: Met + Dox = Metformin + Doxorubicin.

Western blot analysis of Per2 protein levels was analysed prior treatment with metformin treatment in order to determine the effects of metformin on its protein expression in the MDA-MB-231 breast cancer cells. The MDA-MB-231 cancer cells showed a significant reduction in Per2 protein levels with metformin treatment alone (36.39 ± 8.495% vs 100%, p<0.0001) as well as with the combination of metformin and doxorubicin treatment in comparison to the control (55.47 ± 8.144% vs 100%, p<0.001) (**Figure 3.23**).

AMPKα (Thr^{172}) Phosphorylation

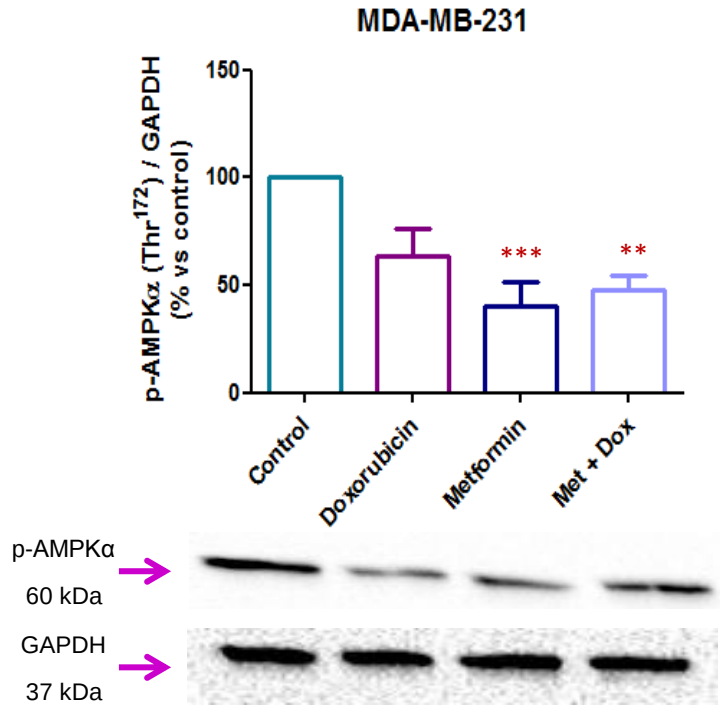

Figure 3.24: Western Blot analysis of p-AMPKα (Thr^{172}) in the MDA-MB-231 (B) breast cancer cells following metformin and doxorubicin treatment. MDA-MB-231 cells were subjected to (1) Control conditions (C), (2) 2.5 µM Doxorubicin (D), (3) 40 mM Metformin (M) and (4) 40 mM Metformin for 24 hours + 2.5 µM Doxorubicin for 24 hours (MD). Statistical analysis: One way ANOVA with Bonferroni post hoc correction. All results are presented as mean ± SEM (n=3). ** = p<0.001 vs control and *** = p<0.0001 vs control. Abbreviations: Met + Dox = Metformin + Doxorubicin.

The MDA-MB-231 cancer cells showed a significant reduction in the phosphorylation of AMPKα following metformin treatment alone (40.21 ± 11.54% vs 100%, p<0.0001), and in combination with doxorubicin treatment when compared to the control (47.67 ± 6.865% vs 100%, p<0.001) (**Figure 3.24**).

p53

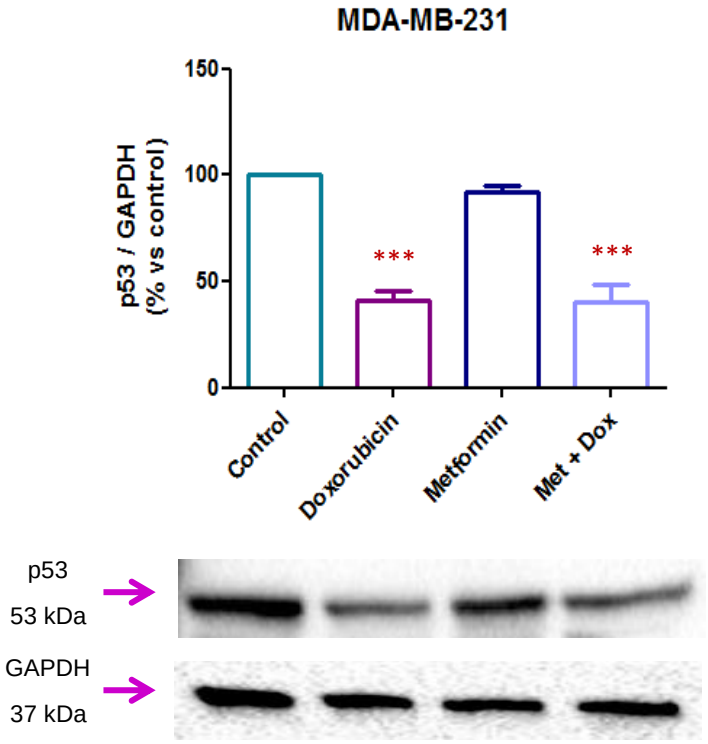

Figure 3.25: Western Blot analysis of p53 in the MDA-MB-231 breast cancer cells following metformin and doxorubicin treatment. MDA-MB-231 cells were subjected to (1) Control conditions (C), (2) 2.5 µM Doxorubicin (D), (3) 40 mM Metformin (M) and (4) 40 mM Metformin for 24 hours + 2.5 µM Dox for 24 hours (MD). Statistical analysis: One way ANOVA with Bonferroni post hoc correction. All results are presented as mean ± SEM (n=3). *** = p<0.0001 vs control. Abbreviations: Met + Dox = Metformin + Doxorubicin.

The MDA-MB-231 cancer cells showed a significant reduction in p53 activity following treatment with doxorubicin alone (41.32 ± 4.255% vs 100%, p<0.0001) as well as with the combination of metformin and doxorubicin treatment in comparison to the control (40.52 ± 7.703% vs 100%, p<0.0001). No significant change in p53 activity was seen in the MDA-MB-231 cancer cells following treatment with metformin alone (91.78 ± 3.242% vs 100%) (**Figure 3.25**).

Caspase-3

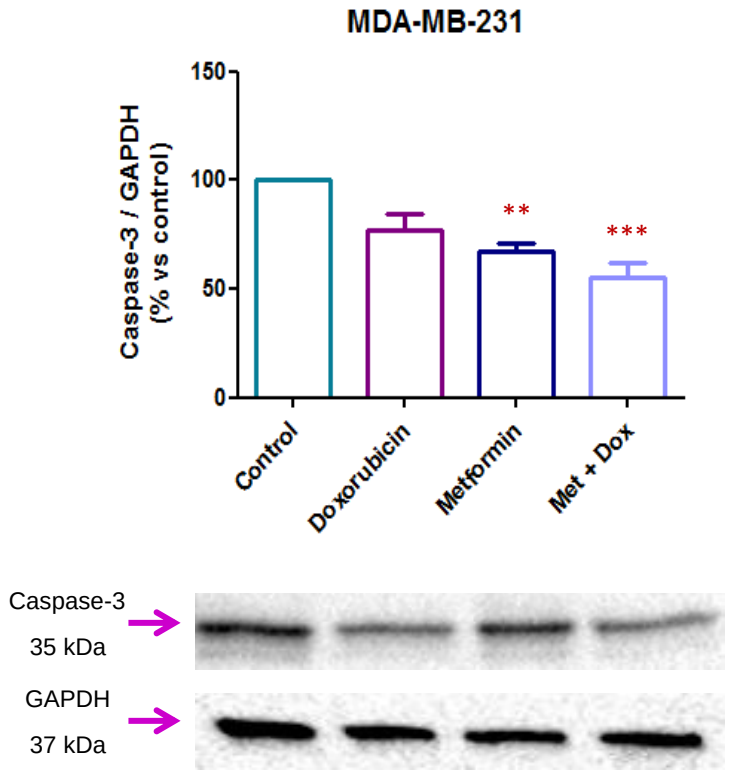

Figure 3.26: Western Blot analysis of Caspase-3 in the MDA-MB-231 breast cancer cells following metformin and doxorubicin treatment. MDA-MB-231 cells were subjected to (1) Control conditions (C), (2) 2.5 µM Doxorubicin (D), (3) 40 mM Metformin (M) and (4) 40 mM Metformin for 24 hours + 2.5 µM Dox for 24 hours (MD). Statistical analysis: One way ANOVA with Bonferroni post hoc correction. All results are presented as mean ± SEM (n=3). ** = $p<0.001$ vs control and *** = $p<0.0001$ vs control. Abbreviations: Met + Dox = Metformin + Doxorubicin.

Caspase-3, an executioner caspase leads to the induction of apoptosis upon its cleavage by upstream initiator caspases. Western blot analysis for caspase-3 was used to assess apoptotic activity in the MDA-MB-231 cells. The MDA-MB-231 cancer cells showed a significant reduction in caspase-3 activity with metformin treatment alone (67.58 ± 3.702% vs 100%, $p<0.001$) which was further reduced with the combination of metformin and doxorubicin treatment in comparison to the control (55.27 ± 6.857% vs 100%, $p<0.0001$) (**Figure 3.26**).

PARP

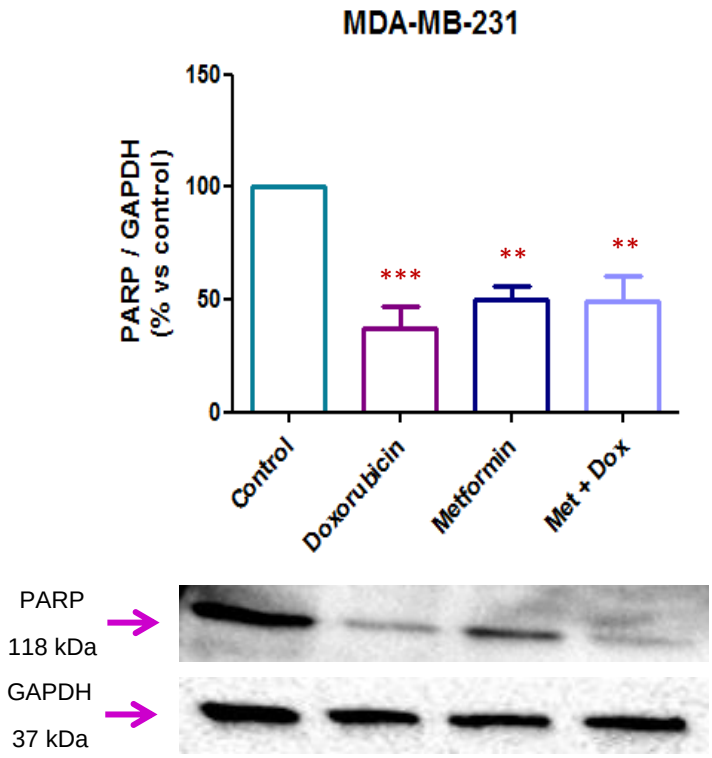

Figure 3.27: Western Blot analysis of PARP in the MDA-MB-231 breast cancer cells following metformin and doxorubicin treatment. MDA-MB-231 cells were subjected to (1) Control conditions (C), (2) 2.5 µM Doxorubicin (D), (3) 40 mM Metformin (M) and (4) 40 mM Metformin for 24 hours + 2.5 µM Doxorubicin for 24 hours (MD). Statistical analysis: One way ANOVA with Bonferroni post hoc correction. All results are presented as mean ± SEM (n=3). *** = p<0.0001 vs control. Abbreviations: Met + Dox = Metformin + Doxorubicin.

PARP protein expression was assessed as a marker of nuclear damage and apoptosis induction in both the MDA-MB-231 cancer cells. The MDA-MB-231 cancer cells showed a significant reduction in PARP levels following doxorubicin (36.89 ± 10.02% vs 100%, p<0.0001), and metformin treatments alone when compared to the control (50.20 ±6.088% vs 100%, p<0.001). A significant reduction in PARP was also seen following the combination of metformin and doxorubicin treatment in comparison to control (49.40 ± 11.02% vs 100%, p<0.001) (**Figure 3.27**).

Table 3.1: A summary of the significant changes in markers of cell death following Per2 silencing in combination with doxorubicin treatment, in the MDA-MB-231 breast cancer cell line. ↑ / ↓ = $p<0.05$, ↑↑ / ↓↓ = $p<0.001$ and ↑↑↑ / ↓↓↓ = $p<0.0001$. Treatment groups: Dox = Doxorubicin, esiPer2 = Per2 silencing, esiPer2 + Dox = Per2 silencing + Doxorubicin.

vs Control		The Role of Per2 in Doxorubicin-induced Cell Death		
		Dox	**esiPer2**	**esiPer2 + Dox**
MTT	Viability	↓↓↓	↓↓↓	↓↓↓
Western Blotting	Per2	NS	↓↓↓	↓↓↓
	p-MDM2 (Ser^{166})	NS	↑	NS
	p-p53 (Ser^{15})	↑↑↑	NS	NS
	CC3	NS	↑	↑
	CP	↑↑↑	↑↑↑	↑↑↑
Hoechst + PI	Live cells	NS	↓	↓↓↓
	Dead cells	↑	↑↑	↑↑↑
Cell Cycle Analysis	G0/G1	NS	↑	NS
	S	NS	NS	↑↑
	G2/M	↑	↓↓	↓↓
	Apoptosis	↑	↑	↑↑
G2/M Transition	Interphase	↑↑↑	↑↑↑	↑↑↑
	p-Aurora	↓↓↓	↓↓↓	↓↓↓
	Mitosis	↓↓	↓	↓↓

Table 3.2: A summary of the significant changes in markers of cell death and autophagy following Per2 silencing in combination with autophagy inhibition using bafilomycin A1 in the MDA-MB-231 breast cancer cell line. ↑ / ↓ = p<0.05, ↑↑ / ↓↓ = p<0.001 and ↑↑↑ / ↓↓↓ = p<0.0001. Treatment groups: Baf = Bafilomycin A1, esiPer2 = Per2 silencing, esiPer2 + Baf = Per2 silencing + Bafilomycin.

vs Control		The Role of Per2 in Autophagy		
		Baf	**esiPer2**	**esiPer2 + Baf**
MTT	Viability	↓↓↓	↓↓↓	↓↓↓
Western Blotting	Per2	NS	↓↓↓	↓↓↓
	AMPKα	NS	↑↑	NS
	p-mTOR (Ser^{2448})	NS	↑↑↑	↑↑
	LC3 II	↑↑	NS	↑↑↑
Hoechst + PI	Live cells	NS	↓	↓↓↓
	Dead cells	NS	↑↑	↑↑↑
Cell Cycle Analysis	G0/G1	↑↑	↑	↑
	S	NS	NS	NS
	G2/M	↓↓	↓	↓↓
	Apoptosis	↑	↑	↑
G2/M Transition	Interphase	↑	↑↑	↑↑
	p-Aurora	↓	↓↓	↓↓
	Mitosis	NS	↓	↓

Table 3.3: A summary of the significant changes in markers of cell viability, markers of cell death and cell cycle analysis following treatment with metformin and doxorubicin in the MDA-MB-231 breast cancer cell line. ↑↑ / ↓↓ = p<0.001 and ↑↑↑ / ↓↓↓ = p<0.0001. Treatment groups: Dox = Doxorubicin, Met = Metformin, Met + Dox = Metformin + Doxorubicin.

vs Control		Metformin: A modulator of Per2 expression and possible adjuvant chemotherapeutic agent		
		Dox	Met	Met + Dox
MTT	Viability	↓↓↓	↓↓↓	↓↓↓
Western Blotting	Per2	↓	↓↓↓	↓↓
	p-AMPKα (Thr^{172})	NS	↓↓↓	↓↓
	p53	↓↓↓	NS	↓↓↓
	Caspase-3	NS	↓↓	↓↓↓
	PARP	↓↓↓	↓↓	↓↓
Cell Cycle Analysis	G0/G1	NS	NS	NS
	S	NS	NS	NS
	G2/M	↑	NS	NS
	Apoptosis	NS	NS	NS

Chapter 4: Discussion

4.1. Introduction

Most peripheral organ and tissue clocks have been shown to express internal circadian oscillations which operate independently of central hypothalamic inputs. Increased reliance on incandescent light and rotating night shift work, associated with modern day living has resulted in a de-synchronization of these intrinsic oscillations giving rise to severe circadian disruptions which have been implicated in the pathogenesis of various diseases including that of breast cancer.

Breast cancer has become a global concern, as the burden of this disease is rapidly on the rise in both developed and developing countries. In South Africa it was estimated that in 2004 alone one in 29 women were newly diagnosed with breast cancer, with numbers set to rise each year (National Cancer Registry., 2004). Furthermore, breast cancer cells have become increasingly resistant to the anti-carcinogenic effects of chemotherapeutic agents like doxorubicin, and as such a critical need for more effective adjuvant therapies aimed at improving cancer cell susceptibility to chemotherapy-induced cell death has arisen.

Therefore this study was designed to provide insight into the molecular nature behind intrinsic peripheral circadian clocks, as well as to assess whether the manipulation of these clocks through the silencing of Per2, a key regulator involved in the resetting of the circadian clock, could sensitize resistant breast cancer cells to the anti-carcinogenic effects of doxorubicin. Prior to the assessment of the role of Per2 in both doxorubicin-induced cell death and autophagy, this study set out to characterize Per2 in a normal

MCF-12A breast epithelial cell line, as well as in the estrogen receptor positive MCF-7 and estrogen receptor negative MDA-MB-231 breast adenocarcinoma cell lines. Western blotting analysis was employed to assess the rhythmic changes in Per2 protein expression over a period of 25 hours. Additionally, fluorescent confocal microscopy was used to determine the cellular localization of Per2 under basal cellular conditions. An *in vitro* experimental model was subsequently employed, which made use of the MDA-MB-231 estrogen receptor negative adenocarcinoma cell line, as they are known to be resistant to doxorubicin-induced cell death (Smith *et al*., 2006). Doxorubicin dose responses were carried out and a concentration, which falls within a clinically relevant range, was chosen based on the ability of doxorubicin to elicit a differential response in MTT reductive capacity of the normal MCF-12A and MDA-MB-231 cancer cells. Per2 was silenced by making use of an esiRNA targeted against the Per2 gene, and silencing was confirmed with western blotting. With the use of various molecular techniques (MTT assay, western blotting and flow cytometry) the role of Per2 in doxorubicin-induced cell death and autophagy was assessed. Additionally, metformin was employed in this study as a pharmacological inhibitor of Per2, in order to substantiate the findings seen with Per2 gene silencing in the context of doxorubicin-induced cell death. The following aims were thus formulated:

- To characterize the role of Per2 in normal breast epithelial cells as well as in ER+ and ER- breast epithelial cells.
- To determine the role of Per2 in doxorubicin-induced cell death.
- To determine the role of Per2 in autophagy.
- To evaluate the role of metformin, a modulator of Per2 expression, as a potential adjuvant chemotherapeutic agent.

4.2. Characterizing the Role of Per2 in Normal, ER+ and ER- Breast Epithelial Cells.

All nucleated cells have been shown to possess intrinsic circadian clocks, which are thought to function in a cell-autonomous fashion, evident by the self-sustained rhythmic oscillations in detached cell culture models (Balsalobre *et al.,* 1998). Therefore, in this part of the study we aimed to elucidate the presence of a rhythmic expression pattern of the circadian Per2 protein in a normal breast epithelial (MCF-12A) cell line, an estrogen receptor positive (ER^+) breast adenocarcinoma cell line (MCF-7) as well as in an estrogen receptor negative (ER^-) cell line (MDA-MB-231). We have demonstrated for the first time that a clear circadian pattern in Per2 **protein** expression in the normal MCF-12A cells as well as in the ER- MDA-MB-231 cancer cells exists. However, the ER+ MCF-7 breast cancer cells showed no rhythmic Per2 protein expression, as protein levels remained fairly constant over 25 hours **(Figure 3.1)**. These results are in accordance with other studies where differential Per2 expression was observed on an **mRNA** level in human breast cancer tissue samples (Chen *et al*., 2005). Additionally, Rossetti and colleagues failed to see rhythmic changes in Per2 when assessing mRNA expression in the MCF-7 cell line (Rossetti *et al.,* 2012).

Two distinct subpopulations of cells expressing the Per2 protein were observed in both the normal MCF-12A breast epithelial cells and the MDA-MB-231 breast adenocarcinoma cells. In both the fluorescently dimmer and brighter subpopulations, Per2 was seen to be located predominantly within the cytoplasm. Co-localization of Per2 in the nucleus was only seen in the fluorescently dimmer subpopulations of both cell lines. These results are in agreement with known literature where both cytoplasmic and nuclear localization of Per2 is seen in the kidney fibroblast-like COS7 cell line (Yagita *et al*., 2002). Additionally, the differences in Per2 protein expression patterns seen in

different populations of the MDA-MB-231 cancer cells, highlights the a-synchronous nature of peripheral circadian clocks as well as the heterogeneity of cancer cell populations (Chen *et al*., 2005). The fact that nuclear localization of Per2 was associated only with diminished cytoplasmic protein expression, may be explained by the fact that Per2 protein levels begin to accumulate within the cytoplasm after its translation at the start of a circadian day (Albrecht, 2002). Per2 protein levels reach threshold levels at the end of a circadian day **(Figure 3.2A and Figure 3.3A)**, where they heterodimerize with accumulated Cry proteins and CKIε - this complex then translocates into the nucleus resulting in the repression of Per2 gene transcription. Once repressed, unbound cytoplasmic Per2 is phosphorylated by CKIε, leading to its degradation by the 26S proteasome pathway thus causing a decrease in cytoplasmic Per2 protein levels **(Figure 3.2B and Figure 3.3B)** and a resetting of the circadian clock (Lefta *et al.,* 2011).

4.3. The Role of Per2 in Doxorubicin-Induced Cell Death

The Per2 gene is an essential regulator of the mammalian circadian clock system, and mutations arising in this gene have been identified in a wide range of human cancers including, colorectal and breast cancer (Yang *et al.*, 2009). Furthermore, circadian Per2 disruption has been implicated in cell cycle dysfunction and apoptosis, evident by the aberrant rhythmic expression of the cell cycle gene, cyclin D1, as well as the negative p53 regulator, MDM2, in Per2 deficient mice (Canaple *et al.*, 2003). Based on this knowledge, we focussed on Per2 as a molecular target for the sensitization of resistant breast cancer cells to doxorubicin treatment. In order to determine the role of Per2 in doxorubicin induced cell death, we made use of an endoribonuclease-prepared siRNA against the mammalian Per2 gene to effectively silence Per2 protein expression. Results

obtained following western blot analysis show that we were able to achieve a silencing efficiency of ±78% in the normal MCF-12A cells and an efficiency of ±99% in the MDA-MB-231 breast cancer cells using 30 nM Per2 esiRNA for a period of 48 hours **(Figure 3.4)**, we therefore used this concentration and time point for all subsequent transfections.

Per2 was silenced in both the normal MCF-12A and MDA-MB-231 breast cancer cells prior to their treatment with 2.5 µM of doxorubicin for 24 hours, in order to determine whether the resistant MDA-MB-231 cancer cells could be sensitized to a lower, clinically relevant, dose of doxorubicin by Per2 circadian disruption. Our results show that 2.5 µM doxorubicin lead to a significant reduction in MTT reductive capacity of the normal MCF-12A cells. Although treatment with 2.5 µM doxorubicin did lead to a significant reduction in the reductive capacity of the MDA-MB-231 cancer cells when compared to the normal MCF-12A cells, doxorubicin treatment was less effective in decreasing the reductive capacity of the MDA-MB-231 cells, demonstrating the resilient nature of these cancer cells to doxorubicin treatment **(Figure 3.6)**. Our results also demonstrate that the silencing of Per2 prior to doxorubicin treatment does in fact sensitize the resistant MDA-MB-231 cancer cells to doxorubicin treatment, as a significant decrease in the MTT reductive capacity of these cells was seen in comparison to doxorubicin treatment alone. These results are contradictory to other studies which show an increase in cell death with the overexpression of Per2 in MCF-7 breast cancer cells (Xiang *et al*., 2008). An explanation for the results we obtained may be due to the fact that the function of the 140 kDa protein isoform of Per2 was assessed in these studies, whereas in our study the smaller 45 kDa protein isoform was assessed. We also observed a significant decrease in the MTT reductive capacity of the MCF-12A cells with Per2 silencing prior to doxorubicin when compared to doxorubicin treatment alone which demonstrates the essential role that Per2 plays in the normal cellular DNA-damage response pathway

(Albrecht *et al.*, 2007). Although this combination therapy was more effective than Dox alone in the MDA-MB-231 cells, the normal MCF-12A cells were also severely affected. This treatment strategy should therefore be targeted specifically to the cancer cells via nanoparticles comprising polyethyleneimine (PEI) and poly(D,L-lactide-*co*-glycolide) (PLGA), to encapsulate a combination of siRNA and chemotherapeutic agent (Patil *et al.*, 2011), in our case the combination of Per2 esiRNA and doxorubicin should be used.

Oncogenic signalling and DNA damage are invariably associated with p53 mediated tumour suppression. In response to DNA damage, the activation of p53 by ATM/ATR and Chk1/Chk2, a set of Ser/Thr kinases (Eymin *et al*., 2006), results in the induction of apoptosis, senescence or cell cycle arrest (Reinhardt *et al.*, 2014). Oncogenic signalling on the other hand is involved in tumour suppression, via the stabilization of p53 in an ARF-dependent mechanism. Activation of p53 by ARF leads to the activation of MDM2, and the subsequent inhibition of p53-ubiquitin ligase activity (Jin *et al.*, 2001). Thus the stabilization of p53 by ARF, leads to an increase in p53 activity, and the induction of apoptosis or senescence (Efeyan *et al.*, 2007).

Mutations arising in p53 are seen in over 50% of all human cancers, with a large proportion of these mutations occurring as a result of missense mutations that give rise to protein products lacking p53-trancriptional activity (Wang *et al*., 2011). The loss of functional p53 may thus account for the ability of these cancer cells to evade cell death. Additionally, p53 aberrations have been associated with an increase in the resistance of cancer cells to chemotherapeutic treatment (Weller, 1998).

Our results obtained from western blot analysis of the MDA-MB-231 breast cancer cells, showed a significant increase in p-MDM2 (Ser^{166}) activity in response to Per2 silencing **(Figure 3.8)**. A slight, non-significant increase in MDM2 (Ser^{166}) phosphorylation was seen with doxorubicin treatment alone, which was associated with a significant increase

in p-p53 (Ser^{15}) activity **(Figure 3.8)**. An increase in MDM2 activity is usually associated with a decrease in functional p-p53 (Ser^{15}) activity, as MDM2 phosphorylation leads to the stabilization and subsequent degradation of p53 (Malmlöf *et al.*, 2007). However, our results showed that p-p53 (Ser^{15}) activity remained unchanged following Per2 silencing and was concomitantly increased with doxorubicin treatment. This may be explained by the fact that the MDA-MB-231 breast cancer cells possess a p53 mutation (codon 280, AGA (arginine) to AAA (lysine)) which leads to the increased expression of dysfunctional p53 (Li *et al.*, 1999).

Our results also show a slight although non-significant increase in cleaved caspase-3 (**Figure 3.9)** with a subsequent significant increase in cleaved PARP in the MDA-MB-231 cancer cells following treatment with 2.5 µM doxorubicin **(Figure 3.10)**. This was unexpected, as findings on human T-cell leukaemia show that doxorubicin leads to the induction of cell death in a caspase-3 dependent manner (Gamen *et al*., 1997). These results may be explained by the fact that once activated caspase-3 leads to the cleavage of PARP, thereby resulting in a rise in cleaved PARP levels (Earnshaw *et al.*, 1999). Additionally, findings in Hela cells shows that active caspase-3 is rapidly degraded (Tawa *et al*., 2004). Thus we may have seen a significantly greater increase after a shorter treatment period. Per2 silencing alone as well as in combination with doxorubicin treatment resulted in a significant increase in both cleaved caspase-3 and cleaved PARP levels which suggests that these cells are committed to cells death through apoptosis.

In order to add to the cell death results obtained by western blotting, MDA-MB-231 cancer cells were stained with Hoechst 33342 and propidium iodide and analysed by flow cytometry **(Figure 3.11)**. Our results show a significant increase in the percentage of dead cells with the treatment of 2.5 µM doxorubicin. Per2 silencing resulted in a significant decrease in the percentage of live cells with a concomitant increase seen in

the dead cell population. Our results also indicate that by silencing Per2 prior to treatment with doxorubicin, the resistant MDA-MB-231 cancer cells become more sensitive to the cytotoxic effects of doxorubicin. These results support the increase in caspase-3 and PARP cleavage seen with our western blotting data. Apoptotic cell death is classically defined by distinct morphological changes which are initiated by cleavage of caspase-3 and subsequent PARP cleavage, nuclear condensation and fragmentation ensues resulting in a loss of membrane integrity, thus allowing the propidium iodide stain to permeabilize the cell and causing an increase in fluorescence as measured by flow cytometry (Riccardi *et al.*, 2006).

Results obtained from cell cycle analysis of the MDA-MB-231 breast cancer cells, show a significant increase in the G2/M phase with a significant increase in apoptosis (Sub-G1) with the treatment of 2.5 µM doxorubicin over 24 hours indicating G2/M cell cycle arrest **(Figure 3.12)**. These results are in agreement with several other studies showing G2/M arrest in the MDA-MB-231 breast cancer cells following doxorubicin treatment (Bar-on *et al.*, 2007 and Siu *et al.*, 1999).

A significant increase in the G0/G1 phase with a concomitant decrease in the G2/M cell cycle phase was seen with Per2 silencing, whereas the combination of Per2 silencing and doxorubicin treatment resulted in cells exiting the cell cycle during the S-phase, this resulted in a significant reduction in the G2/M phase with a concomitant increase in apoptosis. Our results show that Per2 may be involved in the regulation of cell cycle progression as suggested in literature, and this mechanism may be mediated by the effect of Per2 on cyclin D1 and *c-myc* expression (Filipski *et al.*, 2006). However, as we did not assess expression of these key G0/G1 cell cycle regulators in response to Per2 silencing, this still remains to be elucidated.

In order to shed further light on the cell cycle data obtained, particularly during mitosis, G2/M cell cycle transition was also assessed by means of flow cytometry. The phosphorylation of Histone H3 at the Ser^{10} residue is strongly associated with the condensation of chromosomes during mitosis (Goto, 1999), whereas the phosphorylation of the Aurora kinases (A, B and C) is associated with various functions during mitosis, which include but are not limited to mitotic spindle formation, chromosome segregation and cytokinesis (Andrews *et al.*, 2003). The functional influences of these kinases thus span from the beginning of the G2 phase right to the end of mitosis. Additionally, during G2/M cell cycle transition the phosphorylation of Histone H3 is tightly coupled to the expression of the Aurora kinases (Crosio *et al*., 2002). Therefore, cells staining positive for both p-Histone H3 (Ser^{10}) and p-Aurora A (Thr^{288}) / Aurora B (Thr^{232}) / Aurora C (Thr^{198}) indicate cells which are truly mitotic and have progressed through the entire cell cycle (late stage mitosis), whereas those staining positive for only the phosphorylated Aurora kinases are indicative of early mitotic cells.

Our results show that treatment with 2.5 µM doxorubicin results in a severe blunting in mitosis of the MDA-MB-231 cancer cells as a significant reduction in both early and late stage mitosis was seen compared to control **(Figure 3.13)**, this adds to the cell cycle analysis data showing a complete arrest in the G2-phase. Per2 silencing also resulted in a significant decrease in late stage mitosis as well as that of early mitosis; however the decrease in early mitosis was not as severe as that seen with doxorubicin treatment alone. The combination of Per2 silencing and doxorubicin also resulted in a complete inhibition of both early and late mitosis.

4.4. The Role of Per2 in Autophagy

Autophagy or type II programmed cell death, is classically defined by the sequestration of redundant or faulty cellular constituents into double membrane bound vesicles which fuse with internal lysosomes, resulting in their degradation and removal from the cell (Gozuacik *et al.*, 2004). Although autophagy serves an essential “housekeeping” role in normal cells through its ability to remove these faulty constituents, cells fated to die possess increased autophagic activity which results in their excessive destruction by “self-cannibalization” (Levine *et al.*, 2005).

In addition, autophagy has been shown to display circadian rhythmicity in accordance with daily feeding and rest / activity patterns. In rat hepatocytes, autophagy was shown to peak during the rest or fasting periods when plasma glucagon levels peak and intracellular ATP levels are depleted. However, during the active feeding period, plasma insulin levels peak, which results in the activation of the PI3K/Akt pathway, leading to the inhibition of autophagic activity (Sachdeva *et al.*, 2008 and Ma *et al.*, 2012).

The hypoxic and nutrient deprived microenvironment that cancer cells in the centre of a tumour face, causes a shift in cellular metabolism allowing cancer cells to utilize large quantities of glucose for anabolic processes (Kroemer *et al.*, 2008). Additionally, autophagy has been shown to be up-regulated in certain cancer cell types (Ogier-Denis *et al.*, 2003), which confers a survival advantage to the cancer cells as intracellular constituents are broken down and fed into the tricarboxylic acid (TCA) cycle to yield ATP and other catabolites which can be utilized for energy metabolism (Hanahan *et al.*, 2011).

Recently, modulation of the autophagic process has become an attractive therapeutic target against cancer, as it has been postulated that if autophagy does confer a

protective mechanism to cancer cells by allowing them to evade cell death, then it stands to reason that the inhibition of autophagy may force these cells to undergo programmed cell death (Hait *et al.,* 2006). Therefore, for this part of the study we aimed to determine whether the silencing of Per2 could sensitize the chemo-resistant MDA-MDB-231 cancer cells to the inhibition of autophagy, thereby forcing them to undergo programmed cell death.

For this part of the study Per2 was silenced in both the normal MCF-12A and MDA-MB-231 breast cancer cells prior to autophagy inhibition using 10 nM bafilomycin for 8 hours. Our results show that treatment of the normal MCF-12A with bafilomycin A1 had no significant effect on the MTT reductive capacity of these cells, whereas Per2 silencing prior to bafilomycin treatment in the MCF-12A cells resulted in a significant decrease in MTT reductive capacity **(Figure 3.14)**. The resistant MDA-MB-231 breast cancer cells showed a significant decrease in MTT reductive capacity following treatment with 10 nM bafilomycin A1, suggesting that these cells do in fact appear to be sensitive to the inhibition of autophagy. Our results also show that when Per2 was silenced in the MDA-MB-231 cells prior to treatment with bafilomycin, the sensitivity of these cells to autophagic inhibition is greatly enhanced. These results were further supported by flow cytometry analysis by staining cells with Hoechst and propidium iodide **(Figure 3.18)**, as a significant increase in cell death was seen following the silencing of Per2 prior to the inhibition of autophagy by bafilomycin A1.

In order to gain insight into the mechanism whereby Per2 silencing appears to sensitize the MDA-MB-231 cancer cells to autophagy inhibition, western blot analysis was conducted assessing key markers of autophagic activity, namely; AMPKα, p-mTOR (Ser^{2448}) and LC3.

Assessment of AMPKα showed a significant increase following Per2 silencing **(Figure 3.15)**, this result may be explained by the fact that the intrinsic circadian clock is additionally stabilized via the activation of CK1ε by AMPK, leading to the phosphorylation of Per2 and thus its degradation by the 26S proteasome (Eide *et al*., 2005). This might result in a possible feedback mechanism leading to the rise in AMPKα activity which was observed in our results. Interesting to note is that although the silencing of Per2 prior to bafilomycin treatment did lead to an increase in AMPKα activity in comparison to control, the activity still remained lower than with Per2 silencing alone. This decrease could possibly be as a result of a negative feedback mechanism, whereby the inhibition of autophagy by bafilomycin leads to a decrease in the elevated AMPKα activity seen following Per2 silencing.

The mammalian Target of Rapamycin (mTOR), a sensor of nutrient availability, serves as a potent regulator of autophagic activity with a decrease in its activity resulting in the activation of Unc-51-like kinase (ULK1) and Atg13, two of the main initiators of phagophore formation (Lozy *et al.*, 2012). Bafilomycin A1 treatment resulted in a slight but not significant increase in the phosphorylation of mTOR **(Figure 3.16)** and when compared to the control this suggests that autophagy is inhibited (Easton *et al.,* 2006). These results are further supported by the accumulation LC3 II following bafilomycin treatment **(Figure 3.17)**. The increase in both LC3 I and LC3 II levels seen with the silencing of Per2 is suggestive of an increase in autophagic activity in these cells. However, the interpretation of the western blot data for LC3 II accumulation can often be misleading, as an increase in LC3 II can be as a result of impaired autophagy as seen with its accumulation following bafilomycin treatment. Basal autophagy flux can be determined by the change in relative LC3 II levels seen with the pharmacological inhibition or induction of autophagy (Castillo *et al*., 2013); in our study this was determined with bafilomycin treatment.

A significant increase in LC3 II accumulation was seen with the combination of Per2 silencing and bafilomycin treatment when compared to bafilomycin treatment alone, suggestive of an increase in autophagy flux associated with Per2 silencing. The increase in LC3 I seen when Per2 was silenced was abolished when autophagy was inhibited with bafilomycin, suggesting that the increase in autophagy flux may be as a result of increased autophagosomal synthesis in the MDA-MB-231 cancer cells. Traditionally, an increase in mTOR (Ser^{2448}) phosphorylation, as seen when Per2 was silenced both alone and in combination with bafilomycin treatment **(Figure 3.16)**, is associated with the inhibition of autophagy, however, recently it has been shown that autophagy is additionally regulated via mechanisms which are independent of mTOR (Williams et al., 2008). Additionally, C/EBPβ has been shown to induce autophagy by increasing the lipidation of LC3 I into LC3 II, independently of mTOR activation (Ma *et al.*, 2011). Therefore, our results suggest that Per2 is associated with the regulation of autophagy via an mTOR-independent mechanism.

Cell cycle analysis by flow cytometry was assessed in order to determine the underlying mechanisms of how Per2 silencing sensitizes the resistant MDA-MB-231 cancer cells to autophagy inhibition. Our results show that the inhibition of autophagy with bafilomycin results in a significant increase in the G0/G1 phase of the cell cycle with a concomitant decrease in the G2/M phase **(Figure 3.19)**. Therefore, bafilomycin results in G0/G1 cell cycle arrest leading to the apoptotic cell death of the MDA-MB-231 cancer cells. These results are in accordance with other studies which showed G0/G1 cell cycle arrest and the induction of apoptosis in HT-29 human colon cancer cells (Wu *et al*., 2009) as well as in PC12 rat pheochromocytoma cells (Kinoshita *et al*., 1996). Per2 silencing in combination with bafilomycin treatment resulted in the significant increase in cells in the G0/G1 phase with a decrease in the G2/M phase and a subsequent induction of

apoptosis of the MDA-MB-231 cancer cells, however, when compared to treatment with bafilomycin alone no significant changes were observed.

These results may therefore support the notion that both the circadian clock system and autophagy (Young *et al*., 2009) are implicated in cellular senescence, wherein mitotic cells undergo cell cycle arrest (typically in the G0/G1 phase of the cell cycle) in response to genotoxic stress (Campisi *et al.,* 2007). Evident by the fact that Per2 mutations result in increased senescence of vascular endothelial cells (Wang *et al*., 2008) and that Per2 mutant mice exposed to low levels of γ-irradiation display distinct phenotypic changes associated with early aging in addition to an increase rate of mortality (Kondratov, 2007). Furthermore, cellular senescence has also been implicated in the induction of cell death possibly via mitotic catastrophe (Roninson *et al.*, 2001).

As previously mentioned, the increased phosphorylation of histone H3 (Ser^{10}) accompanied by the increased phosphorylation of the aurora kinases (A (Thr^{288}), B (Thr^{232}) and C (Thr^{198})) is associated with cells in the mitotic phase of the cell cycle. Analysis of G2/M transition in the MDA-MB-231 cancer cells showed no significant changes in the percentage of mitotic cells when compared to control, however, a significant increase in resting cells with a shift from late to early mitosis was seen, as the percentage of p-Aurora positive cells was significantly lowered in response to autophagy inhibition **(Figure 3.20)**. Treatment with bafilomycin subsequent to Per2 silencing resulted in an almost complete inhibition of late stage mitosis as well as a significant decrease in the percentage of p-Aurora only cells, confirming the significant decrease we observed in the G2/M phase with the analysis of the cell cycle. Furthermore, these results suggest that Per2 silencing in combination with bafilomycin treatment leads to increased cellular senescence and the induction of cell death via mitotic catastrophe.

4.5. Metformin - A modulator of circadian Per2 expression and a potential adjuvant chemotherapeutic agent.

Since its approval by the food and drug administration (FDA) in 1995, Metformin (1,1-Dimethylbiguanide hydrochloride) still remains the most widely used anti-diabetic drug for the treatment of type II diabetes (Alimova *et al*., 2009). Its effectiveness in the clinical management of diabetes is largely attributed to its ability in reducing serum blood glucose levels via the reduction in hepatic gluconeogenesis in addition to an increase in cellular glucose uptake (Zakikhani *et al.*, 2006).

It is widely accepted that metabolic disturbances associated with diabetes results in an increased risk for the development of breast cancer and adversely affects patient prognosis (Rocha *et al*., 2011). Additionally, alterations in substrate metabolism of nutrient deprived cancer cells confers pro-survival advantages (Warburg *et al.*, 1927) which allow them to effectively evade cell death.

The mechanism behind metformin's efficacy as an anti-carcinogenic agent is attributed to its ability to inhibit mTOR via a liver kinase B1 (LKB1) / AMPK dependent mechanism. Additionally the activation of AMPK by metformin leads to an inhibition of protein synthesis and a rapid induction of cell cycle arrest and / or apoptosis (Goodwin *et al.*, 2009), resulting in the improved prognosis of diabetic cancer patient taking metformin (Hirsch *et al.*, 2009). Furthermore, metformin was shown to inhibit tumour growth of triple negative (estrogen receptor negative, progesterone receptor negative and HER2 negative) breast cancer cells both *in vitro* (Liu *et al*., 2009) as well an in tumour xenograft models in mice (Iliopoulos *et al.*, 2011).

The internal circadian rhythms of peripheral clocks have been shown to play a critical role in cellular metabolism allowing for the synchronization of these intrinsic oscillations to daily feeding activities. The activation of AMPK as a result of nutrient deprived cellular conditions results in the destabilization of the negative feedback loop of the circadian clock system via the degradation of Per2 (Barnea *et al*., 2012). Taking this into account, coupled with the fact that metformin is a potent inducer of intracellular AMPK, for this part of the study we aimed to determine whether the pharmacological inhibition of Per2 with metformin could sensitize resistant MDA-MB-231 breast cancer cells to doxorubicin-induced cell death.

Therefore, in this section the estrogen receptor negative MDA-MB-231 breast cancer cells were treated with 40 mM metformin for 24 hours followed by 2.5 µM doxorubicin for 24 hours. The MDA-MB-231 breast cancer cells showed a significant decrease in MTT reductive capacity with the treatment of doxorubicin treatment alone **(Figure 3.21)**; this was further reduced with metformin pre-treatment prior to doxorubicin. No discernible changes in cell morphology were observed with either metformin treatment alone or in combination with doxorubicin. However, a slight reduction in cell viability was observed with metformin pre-treatment prior to doxorubicin in comparison to control cells.

Our results demonstrated that treatment with 2.5 µM doxorubicin in the MDA-MB-231 cells lead to cell cycle arrest at the G2 check point of the cell cycle, evident by the significant increase seen in the G2/M phase, although an increase in the sub-G1 phase (apoptosis), it was not significant in comparison to control **(Figure 3.22)**. A greater increase may have been observed following a longer treatment time course. No significant effects to the cell cycle of the MDA-MB-231 cancer cells were observed following metformin treatment either alone or in combination with doxorubicin. These results are not in agreement with previous studies, which showed that metformin sensitizes both MCF-7 breast cancer and A549 lung cancer cells to paclitaxel treatment

(Rocha *et al*., 2011). An explanation for the differences seen in our results may be as a result of different glucose concentrations in the growth media. The MDA-MB-231 breast cancer cells are routinely sub-cultured in media containing 25 mM glucose (high glucose conditions) as per guidelines recommended by the ATCC. Research has shown that a significant increase in the clonogenic ability and proliferation of cancer cells is associated with glucose concentrations above that of 5 mM. Additionally, glucose concentrations above 10 mM have been shown to greatly abolish the anti-carcinogenic efficacy of metformin (Wahdan-Alaswad *et al*., 2013). Therefore in order for metformin to sensitize the MDA-MB-231 cancer cells to doxorubicin-induced cell death, cells should have been serum starved and media changed from that containing 25 mM glucose to one containing 5 mM glucose prior to experimentation.

As AMPKα is upstream of CKIε and the degradation of Per2 is directly reliant on its hyper-phosphorylation by CKIε, it is expected that a decrease in Per2 protein expression is coupled to the activation of AMPKα by metformin. However, our results showed that when the MDA-MB-231 cancer cells were treated with metformin the decrease in Per2 protein expression was not associated with an increase in p-AMPKα activity, but rather a reduction in AMPKα phosphorylation was seen **(Figure 3.24)**. When apoptosis was assessed by western blotting for caspase-3 and PARP, a significant reduction in both total caspase-3 and total PARP was seen following metformin treatment alone and in combination with doxorubicin in the MDA-MB-231 cancer cells, indicative of the induction of apoptosis in these cells **(Figure 3.26, Figure 3.27)**. Our results are thus suggestive that, in the estrogen receptor negative MDA-MB-231 cancer cells, metformin induces cell death independently of the activation of AMPKα. A study recently conducted by Kalender and colleagues demonstrated that metformin is able to inhibit mTOR, independently of AMPKα, via a Rag-GTPase dependent mechanism (Kalender *et al*., 2010).

Chapter 5: Final Conclusions

Due to its potent anti-carcinogenic properties, doxorubicin remains one of the most extensively used chemotherapeutic agents for the treatment of solid tumours, including that of breast cancer (Octavia *et al*., 2012). Although effective to a large extent, several problems are associated with this line of therapy. In addition to the severe cumulative dose-dependent side effects, such as that of cardiotoxicity, an increase in the resistance of metastatic breast cancer is an ongoing problem that many cancer patients are faced with (Coley, 2008).

It is widely accepted that circadian disruptions are implicated in the pathogenesis of various diseases including that of cancer. In fact, a significant increase in the prevalence and lifetime risk for the development of breast cancer is seen in women who work prolonged periods of rotating night shift (Innominato *et al.,* 2010). As a result the world health organization recognizes that circadian disruption may be carcinogenic. Furthermore, aberrant Per2 expression, leading to circadian disruption, is seen in a wide variety of cancer cell types (Chen *et al*., 2005 and Fu *et al.*, 2002)

Therefore the initial part of this study was designed to characterize Per2 **protein** expression in a normal breast epithelial cell line as well as in two breast cancer cell lines differing in estrogen receptor status and malignancy. Our results demonstrated for the first time that Per2 **protein** expression fluctuates in a circadian dependent manner in the normal MCF-12A cells, as well as in the metastatic estrogen receptor negative MDA-MB-231 cancer cells over the course of 25 hours. Whereas, the non-metastatic estrogen receptor positive MCF-7 cells, failed to demonstrate a circadian pattern in Per2 protein expression. Furthermore, nuclear Per2 localization was also demonstrated in cells where cytoplasmic localization was lower. These results demonstrate the heterogeneity of

cancer cells within a single population as well as the asynchronous nature of Per2 in different cancer cell types.

Additionally, this study was aimed at determining whether the modulation of Per2 protein expression, via both a genetic (esiRNA transfection) and pharmacological (metformin) approach, could sensitize chemo-resistant breast cancer cells to doxorubicin-induced cell death and autophagy inhibition. Collectively, results obtained for both the pharmacological and genetic modulation of Per2 demonstrate that the resistant nature of the MDA-MB-231 breast cancer cells to doxorubicin treatment was effectively abrogated via the disruption of the intrinsic circadian clock system. The suppression of the 45 kDa Per2 protein by means of a targeted esiRNA approach, in the context of doxorubicin induced cell death, resulted in cell cycle arrest of the MDA-MB-231 breast cancer cells, with a concomitant increase in apoptosis. As both aberrant Per2 expression (Wang *et al.*, 2008) and doxorubicin (Jackson *et al.*, 2006) have been shown to induce cellular senescence in response to genotoxic stress, we propose that the induction of apoptosis seen following the sensitization of MDA-MB-231 breast cancer cells to the cytotoxic effects of doxorubicin, may in part be mediated by mitotic catastrophe following cellular senescence (Figure 5.1). However, the underlying mechanisms behind senescence induced cell death in resistant breast cancer cells warrants further investigation.

In the presence of conditions resulting in intracellular stress, such as that of nutrient deprivation or hypoxia, cancer cells rely heavily on the process of autophagy as a cellular survival mechanism. The increased in basal autophagic flux seen in the chemo-resistant MDA-MB-231 breast cancer cells is thought to confer a pro-survival mechanism, via its ability to fulfil the high metabolic demands of these cells (Tu *et al.*, 2011). The manipulation of the autophagic pathway in highly resistant cancer cells has therefore become an attractive target in overcoming resistance. Increased reliance of the MDA-MB-231 breast cancer cells on autophagy as a cell survival mechanism is evident

by results showing a significant reduction in mitochondrial reductive capacity seen with the inhibition of autophagy by bafilomycin A1. Moreover, it appears that with Per2 silencing an increase in the synthesis of autophagosomes occurs, resulting in increased autophagic flux as a possible compensatory mechanism. We also provided evidence that increased autophagic activity due to Per2 silencing occurs via an mTOR-independent mechanism, as increased AMPKα activity was not accompanied by a decrease in mTOR, instead increased mTOR activity was observed. The main objective of this part of the study was to elucidate whether the manipulation of Per2 protein expression by means of a targeted esiRNA approach would sensitize the MDA-MB-231 cancer cells to autophagic inhibition with bafilomycin A1, thereby forcing cells to undergo cell death. This was satisfied when a significant increase cell death was observed in addition to G0/G1 cell cycle arrest following Per2 silencing prior to autophagic inhibition (Figure 5.1).

Although morphologically distinct, autophagy as a mechanism of cell death and apoptosis are not mutually exclusive processes, instead both work in unison to induce cell death (Thorburn, 2008). AMPK, a known regulator of autophagy, also has the ability to phosphorylate p53 thereby resulting in the induction of apoptosis (Jalving *et al*., 2010). Collectively, our results suggest that circadian disruption as a result of Per2 silencing is involved in both apoptosis and autophagic cell death in the MDA-MB-231 cancer cells. We therefore postulate that this mechanism may be mediated by crosstalk between AMPK and p53 activity (**Figure 5.1**), as Per2 silencing resulted in a significant increase in AMPK activity. Although p53 (Ser^{15}) phosphorylation was elevated in response to Per2 silencing, this increase was not statistically significant. A significant increase may have been observed following a longer treatment period. These results demonstrate the clear need for more extensive research in order to fully elucidate the

mechanism whereby these two cell death pathways converge to promote cancer cell death following Per2 silencing.

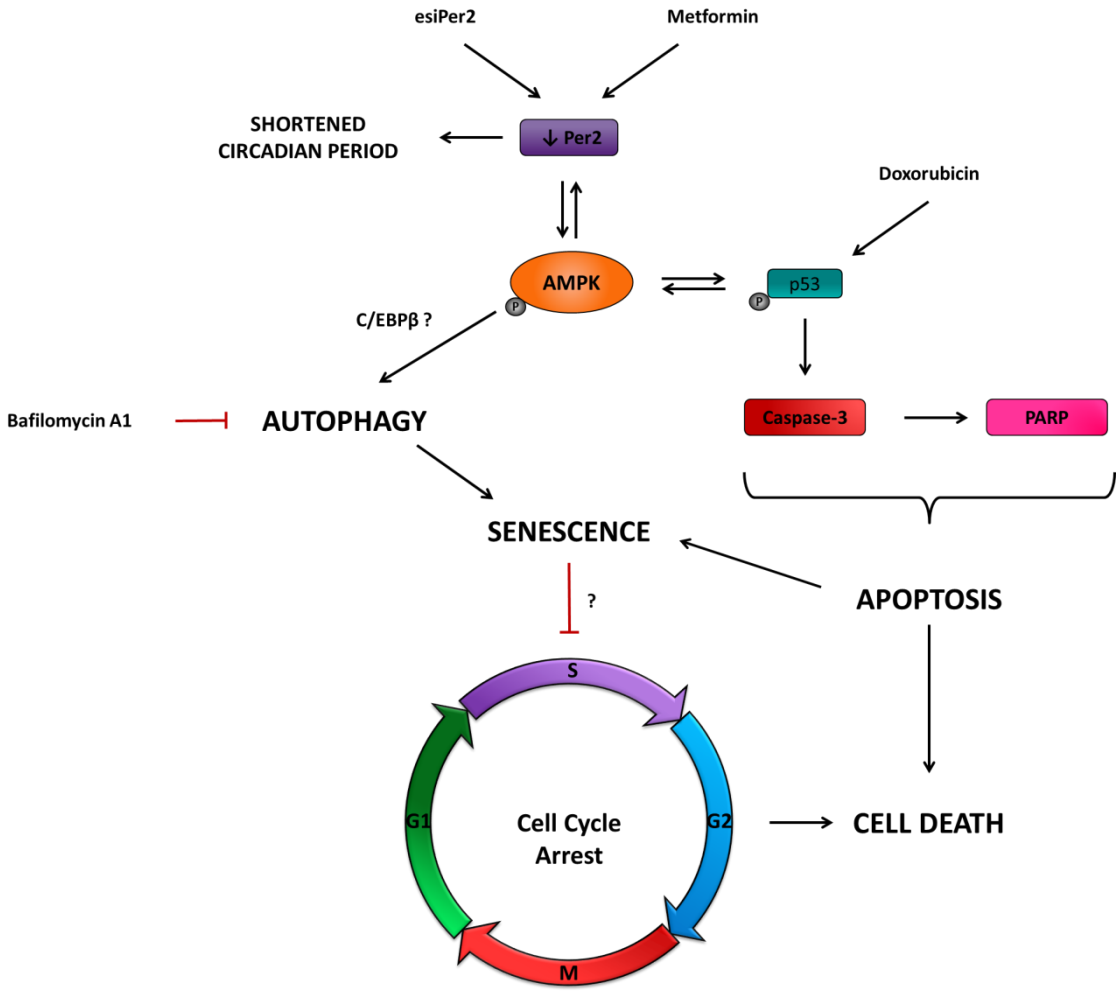

Figure 5.1: Proposed mechanism of action involved in sensitizing chemoresistant MDA-MB-231 breast cancer cells to doxorubicin-induced cell death and autophagy inhibition following Per2 manipulation. The reduction in Per2 protein expression following either genetic inhibition (esiRNA) or pharmacological (Metformin) leads to the phosphorylation and activation of AMPKα, an intracellular nutrient sensor. Increased AMPK activity is known to induce phagophore formation and thus results in an increase in basal autophagic flux. The pharmacological inhibition of autophagy using bafilomycin A1, leads to G0/G1 cell cycle arrest, possibly by resulting in cellular senescence and mitotic catastrophe. Doxorubicin is known to induce cell death in the MDA-MB-231 breast cancer cells; however, these cells have become increasingly resistant to doxorubicin treatment. Silencing Per2 in the MDA-MB-231 breast cancer cells overcomes this resistance to doxorubicin, and as such greatly enhances caspase-3 and PARP cleavage, resulting in cell cycle arrest and increased cell death. Therefore, Per2 silencing in the MDA-MB-231 cancer cells prior to doxorubicin or bafilomycin A1 treatment effectively sensitizes these resistant cancer cells to both doxorubicin-induced cell death and autophagic inhibition.

Chapter 6: Limitations and Future Studies

Increasing evidence shows a complex interplay between the circadian clock system and the regulation of metabolism exists, with the disruption of the circadian clock leading to severe metabolic derangements. Recently, Per2 has been shown to directly repress peroxisome proliferator activated receptor gamma (PPARγ), a key regulator of adipogenesis and insulin sensitivity, thus mutations arising in Per2 have been linked directly to alterations in lipid metabolism (Grimaldi *et al*., 2010). Therefore, metabolic profiling of the MDA-MB-231 cancer cells, both in the presence and absence of Per2, may provide further insight into the role of this protein in cancer cell metabolism. Furthermore, the induction of autophagy by PPARγ in cancer may result in the release of intracellular free fatty acids which can be fed into the TCA cycle, thereby conferring pro-survival properties (Zhou *et al*., 2010). As such a worthy avenue of exploration would be to assess the ATP production and consumption in response to Per2 silencing alone as well as in conjunction with autophagic manipulation using bafilomycin A1 and Rapamycin.

Post-translational modifications, including phosphorylation, play a critical role in regulating Per2 protein stability and cellular localization. Alterations in the phosphorylation state of Per2, specifically those arising from mutations in the Ser^{662} residue, are responsible for shortened circadian periods (Xu *et al*., 2007). However, the exact role that altered Per2 phosphorylation states play in the metabolic signalling of circadian clocks remains to be elucidated. This may be achieved by means of phosphoamino acid analysis, which relies on the phosphorylation of proteins using ^{32}P-ATP and then separating both phosphorylated and dephosphorylated proteins using thin

layer chromatography, exposure to ninhydrin and autoradiography (Sickmann *et al.*, 2001).

Additionally, as different isoforms of the Per2 protein exist, it would be of great importance to assess the function of these isoforms both in cancer cell death and metabolism in order to determine whether specific isoforms of Per2 play a role in cell death. Furthermore, to fully elucidate the role that Per2 plays in both apoptosis and autophagy the use of an *in vitro* overexpression model of the 45 kDa Per2 protein isoform in both the normal MCF-12A and MDA-MB-231 cancer cell lines should be conducted.

Literature suggests that Per2 serves a critical mediator linking the estrogen receptor to the circadian clock system (Gery *et al.*, 2007), it would therefore be interesting to determine the effects of both silencing and overexpression of Per2 in an estrogen receptor positive breast cancer cell line (MCF-7) in order to assess the effects of the estrogen signalling pathway on both doxorubicin-induced cell death and autophagic inhibition.

The culturing of cells in a 3-dimensional *in vitro* setting instead of the traditional 2-dimensional monolayer approach provides a more physiological representation of the *in vivo* tumour microenvironment. As cells cultured on a reconstructed basement membrane, lead to the formation of acini-like spheroids which respond differently to chemotherapeutic intervention (Pampaloni *et al.*, 2007). Therefore, it would be of value to determine whether MDA-MB-231 cancer cells cultured in 3-dimension can also be sensitized to doxorubicin-induced cell death and autophagy inhibition.

Finally, the efficacy of metformin is largely dependent on glucose concentrations, and hyperglycaemia (>10 mM glucose) severely blunts the anti-proliferative effects of metformin in highly resistant MDA-MB-231 breast cancer cells (Wahdan-Alaswad *et al*.,

2013). Therefore, repeating these experiments under normoglycaemic (5 mM glucose) conditions would be beneficial in elucidating the mechanism of action of the anti-carcinogenic properties of metformin.

References

- Albrecht, U. (2002). Regulation of mammalian circadian clock genes. *Journal of Applied Physiology*, *92*(3), 1348–55. doi:10.1152/japplphysiol.00759.2001
- Albrecht, U., Bordon, a, Schmutz, I., & Ripperger, J. (2007). The multiple facets of Per2. *Cold Spring Harbor Symposia on Quantitative Biology*, *72*, 95–104. doi:10.1101/sqb.2007.72.001
- Alimova, I. N., Liu, B., Fan, Z., Edgerton, S. M., Dillon, T., Lind, S. E., & Thor, A. D. (2009). Metformin inhibits breast cancer cell growth, colony formation and induces cell cycle arrest in vitro. *Cell Cycle (Georgetown, Tex.)*, *8*(6), 909–15.
- Andrews, P. D., Knatko, E., Moore, W. J., & Swedlow, J. R. (2003). Mitotic mechanics: the auroras come into view. *Current Opinion in Cell Biology*, *15*(6), 672–683. doi:10.1016/j.ceb.2003.10.013
- Antoch, M. P., & Kondratov, R. V. (2010). Circadian proteins and genotoxic stress response. *Circulation Research*, *106*(1), 68–78. doi:10.1161/CIRCRESAHA.109.207076
- Ashcroft, M., & Vousden, K. H. (1999). Regulation of p53 stability. *Oncogene*, *18*(53), 7637–43. doi:10.1038/sj.onc.1203012
- Aubel-Sadron, G., & Londos-Gagliardi, D. (1984). Daunorubicin and doxorubicin, anthracycline antibiotics, a physicochemical and biological review. *Biochimie*, *66*(5), 333–52.
- Balsalobre, a, Damiola, F., & Schibler, U. (1998). A serum shock induces circadian gene expression in mammalian tissue culture cells. *Cell*, *93*(6), 929–37.
- Barnea, M., Haviv, L., Gutman, R., Chapnik, N., Madar, Z., & Froy, O. (2012). Metformin affects the circadian clock and metabolic rhythms in a tissue-specific manner. *Biochimica et Biophysica Acta*, *1822*(11), 1796–806. doi:10.1016/j.bbadis.2012.08.005

- Bar-on, Ortal. Shapira, Ma'anit. Hershko, D. D. (2007). Differential effects of doxorubicin treatment on cell cycle arrest and Skp2 expression in breast cancer cells. *Anti-Cancer Drugs*, *18*(10), 1113–1121.
- Belda-Iniesta, C., Pernía, O., & Simó, R. (2011). Metformin: a new option in cancer treatment. *Clinical & Translational Oncology*, *13*, 363–367. doi:10.1007/s12094-011-0669-y
- Boulares, a. H. (1999). Role of Poly(ADP-ribose) Polymerase (PARP) Cleavage in Apoptosis. Caspase 3-Resistant Parp Mutant Increases Rates Of Apoptosis In Transfected Cells. *Journal of Biological Chemistry*, *274*(33), 22932–22940. doi:10.1074/jbc.274.33.22932
- Bremer, E., van Dam, G., Kroesen, B. J., de Leij, L., & Helfrich, W. (2006). Targeted induction of apoptosis for cancer therapy: current progress and prospects. *Trends in Molecular Medicine*, *12*(8), 382–93. doi:10.1016/j.molmed.2006.06.002
- Brown, K. a, Samarajeewa, N. U., & Simpson, E. R. (2013). Endocrine-related cancers and the role of AMPK. *Molecular and Cellular Endocrinology*, *366*(2), 170–9. doi:10.1016/j.mce.2012.06.016
- Campisi, J., & d'Adda di Fagagna, F. (2007). Cellular senescence : when bad things happen to good cells. *Nature*, *8*, 729 – 740.
- Canaple, L., Kakizawa, T., & Laudet, V. (2003). The Days and Nights of Cancer Cells. *Cancer Research*, *63*, 7545–7552.
- Caroline F. Thorn, Connie Oshiro, Sharon Marsh, Tina Hernandez-Boussard, Howard McLeod, Teri E. Klein, and R. B. A. (2011). Doxorubicin pathways: pharmacodynamics and adverse effects. *Pharmacogenet Genomics*, *21*(7), 440–446. doi:10.1097/FPC.0b013e32833ffb56.
- Casares, N., Pequignot, M. O., Tesniere, A., Ghiringhelli, F., Roux, S., Chaput, N., Kroemer, G. (2005). Caspase-dependent immunogenicity of doxorubicin-induced tumor

cell death. *The Journal of Experimental Medicine*, *202*(12), 1691–701. doi:10.1084/jem.20050915

- Castillo, K., Valenzuela, V., Matus, S., Nassif, M., Oñate, M., Fuentealba, Y., Hetz, C. (2013). Measurement of autophagy flux in the nervous system in vivo. *Cell Death & Disease*, *4*, e917. doi:10.1038/cddis.2013.421
- Chen, N., & Debnath, J. (2010). Autophagy and tumourigenesis. *FEBS Letters*, *584*(7), 1427–35. doi:10.1016/j.febslet.2009.12.034
- Chen, S., Choo, K., Hou, M., Yeh, K., Kuo, S., & Chang, J. (2005). Deregulated expression of the PER1 , PER2 and PER3 genes in breast cancers, *26*(7). doi:10.1093/carcin/bgi075
- Chlebowski, R. T., Mctiernan, A., Wactawski-wende, J., Manson, J. E., Aragaki, A. K., Rohan, T., Euhus, D. M. (2013). Diabetes, Metformin, and Breast Cancer in Postmenopausal Women. *Journal of Clinical Oncology*, *30*(23), 2844 – 2852. doi:10.1200/JCO.2011.39.7505
- Clairambault, J. (2010). Circadian rhythm and cell population growth. *Mathematical and Computer Modelling,* 53(7-8), 1558–1567.
- Cohen, G. M. (1997). Caspases: the executioners of apoptosis. *The Biochemical Journal*, *326*(1), 1–16.
- Coley, H. M. (2008). Mechanisms and strategies to overcome chemotherapy resistance in metastatic breast cancer. *Cancer Treatment Reviews*, *34*(4), 378–90. doi:10.1016/j.ctrv.2008.01.007
- Crosio, C., Fimia, G. M., Loury, R., Okano, Y., Zhou, H., Sen, S., Allis, C. D. (2002). Mitotic Phosphorylation of Histone H3 : Spatio-Temporal Regulation by Mammalian Aurora Kinases. *Molecular and Cellular Biology*, *22*(3), 874 – 885. doi:10.1128/MCB.22.3.874
- Curtis, A. M., Bellet, M. M., Sassone-Corsi, P., & O'Neill, L. a J. (2014). Circadian Clock Proteins and Immunity. *Immunity*, *40*(2), 178–186. doi:10.1016/j.immuni.2014.02.002

- Dalby, K. N., Tekedereli, I., Lopez-Berestein, G., & Ozpolat, B. (2010). Targeting the prodeath and prosurvival functions of autophagy as novel therapeutic strategies in cancer. *Autophagy*, *6*(3), 322–9.
- Dowling, R. J. O., Zakikhani, M., Fantus, I. G., Pollak, M., & Sonenberg, N. (2007). Metformin inhibits mammalian target of rapamycin-dependent translation initiation in breast cancer cells. *Cancer Research*, *67*(22), 10804–12. doi:10.1158/0008-5472.CAN-07-2310
- Earnshaw, W. C., Martins, L. M., & Kaufmann, S. H. (1999). Mammalian Caspases: Structure, Activation, Substrates, and Functions During Apoptosis. *Annu. Rev. Biochem.*, *68*, 383–424.
- Easton, J. B., & Houghton, P. J. (2006). mTOR and cancer therapy. *Oncogene*, *25*(48), 6436–46. doi:10.1038/sj.onc.1209886
- Efeyan, A., & Serrano, M. (2007). p53: Guardian of the Genome and Policeman of the Oncogenes. *Cell Cycle*, 6(9), 1006–1010.
- Eide, E. J., Woolf, M. F., Kang, H., Woolf, P., Hurst, W., Camacho, F., Virshup, D. M. (2005). Control of Mammalian Circadian Rhythm by CKI ε -Regulated Proteasome-Mediated PER2 Degradation. *Molecular and Cellular Biology*, *25*, 2795 – 2807. doi:10.1128/MCB.25.7.2795
- Elmore, S. (2007). Apoptosis: A Review of Programmed Cell Death. *Toxicology and Pathology*, *35*(4), 495–516.
- Eymin, B., Claverie, P., Salon, C., Leduc, C., Col, E., Brambilla, E., Gazzeri, S. (2006). p14ARF activates a Tip60-dependent and p53-independent ATM/ATR/CHK pathway in response to genotoxic stress. *Molecular and Cellular Biology*, *26*(11), 4339–50. doi:10.1128/MCB.02240-05
- Feridooni, T., Hotchkiss, A., Remley-Carr, S., Saga, Y., & Pasumarthi, K. B. S. (2011). Cardiomyocyte specific ablation of p53 is not sufficient to block doxorubicin induced

cardiac fibrosis and associated cytoskeletal changes. *PloS One*, *6*(7), 1-12. doi:10.1371/journal.pone.0022801

- Fernald, K., & Kurokawa, M. (2013). Evading apoptosis in cancer. *Trends in Cell Biology*, *23*(12), 620–33. doi:10.1016/j.tcb.2013.07.006
- Filipski, E., King, V. M., Li, X., Granda, T. G., Mormont, M., Liu, X., Le, F. (2002). Host Circadian Clock as a Control Point in Tumor Progression. *Journal of the National Cancer Institute*, *94*(9), 690 – 697.
- Filipski, E., Li, X. M., & Lévi, F. (2006). Disruption of circadian coordination and malignant growth. *Cancer Causes & Control : CCC*, *17*(4), 509–14. doi:10.1007/s10552-005-9007-4
- Fu, L., Pelicano, H., Liu, J., Huang, P., & Lee, C. (2002). The circadian gene Period2 plays an important role in tumor suppression and DNA damage response in vivo. *Cell*, *111*(1), 41–50.
- Fulda, S., & Debatin, K.-M. (2006). Extrinsic versus intrinsic apoptosis pathways in anticancer chemotherapy. *Oncogene*, *25*(34), 4798–811. doi:10.1038/sj.onc.1209608
- Gamen, S., Anel, A., Lasierra, P., Alava, M. a, Martinez-Lorenzo, M. J., Piñeiro, A., & Naval, J. (1997). Doxorubicin-induced apoptosis in human T-cell leukemia is mediated by caspase-3 activation in a Fas-independent way. *FEBS Letters*, *417*(3), 360–364. doi:10.1016/S0014-5793(97)01282-9
- Gery, S., Virk, R. K., Chumakov, K., Yu, a, & Koeffler, H. P. (2007). The clock gene Per2 links the circadian system to the estrogen receptor. *Oncogene*, *26*(57), 7916–20. doi:10.1038/sj.onc.1210585
- Gewirtz, D. A. (1999). A Critical Evaluation of the Mechanisms of Action Proposed for the Antitumor Effects of the Anthracycline Antibiotics Adriamycin and Daunorubicin, *57*(98), 727–741.
- Goodwin, P. J., Ligibel, J. a, & Stambolic, V. (2009). Metformin in breast cancer: time for action. *Journal of Clinical Oncology. 27*(20), 3271–3. doi:10.1200/JCO.2009.22.1630

- Goto, H. (1999). Identification of a Novel Phosphorylation Site on Histone H3 Coupled with Mitotic Chromosome Condensation. *Journal of Biological Chemistry*, *274*(36), 25543–25549. doi:10.1074/jbc.274.36.25543
- Gottesman, M. M. (2002). Mechanisms of cancer drug resistance. *Annu. Rev. Medicine*, *53*, 615 – 627.
- Gozuacik, D., & Kimchi, A. (2004). Autophagy as a cell death and tumor suppressor mechanism. *Oncogene*, *23*(16), 2891–906. doi:10.1038/sj.onc.1207521
- Grasso, S., Menéndez-gutiérrez, M. P., Carrasco-garcía, E., Mayor-lópez, L., Tristante, E., Rocamora-reverte, L., Martínez-lacaci, I. (2012). Cell Death and Cancer , Novel Therapeutic Strategies. In *Cell Death and Cancer, Novel herapeutic Strategies*. 67 – 110.
- Green, C. B., Takahashi, J. S., & Bass, J. (2008). The meter of metabolism. *Cell*, *134*(5), 728–42. doi:10.1016/j.cell.2008.08.022
- Grimaldi, B., Bellet, M. M., Katada, S., Astarita, G., Hirayama, J., Amin, R. H., Sassone-Corsi, P. (2010). PER2 controls lipid metabolism by direct regulation of PPARγ. *Cell Metabolism*, *12*(5), 509–20. doi:10.1016/j.cmet.2010.10.005
- Hait, W. N., Jin, S., & Yang, J.-M. (2006). A matter of life or death (or both): understanding autophagy in cancer. *Clinical Cancer Research, 12*(7 Pt 1), 1961–5. doi:10.1158/1078-0432.CCR-06-0011
- Hanada, T., Noda, N. N., Satomi, Y., Ichimura, Y., Fujioka, Y., Takao, T., Ohsumi, Y. (2007). The Atg12-Atg5 conjugate has a novel E3-like activity for protein lipidation in autophagy. *The Journal of Biological Chemistry*, *282*(52), 37298–302. doi:10.1074/jbc.C700195200
- Hanahan, D., & Weinberg, R. A. (2011). Hallmarks of cancer: the next generation. *Cell*, *144*(5), 646–674.

- Hastings, M. H., Reddy, A. B., & Maywood, E. S. (2003). A Clockwork Web : Circadian Timing in Brain and Periphery, in Health and Disease. *Nature Reviews, Neuroscience*, *4*, 649 – 661. doi:10.1038/nrn1177
- Hastings, M., Neill, J. S. O., & Maywood, E. S. (2007). Circadian clocks : regulators of endocrine and metabolic rhythms. *Journal of Endocrinology*, *195*, 187 – 198. doi:10.1677/JOE-07-0378
- Haupt, S., Berger, M., Goldberg, Z., & Haupt, Y. (2003). Apoptosis - the p53 network. *Journal of Cell Science*, *116*(Pt 20), 4077–85. doi:10.1242/jcs.00739
- Hippert, M. M., O'Toole, P. S., & Thorburn, A. (2006). Autophagy in cancer: good, bad, or both? *Cancer Research*, *66*(19), 9349–51. doi:10.1158/0008-5472.CAN-06-1597
- Hirsch, H. a, Iliopoulos, D., Tsichlis, P. N., & Struhl, K. (2009). Metformin selectively targets cancer stem cells, and acts together with chemotherapy to block tumor growth and prolong remission. *Cancer Research*, *69*(19), 7507–7511. doi:10.1158/0008-5472.CAN-09-2994
- Horn, H F and Vousden, K. H. (2007). Coping with stress: multiple ways to activate p53. *Oncogene*, *26*(9), 1306 – 1316.
- Houtgraaf, J. H., Versmissen, J., & van der Giessen, W. J. (2006). A concise review of DNA damage checkpoints and repair in mammalian cells. *Cardiovascular Revascularization Medicine : Including Molecular Interventions*, *7*(3), 165–72. doi:10.1016/j.carrev.2006.02.002
- Hunt, T., & Sassone-Corsi, P. (2007). Riding tandem: circadian clocks and the cell cycle. *Cell*, *129*(3), 461–4. doi:10.1016/j.cell.2007.04.015
- Iliopoulos, D., Hirsch, H. a, & Struhl, K. (2011). Metformin decreases the dose of chemotherapy for prolonging tumor remission in mouse xenografts involving multiple cancer cell types. *Cancer Research*, *71*(9), 3196–3201. doi:10.1158/0008-5472.CAN-10-3471

- Innominato, P. F., Lévi, F. a, & Bjarnason, G. a. (2010). Chronotherapy and the molecular clock: Clinical implications in oncology. *Advanced Drug Delivery Reviews*, *62*(9-10), 979–1001. doi:10.1016/j.addr.2010.06.002
- Jackson, J. G., & Pereira-smith, O. M. (2006). Primary and Compensatory Roles for RB Family Members at Cell Cycle Gene Promoters That Are Deacetylated and Downregulated in Doxorubicin-Induced Senescence of Breast Cancer Cells. *Molecular and Cellular Biology*, *26*(7), 2501 – 2510. doi:10.1128/MCB.26.7.2501
- Jalving, M., Gietema, J. a, Lefrandt, J. D., de Jong, S., Reyners, A. K. L., Gans, R. O. B., & de Vries, E. G. E. (2010). Metformin: taking away the candy for cancer? *European Journal of Cancer*, *46*(13), 2369–80. doi:10.1016/j.ejca.2010.06.012
- Jemal, A., Bray, F., & Ferlay, J. (2011). Global Cancer Statistics. *A Cancer Journal for Clinicians*, *61*(2), 69–90. doi:10.3322/caac.20107.
- Jin, S., & Levine, A. J. (2001). The p53 Functional Circuit. *Cell Science*, *114*, 4139–4140.
- Jordan, S. D., & Lamia, K. a. (2013a). AMPK at the crossroads of circadian clocks and metabolism. *Molecular and Cellular Endocrinology*, *366*(2), 163–9. doi:10.1016/j.mce.2012.06.017
- Kalender, A., Selvaraj, A., Kim, S. Y., Gulati, P., Brûlé, S., Viollet, B., … Thomas, G. (2010). Metformin, independent of AMPK, inhibits mTORC1 in a rag GTPase-dependent manner. *Cell Metabolism*, *11*(5), 390–401. doi:10.1016/j.cmet.2010.03.014
- Karantza-Wadsworth, V., Patel, S., Kravchuk, O., Chen, G., Mathew, R., Jin, S., & White, E. (2007). Autophagy mitigates metabolic stress and genome damage in mammary tumourigenesis. *Genes & Development*, *21*(13), 1621–35. doi:10.1101/gad.1565707
- Keizer, H. G., Pinedo, H. M., Schuurhuis, G. J., & Joenje, H. (1990). Doxorubicin (adriamycin): a critical review of free radical-dependent mechanisms of cytotoxicity. *Pharmacology & Therapeutics*, *47*(2), 219–231.
- Kelleher, F. C., Rao, A., & Maguire, A. (2014). Circadian molecular clocks and cancer. *Cancer Letters*, *342*(1), 9–18. doi:10.1016/j.canlet.2013.09.040

- Kerr, J. F. R., Ph, D., Winterford, C. M., Dipl, A., Biol, A., & Harmon, B. V. (1994). Apoptosis Its Significance in Cancer and Cancer Therapy. *Cancer*, *73*(8), 2013 – 2026.
- King, K. Cidlowski, J. (1998). Cell Cycle Regultion and Apoptosis. *Annu. Rev. Physiol.*, *60*, 601 – 617.
- Kinoshita, K., Waritani, T., Noto, M., Takizawa, K., Minemoto, Y., Nishikawa, Y., & Ohkuma, S. (1996). Bafilomycin A1 induces apoptosis in PC12 cells independently of intracellular pH. *FEBS Letters*, *398*, 61–66.
- Komatsu, M., Waguri, S., Koike, M., Sou, Y.-S., Ueno, T., Hara, T., Tanaka, K. (2007). Homeostatic levels of p62 control cytoplasmic inclusion body formation in autophagy-deficient mice. *Cell*, *131*(6), 1149–63. doi:10.1016/j.cell.2007.10.035
- Kondo, Y., Kanzawa, T., Sawaya, R., & Kondo, S. (2005). The role of autophagy in cancer development and response to therapy. *Nature Reviews. Cancer*, *5*(9), 726–34. doi:10.1038/nrc1692
- Kondratov, R. V. (2007). A role of the circadian system and circadian proteins in aging. *Ageing Research Reviews*, *6*(1), 12–27. doi:10.1016/j.arr.2007.02.003
- Kroemer, G., & Pouyssegur, J. (2008). Tumor cell metabolism: cancer's Achilles' heel. *Cancer Cell*, *13*(6), 472–82. doi:10.1016/j.ccr.2008.05.005
- Lamia, K. a, Sachdeva, U. M., DiTacchio, L., Williams, E. C., Alvarez, J. G., Egan, D. F., Evans, R. M. (2009). AMPK regulates the circadian clock by cryptochrome phosphorylation and degradation. *Science*, *326*(5951), 437–40. doi:10.1126/science.1172156
- Lefta, M., Wolff, G., & Esser, K. a. (2011). Circadian rhythms, the molecular clock, and skeletal muscle. *Current topics in developmental biology* 96(1), 231–71. doi:10.1016/B978-0-12-385940-2.00009-7
- Levine, B. (2007). Autophagy and cancer. *Nature*, *446*, 745 – 747.
- Levine, B., & Kroemer, G. (2008). Autophagy in the pathogenesis of disease. *Cell*, *132*(1), 27–42. doi:10.1016/j.cell.2007.12.018

- Levine, B., & Yuan, J. (2005). Autophagy in cell death : an innocent convict? *The Journal of Clinical Investigation*, *115*(10), 2679 – 2688. doi:10.1172/JCI26390.or
- Li, Y., Upadhyay, S., Bhuiyan, M., & Sarkar, F. H. (1999). Induction of apoptosis in breast cancer cells MDA-MB-231 by genistein. *Oncogene*, *18*, 3166–3172.
- Liu, B., Fan, Z., Edgerton, S. M., Deng, X., Alimova, I. N., Lind, S. E., & Thor, A. D. (2009). Metformin induces unique biological and molecular responses in triple negative breast cancer cells. *Cell Cycle*, *8*(13), 2031–2040.
- Liu, Y.-Y., Yu, J. Y., Yin, D., Patwardhan, G. A., Gupta, V., Hirabayashi, Y., Cabot, M. C. (2008). A role for ceramide in driving cancer cell resistance to doxorubicin. *FASEB Journal, 22*(7), 2541–51. doi:10.1096/fj.07-092981
- Lown, J. W. (1983). The mechanism of action of quinone antibiotics. *Molecular and Cellular Biochemistry*, *55*(1), 17–40.
- Lozy, F., & Karantza, V. (2012). Autophagy and cancer cell metabolism. *Seminars in Cell & Developmental Biology*, *23*(4), 395–401. doi:10.1016/j.semcdb.2012.01.005
- Ma, D., Li, S., Molusky, M. M., & Lin, J. D. (2012). Circadian autophagy rhythm: a link between clock and metabolism? *Trends in Endocrinology and Metabolism*, *23*(7), 319 – 325. doi:10.1016/j.tem.2012.03.004
- Ma, D., Panda, S., & Lin, J. D. (2011). Temporal orchestration of circadian autophagy rhythm by C/EBPβ. *The EMBO Journal*, *30*(22), 4642–51. doi:10.1038/emboj.2011.322
- Malmlöf, M., Roudier, E., Högberg, J., & Stenius, U. (2007). MEK-ERK-mediated phosphorylation of Mdm2 at Ser-166 in hepatocytes. Mdm2 is activated in response to inhibited Akt signaling. *The Journal of Biological Chemistry*, *282*(4), 2288–96. doi:10.1074/jbc.M604953200
- Masri, S., Cervantes, M., & Sassone-Corsi, P. (2013). The circadian clock and cell cycle: interconnected biological circuits. *Current Opinion in Cell Biology*, *25*(6), 730–4. doi:10.1016/j.ceb.2013.07.013
- Massague, J. (2004). G1 cell-cycle control and cancer. *Nature*, *432*, 298 – 306.

- Mathew, R., & White, E. (2011). Autophagy in tumourigenesis and energy metabolism: friend by day, foe by night. *Current Opinion in Genetics & Development*, *21*(1), 113–9. doi:10.1016/j.gde.2010.12.008
- Mehmet, H., & Hansen, B. (2000). Caspases find a new place to hide A bright future for dark matter. *Nature*, *403*, 29 – 30.
- Mizushima, N., Levine, B., Cuervo, A. M., & Klionsky, D. J. (2008). Autophagy fights disease through cellular self-digestion. *Nature*, *451*(7182), 1069–75. doi:10.1038/nature06639
- Morgan, D. (1995). Principles of CDK regulation. *Nature*, *374*(6518), 131–4. doi:10.1038/374131a0
- Mormont, M. (2003). Cancer Chronotherapy : Principles , Applications , and Perspectives. *Cancer*, *97*(1), 155 – 168. doi:10.1002/cncr.11040
- Morselli, E., Galluzzi, L., Kepp, O., Vicencio, J.-M., Criollo, A., Maiuri, M. C., & Kroemer, G. (2009). Anti- and pro-tumor functions of autophagy. *Biochimica et Biophysica Acta*, *1793*(9), 1524–32. doi:10.1016/j.bbamcr.2009.01.006
- Noatynska, A., Tavernier, N., Gotta, M., & Pintard, L. (2013). Coordinating cell polarity and cell cycle progression: what can we learn from flies and worms? *Open Biology*, *3*(8), 1-13. doi:10.1098/rsob.130083
- Octavia, Y., Tocchetti, C. G., Gabrielson, K. L., Janssens, S., Crijns, H. J., & Moens, A. L. (2012). Doxorubicin-induced cardiomyopathy: from molecular mechanisms to therapeutic strategies. *Journal of Molecular and Cellular Cardiology*, *52*(6), 1213–25. doi:10.1016/j.yjmcc.2012.03.006
- Ogier-Denis, E., & Codogno, P. (2003). Autophagy: a barrier or an adaptive response to cancer. *Biochimica et Biophysica Acta (BBA) - Reviews on Cancer*, *1603*(2), 113–128. doi:10.1016/S0304-419X(03)00004-0

- Pampaloni, F., Reynaud, E., & Stelzer, E. (2007). The third dimension bridges the gap between cell culture and live tissue. *Nature Reviews. Molecular Cell Biology*, *8.10*, 839 – 847.
- Patil, Y., Swaminathan, S., Sadhukha, T., Ma, L., & Panyam, J. (2011). The use of nanoparticle-mediated targeted gene silencing and drug delivery to overcome tumor drug resistance. *Biomaterials*, *31*(2), 612–626. doi:10.1016/j.biomaterials.2009.09.048.
- Porter, a G., & Jänicke, R. U. (1999). Emerging roles of caspase-3 in apoptosis. *Cell Death and Differentiation*, *6*(2), 99–104. doi:10.1038/sj.cdd.4400476
- Rabinowitz, J. D., & White, E. (2010). Autophagy and metabolism. *Science*, *330*(6009), 1344–8. doi:10.1126/science.1193497
- Rana, S., & Mahmood, S. (2010). Circadian rhythm and its role in malignancy. *Journal of Circadian Rhythms*, *8*(3), 1-13. doi:10.1186/1740-3391-8-3
- Reinhardt, H. C., & Schumacher, B. (2012). The p53 network : Cellular and systemic DNA damage responses in aging and cancer. *Trends in Genetics*, *28*(3), 128–136. doi:10.1016/j.tig.2011.12.002.
- Reiter, R. J., Tan, D. X., Erren, T. C., Fuentes-broto, L., & Paredes, S. D. (2009). Light-Mediated Perturbations of Circadian Timing and Cancer Risk : A Mechanistic Analysis. *Integrative Cancer Therapies*. 8(4), 354-360. doi:10.1177/1534735409352026
- Reppert, S. M., & Weaver, D. R. (2002). Coordination of circadian timing in mammals. *Nature*, *418*(6901), 935–41. doi:10.1038/nature00965
- Riccardi, C., & Nicoletti, I. (2006). Analysis of apoptosis by propidium iodide staining and flow cytometry. *Nature Protocols*, *1*(3), 1458–61. doi:10.1038/nprot.2006.238
- Robertson, J. D., Orrenius, S., & Zhivotovsky, B. (2000). Review: nuclear events in apoptosis. *Journal of Structural Biology*, *129*(2-3), 346–58. doi:10.1006/jsbi.2000.4254
- Rocha, G. Z., Dias, M. M., Ropelle, E. R., Osório-Costa, F., Rossato, F. a, Vercesi, A. E., Carvalheira, J. B. C. (2011). Metformin amplifies chemotherapy-induced AMPK

activation and antitumoral growth. *Clinical Cancer Research*, *17*(12), 3993–4005. doi:10.1158/1078-0432.CCR-10-2243

- Roninson, I. B., Broude, E. V, & Chang, B. D. (2001). If not apoptosis, then what? Treatment-induced senescence and mitotic catastrophe in tumor cells. *Drug Resistance Updates. 4*(5), 303–13. doi:10.1054/drup.2001.0213
- Rossetti, S., Esposito, J., Corlazzoli, F., Gregorski, A., & Sacchi, N. (2012). Entrainment of breast (cancer) epithelial cells detects distinct circadian oscillation patterns for clock and hormone receptor genes. *Cell Cycle. 11*(2), 350–60. doi:10.4161/cc.11.2.18792
- Rubinsztein, D. C., Gestwicki, J. E., Murphy, L. O., & Klionsky, D. J. (2007). Potential therapeutic applications of autophagy. *Nature Reviews. Drug Discovery*, *6*(4), 304–12. doi:10.1038/nrd2272
- Sachdeva, U. M., & Thompson, C. B. (2008). Diurnal rhythms of autophagy. *Autophagy*, *4*(5), 581–589.
- Sahar, S., & Sassone-Corsi, P. (2009). Metabolism and cancer: the circadian clock connection. *Nature Reviews Cancer*, *9*(12), 886–896.
- Sainz, R. M., Mayo, J. C., Rodriguez, C., Tan, D. X., Lopez-Burillo, S., & Reiter, R. J. (2003). Melatonin and cell death: differential actions on apoptosis in normal and cancer cells. *Cellular and Molecular Life Sciences*, *60*(7), 1407–26. doi:10.1007/s00018-003-2319-1
- Sancar, A., Lindsey-Boltz, L. a, Kang, T.-H., Reardon, J. T., Lee, J. H., & Ozturk, N. (2010). Circadian clock control of the cellular response to DNA damage. *FEBS Letters*, *584*(12), 2618–25. doi:10.1016/j.febslet.2010.03.017
- Sauna, Z. E., & Ambudkar, S. V. (2000). Evidence for a requirement for ATP hydrolysis at two distinct steps during a single turnover of the catalytic cycle of human P-glycoprotein. *Proceedings of the National Academy of Sciences of the United States of America*, *97*(6), 2515–20.

- Schernhammer, E. S., Laden, F., Speizer, F. E., Willett, W. C., Hunter, D. J., Kawachi, I., & Colditz, G. a. (2001). Rotating night shifts and risk of breast cancer in women participating in the nurses' health study. *Journal of the National Cancer Institute*, *93*(20), 1563–8.
- Senchenkov, a, Litvak, D. a, & Cabot, M. C. (2001). Targeting ceramide metabolism--a strategy for overcoming drug resistance. *Journal of the National Cancer Institute*, *93*(5), 347–57.
- Shintani, T., & Klionsky, D. J. (2004). Autophagy in health and disease: a double-edged sword. *Science. 306*(5698), 990–995.
- Sickmann, A., & Meyer, H. E. (2001). Phosphoamino acid analysis. *Proteomics*, *1*, 200–206.
- Singletary, K., & Milner, J. (2008). Diet, autophagy, and cancer: a review. *Cancer Epidemiology, Biomarkers & Prevention*, *17*(7), 1596–610. doi:10.1158/1055-9965.EPI-07-2917
- Siu, W. Y., Yam, C. H., & Poon, R. Y. C. (1999). G1 versus G2 cell cycle arrest after adriamycin-induced damage in mouse. *FEBS Letters*, *461*, 299–305.
- Sjöström, J., & Bergh, J. (2001). How apoptosis is regulated , and what goes wrong in cancer. *BMJ*, *322*, 1538–1539.
- Smith, L., Watson, M. B., O'Kane, S. L., Drew, P. J., Lind, M. J., & Cawkwell, L. (2006). The analysis of doxorubicin resistance in human breast cancer cells using antibody microarrays. *Molecular Cancer Therapeutics*, *5*(8), 2115–20. doi:10.1158/1535-7163.MCT-06-0190
- Stevens, R. G. (2009). Light-at-night, circadian disruption and breast cancer : assessment of existing evidence. *International Journal of Epidemiology*, *38*, 963–970. doi:10.1093/ije/dyp178

- Straif, K., Baan, R., Grosse, Y., Secretan, B., Ghissassi, F. El, Bouvard, V., Cogliano, V. (2007). Carcinogenicity of shift-work, painting, and fire-fighting. *The Lancet Oncology*, *8*(12), 1065–1066. doi:10.1016/S1470-2045(07)70373-X
- Tacar, O., Sriamornsak, P., & Dass, C. R. (2013). Doxorubicin: an update on anticancer molecular action, toxicity and novel drug delivery systems. *The Journal of Pharmacy and Pharmacology*, *65*(2), 157–70. doi:10.1111/j.2042-7158.2012.01567.x
- Tawa, P., Hell, K., Giroux, a, Grimm, E., Han, Y., Nicholson, D. W., & Xanthoudakis, S. (2004). Catalytic activity of caspase-3 is required for its degradation: stabilization of the active complex by synthetic inhibitors. *Cell Death and Differentiation*, *11*(4), 439–47. doi:10.1038/sj.cdd.4401360
- Thorburn, A. (2008). Apoptosis and autophagy: regulatory connections between two supposedly different processes. *Apoptosis : An International Journal on Programmed Cell Death*, *13*(1), 1–9. doi:10.1007/s10495-007-0154-9
- Thornberry, N. a. (1998). Caspases: Enemies Within. *Science*, *281*(5381), 1312–1316. doi:10.1126/science.281.5381.1312
- Tu, Y.-F., Kaipparettu, B. a, Ma, Y., & Wong, L.-J. C. (2011). Mitochondria of highly metastatic breast cancer cell line MDA-MB-231 exhibits increased autophagic properties. *Biochimica et Biophysica Acta*, *1807*(9), 1125–32. doi:10.1016/j.bbabio.2011.04.015
- Ünsal-kaçmaz, K., Mullen, T. E., & William, K. (2005). Coupling of Human Circadian and Cell Cycles by the Timeless Protein Coupling of Human Circadian and Cell Cycles by the Timeless Protein. *Molecular and Cellular Biology*, *25*(8), 3109 – 3116. doi:10.1128/MCB.25.8.3109
- Vermeulen, K., Van Bockstaele, D. R., & Berneman, Z. N. (2003). The cell cycle: a review of regulation, deregulation and therapeutic targets in cancer. *Cell Proliferation*, *36*(3), 131–49. Retrieved from http://www.ncbi.nlm.nih.gov/pubmed/12814430
- Vousden, K. H., & Lane, D. P. (2007). P53 in Health and Disease. *Nature Reviews. Molecular Cell Biology*, *8*(4), 275–83. doi:10.1038/nrm2147

- Wahdan-Alaswad, R., Fan, Z., Edgerton, S. M., Liu, B., Deng, X.-S., Arnadottir, S. S., Thor, A. D. (2013). Glucose promotes breast cancer aggression and reduces metformin efficacy. *Cell Cycle*, *12*(24), 3759–69. doi:10.4161/cc.26641
- Wang, C.-Y., Wen, M.-S., Wang, H.-W., Hsieh, I.-C., Li, Y., Liu, P.-Y., Liao, J. K. (2008). Increased vascular senescence and impaired endothelial progenitor cell function mediated by mutation of circadian gene Per2. *Circulation*, *118*(21), 2166–73. doi:10.1161/CIRCULATIONAHA.108.790469
- Wang, X.-S., Armstrong, M. E. G., Cairns, B. J., Key, T. J., & Travis, R. C. (2011). Shift work and chronic disease: the epidemiological evidence. *Occupational Medicine*, *61*(2), 78–89. doi:10.1093/occmed/kqr001
- Wang, Y., Suh, Y., Fuller, M. Y., Jackson, J. G., Xiong, S., Terzian, T., Lozano, G. (2011). Restoring expression of wild-type p53 suppresses tumor growth but does not cause tumor regression in mice with a p53 missense mutation. *Journal of Clinical Investigation*, *121*(3), 893 – 904. doi:10.1172/JCI44504DS1
- Warburg, O., Wind, F., & Negelein, E. (1927). The metabolism of tumors in the body. *The Journal of General Physiology*, 521 – 530.
- Weller, M. (1998). Predicting response to cancer chemotherapy: the role of p53. *Cell and Tissue Research*, *292*(3), 435–445. doi:10.1007/s004410051072
- Whibley, C Pharoah, P Hollstein, M. (2009). p53 polymorphisms: cancer implications. *Nature Reviews. Cancer*, *9*, 95 – 107.
- Williams, A., Sarkar, S., Cuddon, P., Ttofi, E. K., Saiki, S., Kane, J. O., Rubinsztein, D. C. (2008). Novel targets for Huntington ' s disease in an mTOR-independent autophagy pathway. *Nature Chemical Biology*, *4*(5), 295–305. doi:10.1038/nchembio.79.
- Wu, Y. C., Wu, W. K. K., Li, Y., Yu, L., Li, Z. J., Wong, C. C. M., Cho, C. H. (2009). Inhibition of macroautophagy by bafilomycin A1 lowers proliferation and induces apoptosis in colon cancer cells. *Biochemical and Biophysical Research Communications*, *382*(2), 451–6. doi:10.1016/j.bbrc.2009.03.051

- Xiang, S., Coffelt, S. B., Mao, L., Yuan, L., Cheng, Q., & Hill, S. M. (2008). Period-2: a tumor suppressor gene in breast cancer. *Journal of Circadian Rhythms*, *6*, 4. doi:10.1186/1740-3391-6-4
- Xu, Y., Toh, K. L., Jones, C. R., Shin, J.-Y., Fu, Y.-H., & Ptácek, L. J. (2007). Modeling of a human circadian mutation yields insights into clock regulation by PER2. *Cell*, *128*(1), 59–70. doi:10.1016/j.cell.2006.11.043
- Yagita, K., Tamanini, F., Yasuda, M., Hoeijmakers, J. H. J., Horst, G. T. J. Van Der, & Okamura, H. (2002). Nucleocytoplasmic shuttling and mCRY-dependent inhibition of ubiquitylation of the mPER2 clock protein. *The EMBO Journal*, *21*(6), 1301–1314.
- Yang, F., Teves, S. S., Kemp, C. J., & Henikoff, S. (2014). Doxorubicin, DNA torsion, and chromatin dynamics. *Biochimica et Biophysica Acta*, *1845*(1), 84–9. doi:10.1016/j.bbcan.2013.12.002
- Yang, X., Downes, M., Yu, R. T., Bookout, A. L., He, W., Straume, M., Evans, R. M. (2006). Nuclear receptor expression links the circadian clock to metabolism. *Cell*, *126*(4), 801–10. doi:10.1016/j.cell.2006.06.050
- Yang, X., Wood, P. a, Ansell, C., & Hrushesky, W. J. M. (2009). Circadian time-dependent tumor suppressor function of period genes. *Integrative Cancer Therapies*, *8*(4), 309–16. doi:10.1177/1534735409352083
- Young, A. R. J., Narita, M., Ferreira, M., White, E., Lowe, S. W., Kirschner, K., Watt, F. M. (2009). Autophagy mediates the mitotic senescence transition Autophagy mediates the mitotic senescence transition. *Genes & Development*, *23*, 798–803. doi:10.1101/gad.519709
- Zakikhani, M., Dowling, R., Fantus, I. G., Sonenberg, N., & Pollak, M. (2006). Metformin is an AMP kinase-dependent growth inhibitor for breast cancer cells. *Cancer Research*, *66*(21), 10269–73. doi:10.1158/0008-5472.CAN-06-1500

- Zhou, J., Zhang, W., Liang, B., Casimiro, M. C., Whitaker-, D., Wang, M., Wang, C. (2010). PPARγ Activation Induces Autophagy in Breast Cancer Cells. *International Journal of Cell Biology*, *41*(11), 2334–2342. doi:10.1016/j.biocel.2009.06.007.

Appendix A: Protocols

Protocol 1: Cell Culture

Before work was started in the laminar flow hood, hands were washed and gloves were worn. Hands were sprayed with 70% ethanol each time before putting inside the hood to maintain sterility.

a) Cracking a vial

- Carefully remove a vial of required cells (MCF-12A, MCF-7 or MDA-MB-231 cells) from the liquid nitrogen tank and gently immerse the vial in the water bath set at 37 ºC (take extreme care not to get the lid of the cryovial wet, in order to ensure sterility). Allow cells to thaw until there is only a small frozen pellet of cells
- Remove cells from the cryovial and place them into a sterile 15 ml falcon tube containing 2 ml warm growth media (see Appendix B) and centrifuge at 1500 RPM for 3 min.
- Carefully aspirate the supernatant and re-suspend the pellet in 4 ml of warm growth media using a serological pipette.
- Place cells into a sterile T25 flask and incubate at an atmosphere of 37 ºC and a humidity of 5% CO_2.
- Wash cells with warm sterile PBS (see Appendix B) and replace growth media every day until cells reach a confluency of 70 – 80%.
- Once 70 - 80% confluency is reached cells are ready to be split.

b) Splitting and seeding

- Cells are ready to be split when 70 - 80% confluency is reached. Cell confluency is subjectively measured by viewing cells under a 20x objective using an inverted microscope.
- Place growth media, PBS and trypsin in a water bath set at 37 ºC and allow them to warm up.
- Media was aspirated and the cell monolayer was washed twice with warm PBS (see Appendix B) in order to completely remove growth media and all cell debris
- 2ml of warm 0.25% trypsin-EDTA was added to lift adherent cells, by gently agitation in a 37 ºC shaking incubator set to low speed for ± 4 min.
- Once all cells had loosened, trypsin was neutralized by adding double the amount of warm growth media to the cells to avoid trypsin from killing the cells.
- Cells were then transferred to sterile 15 ml falcon tubes and centrifuged for 3 min at 1500 RPM.
- The supernatant (media and trypsin) was carefully removed so as not to disturb the pellet (cells). Cells were then re-suspended in fresh growth media using a serological pipette.
- Cells were then either split into new flasks and allowed to proliferate or counted using a haemocytometer and standard counting techniques before seeding for experimentation was done.
- For experimental procedures the normal MCF-12A breast epithelial cells, MCF-7 breast cancer or MDA-MB-231 breast cancer cells, were seeded into either 6 well plates or T25 flasks at a density of ± 150 000 cells in 2 ml growth media or ± 400 000 cells in 4 ml growth media per well / flask respectively.

c) Freezing down cells

- Once cells reached a confluency of 70 – 80%, old media was aspirated and discarded using a sterile pipette
- The cell monolayer was washed twice with warm PBS in order to completely remove growth media and all cell debris.
- 2 ml / 4 ml warm trypsin was added to T25 and T75 flasks respectively and cells were gently agitated by placing them in a 37 ºC shaking incubator set at low speed for ± 4 min, until all cells had detached from the bottom of the flask.
- Double the amount of warm growth media was then added and cells were transferred to a sterile 15 ml falcon tube and centrifuged at 1500 RPM for 3 min.
- Supernatant was hen decanted and the pellet re-suspended in freezing media (see Appendix B) that was freshly made up.
- Cells were then placed at -20 ºC for 2 hours before being transferred to the -80 ºC freezer overnight. The next morning cells were transferred to the liquid nitrogen tank for storage.

Protocol 2: Treatments

a) Doxorubicin

- Under sterile conditions 10 mg of Doxorubicin Hydrochloride (Mr: 579.98 g/mol) was dissolve in exactly 5071 μL growth medium to obtain a stock concentration of 3.4 mM
- The solution was then vortex and filter-sterilized
- 100 µl aliquots were then prepared in order to avoid freeze-thaw cycles, and epi's were wrapped individually in tinfoil before being stored at -20℃.
- **NB**: Doxorubicin is light sensitive therefore when working with the solution care was taken to protect Dox from light by covering it with foil and ensuring the lights were switched off.
- **Day of use:** An epi containing doxorubicin was removed from the freezer and allowed to thaw by placing it in the hood at room temperature. Appropriate dilutions were made by adding Dox to warm growth media to obtain a final working concentration of 2.5 µM.
- Old media was aspirated and discarded from 70 – 80% confluent cells using a sterile pipette
- The cell monolayer was washed twice with warm PBS in order to completely remove growth media and all cell debris, and the 2.5 µM doxorubicin solution was added to cells.
- Flasks were then wrapped in tinfoil, labelled and allowed to incubate for 24 hours at an atmosphere of 37 ºC and a humidity of 5% CO_2.

b) Bafilomycin A1

- Under sterile conditions 10 µg of Bafilomycin A1 (Mr: 622.83 g/mol) was dissolve in exactly 5000 µl of sterile PBS to obtain a stock concentration of 3.2 µM
- The solution was then vortex and filter-sterilized
- 160 µl aliquots were then prepared in order to avoid freeze-thaw cycles, and epis were stored at -20℃.
- **Day of use:** An epi containing bafilomycin was removed from the freezer and allowed to thaw by placing it in the hood at room temperature. Appropriate dilutions were made by adding baf to warm growth media to obtain a final working concentration of 10 nM.
- Old media was aspirated and discarded from 70 – 80% confluent cells using a sterile pipette
- The cell monolayer was washed twice with warm PBS in order to completely remove growth media and all cell debris, and the 10 nM bafilomycin solution was added to cells.
- Cells were then allowed to incubate for 8 hours at an atmosphere of 37 ºC and a humidity of 5% CO_2.

c) Metformin - 1,1-Dimethylbiguanide hydrochloride

- 40 mM working concentrations of Metformin (Mr: 165.62 g/mol) were made up fresh on the day of treatment by weighing out the appropriate amount of metformin powder and dissolving it in warm sterile PBS.
- Solution was then vortex to ensure even distribution.
- Old media was aspirated and discarded from 70 – 80% confluent cells using a sterile pipette
- The cell monolayer was washed twice with warm PBS in order to completely remove growth media and all cell debris, and the 40 mM metformin solution was added to cells.
- Cells were then allowed to incubate for 24 hours at an atmosphere of 37 ºC and a humidity of 5% CO_2.

Protocol 3: Forward Transfection

Method:

- Seed cells in 6 well culture dishes 24 hours prior to transfection.
- Prepare master mix by diluting 30 nM of Per2 esiRNA into 100 µl of serum and antibiotic free medium per well.
- Add 12 µl HiPerfect transfection reagent per 100 µl of mix prepared.
- Allow to incubate for 20 minutes to ensure the formation of esiRNA: HiPerfect complexes.
- Add antibiotic free growth media to produce a final volume of 2ml and add drop-wise onto cells.
- Gently swirl plates to distribute media evenly over cells
- Incubate until cells are ready to treat 48 hours later.

Protocol 4: Protein Extraction

In order to avoid protein de-phosphorylation and proteolysis, all protein extraction steps where carries out on ice in a 4ºC walk-in fridge.

- All eppendorf tubes were labelled according to treatment group.
- Once cells reached a confluency of 70 – 80%, old media was aspirated and discarded using a sterile pipette.
- The cell monolayer was washed twice with ice cold PBS in order to completely remove growth media and all cell debris.
- 100 µl of ice cold RIPA buffer was added to each sample and cells were left on ice for 5 min, after which cells were gently detached from plastic ware using a plastic cell scraper which was rinsed in ethanol between different treatment groups.
- Cells were broken up in order to release protein content by sonication for 8 seconds at 3 Hz while sample was maintained on ice. Microtip™ was rinsed with ethanol between different samples, in order to prevent cross-contamination.
- All samples were left on ice in a 4ºC fridge for ± 1 hour until all foam had settled.
- All insoluble cellular debris was removed by micro-centrifugation at 8000 RPM for a period of 30 seconds.
- Supernatant was decanted into new epppendorf tubes that were pre-chilled and labelled according to treatment group, cell line and date.
- All lysate samples were stored at -80ºC until use.

Protocol 5: Protein Quantification and Sample Preparation

- Prior to use, a 200 µg/ml BSA working solution was prepared by diluting a 1 mg/ml BSA stock solution in a 1:4 ration with dH_2O as a solvent.
- Eppendorf tubes were labelled according to each treatment group and dilution standard.
- A standard curve was set up by means of a BSA dilution series as follows:

Concentration (µg)	BSA (µl)	dH_2O
0	0	100
2	10	90
4	20	80
8	40	60
12	60	40
16	80	20
20	100	0

- Each treatment sample to be tested was prepared by pipetting 5 µl of protein lysate into the labelled eppendorf tubes and diluting them in 95 µl of dH_2O. Samples were briefly vortexed prior to pipetting.
- 900 µl of working Bradford solution was added into each Eppendorf tube and samples were vortexed briefly to distribute solutions.
- Absorbance values of all standards and treatment samples were measured using a spectrophotometer set to a wavelength of 595 nm.
- A standard curve was plotted using the BSA serial dilution absorbencies and protein content of treatment samples was quantified by means of interpolation.

Protocol 5: Sample Preparation

- Desired number of eppendorf tubes for each experimental group, were labelled and appropriate volume of lysate to yield a protein content of 50 µg was pipetted into appropriate tubes.
- Lammli sample buffer equal to a third of the final volume was added to in order to fix each aliquoted sample.
- Samples were boiled for 5 min in a heating block set to a temperature of 95ºC . Ensure that all eppendorf tubes had pin-sized holes made into their lids in order to prevent a build-up of pressure.
- If samples are not to be used immediately, store all samples upright in cryoboxes in the -80ºC freezer.

Protocol 6: SDS-PAGE and Western Blot Analysis

a) Preparation of Polyacrylamide Gels

- Thoroughly clean glass 1 mm spacer plates and short plates with 70% ethanol and rise with dH_2O.
- Assemble the glass spacer and short plates in the green casting frame. Ensuring that they are perfectly lined up at the bottom. Place the green casting frame by securing clips and placing the casting frame onto the rubber gasket in the casting stand. Press down onto the casting frame to ensure a tight seal so as to prevent leakages.
- Make up a 10% or 12% stain free polyacrylamide resolving gel (see Appendix B), depending on the size range of proteins to be separated.
- Using a plastic Pasteur pipette, gently pipette the resolving gel solution in between the glass plates, leaving enough space for the stacking gel.
- Pipette isobutanol over the resolving gel, so create a barrier against the air and to prevent evaporation.
- Allow the gel to set at room temperature. The gel is completely polymerized once a sharp interface between the resolving gel and the isobutanol appears.
- Remove the isobutanol and gently rinse with dH_2O
- Make up a 4% stain free polyacrylamide stacking gel (see Appendix B) and add the solution gently on top of the resolving gel using a plastic Pasteur pipette. Gently insert a 10 or 12 well comb into the stacking solution ensuring it is aligned perfectly and that no bubbles have been trapped under the comb.
- Allow the gel to completely polymerize before removing the comb.
- Before the gel can be used, gently rinse the wells out with dH_2O.

b) SDS - Polyacrylamide Gel Electrophoresis (PAGE)

- Prepare a 1x Running buffer solution by diluting a 10x stock solution (see Appendix B) in dH_2O.
- Retrieve all samples to be run from the -80ºC freezer as well as protein molecular weight marker from the -20ºC freezer and allow to thaw on ice.
- Boil samples for a second time in a heating block set to a temperature of 95ºC. Once boiled immediately place samples on ice to prevent protein form being denatured further.
- Briefly pulse centrifuge samples to ensure that the sample is all at the bottom of the eppendorf tubes.
- Assemble gels into the U-shaped adapter cassette, ensuring the short glass plates are facing into the centre.
- Place the assembled cassette into the electrophoresis tank and fill the inner compartment with 1x running buffer. Make sure that no running buffer leaks form the inner compartment
- Gently pipette 5 µl of molecular weight marker in the well of the first lane. This allows for the monitoring of the electrophoretic run.
- Load 50 µg of protein samples into wells following the marker.
- Gently fill the outer compartment of the electrophoresis tank with 1x running buffer. Attach the lid ensuring leads are not tangled and attached correctly.
- An initial run of 100 V (constant) and 200 mA, until samples have migrated through the stacking gel. Thereafter, run gels at 200 V (constant) and 200 mA until the front reaches the bottom of the gel.
- Migration efficiency is determined by activating the gel for 2.5 minutes using the ChemDoc^{MP} stain free gel protocol, and visualizing protein separation.

c) Transferring

- Remove prepared transfer buffer from the 4ºC fridge at the time of use.
- Cut PVDF membrane and blotting paper to the same size as the gel. Activate PVDF membrane by briefly placing the membrane in 100% methanol and rinse with dH_2O before soaking in ice cold transfer buffer. Once activated the membrane turns slightly transparent.
- Soak blotting paper and membrane in transfer buffer until use.
- Allow gels with fractionated protein pattern to equilibrate in transfer buffer with gently agitation for 10 – 15 min.
- Construct the horizontal semi-dry transfer sandwich by placing a soaked blotting pad onto the TransBlot® Turbo™ transfer cassette, place the activated membrane on top of the blotting pad followed by the polyacrylamide gel and a second blotting pad. Ensure that no air bubbles are trapped in the sandwich by gently rolling them out between each layer using a roller rinsed in transfer buffer.
- Close the cassette, ensuring that the sandwich is not disturbed. Transfer proteins to the membrane for 30 minutes at 25 V and 1.0 A.
- Protein transfer can be visualized using the stain free blot protocol on the Chemi-Doc™ MP (BioRad) imaging system.
- Wash membranes 3x in 1x TBS-Tween 20 solution for 5 min each.

d) Immunodetection

- In order to prevent non-specific binding of antibodies, membranes were blocked by incubation in 5% (w/v) fat free milk solution for 2 hours. If proteins detected are in their phosphorylated state a 3% BSA blocking solution was used as the

milk contains the phosphorylated protein casein which will bind non-specifically to antibodies.

- Membranes were then washed 3x in TBS-T for 5 min each, before being placed into a 1:1000 primary antibody solution in TBS-T overnight on a rotator.
- Prior to incubation in a 1:10000 solution of secondary antibody in TBS-T for 1 hour at room temperature, membranes were washed 3x in TBS-T for 5 min each.
- Protein detection was carried out with the use of the ECL western blotting substrate detection kit on the Chemi-Doc™ MP (BioRad) imaging system.

Protocol 7: Immunocytochemistry – Per2 and Hoechst 33342

For this technique, cells were grown in 8 well chamber plates which were first UV sterilized by placing them face open in the hood under the UV light for a period of 4 hours. Cells were cultured as previously described (Protocol 1). All staining techniques were performed in the Histology lab where there is minimal light.

Method

- Medium was removed from cells and washed 3x with sterile PBS (0.1M)
- 100 µl fixative (1:1 methanol/acetone) per well was added and incubated for 10 min at 4ºC. This process was carried out whilst cells were kept on ice.
- The fixative was then removed and the coverslips were allowed to air dry for 20 min at room temperature
- The cells were then rinsed 3x with 200 µl ice cold sterile PBS.
- 200µl of a 5% donkey serum made in PBS (see Appendix B) was added to each well and incubated for 20 min at room temp
- After the time had elapsed, the serum was drained (NOT washed) and 200µl primary antibody solution in a 1:50 dilution (in this case a Per2 primary antibody was used) was added to each well and incubated overnight at 4ºC.
- The cells were then rinsed once with PBS, only 200µl was used for each well and 200µl secondary antibody solution in a 1:200 dilution (in this case an anti-rabbit AlexaFluor488 conjugated secondary antibody) was added. Incubation continued for 30 min at room temp. The secondary used was tagged with a fluorophore and was not grown in the same animal as the primary antibody.

- REMEMBER TO VORTEX THE SECONDARY ANTIBODY SOLUTION TO AVOID THE FORMATION OF CRYSTALS
- In addition, 100µl Hoechst 33342 solution was added on top of the secondary antibody solution and incubated or another 10 min at room temp.
- The coverslips were lastly rinsed 3x with sterile PBS and a small drop of fluorescent mounting medium was added to each well to mount cells.
- 8-well chamber plates can now be used or stored wrapped in foil to avoid light for up to 2 weeks at -20ºC

Protocol 8: MTT Assay

Method:

Three independent experiments were conducted in triplicate.

- An Isopropanol solution (1%): containing 1 ml concentrated HCl and 99 ml Isopropanol was made.
- Triton solution (0.1 %) containing 0.1 ml Triton-X-100 was made up to 100 ml with distilled water.
- An Isopropanol / Triton solution was made in a 50:1 ratio, where 50 ml of 1% Isopropanol was added to 1 ml of 0.1% Triton. 1%
- MTT (0.01 g/1 ml PBS) solution was made up just before use. MTT is photosensitive, thus the solution was covered in foil.
- Medium was removed from treated cells.
- PBS (1.5 ml) and MTT (500 µl) was added and allowed to incubate, in 6 well plates covered with foil for 1 to 2 hours at 37ºC.
- After incubation time, MTT solution was removed and 2ml of the Isopropanol / Triton solution was added to each well and plates covered in foil were placed on a shaker for 5 minutes.
- The contents of each wells was transferred to 2 ml eppendorf tubes, centrifuged for 2mins at RPM 1500.
- The absorbance values of the supernatant were read at 540 nm using a spectrophotometer with Isopropanol / Triton solution was used as a blank.
- If absorbance was greater than one the supernatant was diluted with the Isopropanol / Triton solution and read at 540 nm again.

Protocol 9: Hoechst and Propidium Iodide (PI) staining technique

Method

- Medium was removed from cells and washed 3x with sterile PBS (0.1M)
- 100µl of PI solution (see appendix B) was added to each coverslip and incubated for 20 minutes at 4ºC
- PI solution was then removed and cells were rinsed 2x with sterile PBS
- A cold fixative (1:1 methanol/acetone), enough to cover the monolayer of cells, was added to each coverslip and incubated for 10 min at 4ºC
- The fixative was removed and the coverslips were left to air dry completely for a further 10 min
- After the time had elapsed, 150µl of Hoechst solution (see Appendix B) was added to each coverslip and incubated for 10 min at 4ºC
- Hoechst solution was removed and cells were rinsed 5x with sterile PBS to avoid or minimize background noise
- The coverslips were allowed to dry before being mounted on a microscope slide using a small drop of fluorescent mounting medium
- The slides were now placed ace down on tissue paper and covered in foil to protect them from light
- The slides can now be stored at -20ºC for up to 2 weeks

Protocol 10: Cell Cycle Analysis

Method

- Add 3 ml Trypsin/EDTA (0.25%) to each flask and place on the cell shaker for 5 minutes or until the cells have detached from the surface of the flask.
- Add 6 ml of appropriate culture medium to each flask.
- Transfer each resulting cell suspension to a separate, sterile 15 ml falcon tube.
- Centrifuge at 400 x g for 5 minutes at room temperature.
- Carefully decant all the supernatant, and tap off the last drop onto a tissue.
- Wash the pellet with sterile room temperature PBS.
- Centrifuge at 400 x g for 5 minutes at room temperature.
- Add 250 µl of trypsin buffer (Solution A) to each tube and mix by tapping. (Do not vortex).
- Allow solution A to react for 10 minutes at room temperature.
- Do not remove solution A.
- Add 200 µl of trypsin inhibitor and RNase buffer was added to each tube and mix gently by hand tapping. (Do not vortex).
- Incubate for 10 minutes at room temperature.
- Add 200 µl of ice cold propidium iodide stain solution was added to each tube and incubated on ice in the dark for a further 10 minutes.

- Filter samples through a 50 µm nylon mesh into 12x75 mm tubes.

- Analyse using flow cytometry

Protocol 11: G2/M Transition Analysis – Flow Cytometry

Method

- Add 3 ml Trypsin/EDTA (0.25%) to each flask and place on the cell shaker for 5 minutes or until the cells have detached from the surface of the flask.
- Add 6 ml of appropriate culture medium to each flask.
- Transfer each resulting cell suspension to a separate, sterile 15 ml falcon tube.
- Centrifuge at 1500 RPM for 3 minutes at room temperature.
- Carefully decant all the supernatant, and re-suspended in 1 ml PBS.
- Add formaldehyde to a final concentration of 4% and fix cells at 37ºC for 10 min.
- Place cells on ice and chill for 1min
- Remove fixative by centrifugation and permeabilize cells by adding 90% ice cold methanol to cells and incubate cells on ice for 30 min
- Add 2-3 ml incubation buffer (0.5g BSA dissolved in 100 ml PBS) to cells and rinsed twice by centrifugation.
- Dilute conjugated primary antibodies in incubation buffer (1:50) and incubate for 1 hour at room temperature.
- Wash cells by centrifugation in incubation buffer before re-suspending in 0.5 ml PBS and analysing on the flow cytometer.

Appendix B: Recipes

Growth Medium

a) MCF-7 and MDA-MB-231 cancer cells

- 500ml Dulbecco's Modified Eagles Medium (DMEM)
- 56ml Fetal Bovine Serum (FBS)
- 5.6ml PenStrep

b) MCF-12A normal breast epithelial cells

- 250 ml MCF-7 / MDA-MB-231 growth media
- 250 ml Hams F12 nutrient mixture containing 10% FBS and 1% Penstrep
- 1110 µl Insulin (30 / 70 Humalin)
- 50 µl Cholera toxin
- 25 µl Hydrocortisone

1X Phosphate Buffered Saline (PBS) – 0.1M

Dissolve the following in 1L of water

- 16g NaCl
- 0.4g KCl
- 2.88g Na_2HPO_4 (di Sodium hydrogen phosphate)
- 0.48g KH_2PO_4 (Potassium dihydrogen phosphate)

Adjust pH to 7.4, fill up to the 2L mark with distilled water and sterilize by autoclaving.

Propidium Iodide and Hoechst 33342 stain

- Dissolve 5µl PI in 1000µl sterile PBS
- Dissolve 5µl Hoechst 33342 in 1000µl sterile PBS
- These solutions are made fresh and must be kept on ice away from light

BSA (Bovine serum albumin) – 1mg/ml

- For 1ml BSA, weigh out 1mg BSA and add 1000µl distilled water
- Or use during Western blotting, this BSA needs to be diluted. Pipette 100µl from 1mg/ml stock solution in a new eppendorf tube and add 400µl distilled water
- Mix well

Bradford Reagent (1L)

- Weigh out 500mg Coomassie Brilliant Blue G and add it to 25ml 95% ethanol
- Add 500ml phosphoric acid and mix well
- Fill up to 1L mark with distilled water and store at 4ºC
- For use during Western Blotting, this solution needs to be filtered 2x and then a 1:5 dilution needs to be made.

3X Sample Buffer

- Measure 33.3ml stacking Tris (0.5M) and place in a beaker
- Weigh out 8.8g SDS and 20g glycerol and place in the beaker
- Add a pinch of bromo-phenol blue to the mixture

- Add and make up to 75.47ml with distilled water

Tris pH 8.8 (500ml)

- Weigh out 68.1g Tris (1.124M) and 1.5g SDS (0.3%) and place in a beaker
- Add 400ml distilled water, stir and then adjust pH to 8.8 using HCl
- Add 100ml distilled water to make the final volume of 500ml

Tris pH 6.8 (500ml)

- Weigh out 30.3g Tris (0.5M) and 2g SDS (0.4%) and place in a beaker
- Add 400ml distilled water, stir and then adjust pH to 6.8 using HCl
- Add 100ml distilled water to make up final volume of 500ml

Tris pH 6.8 (100ml) for Sample Buffer

- Weigh out 6.06g Tris (0.5M) and add 4ml 10% SDS and place in a beaker
- Add 80ml distilled water, stir and adjust pH to 6.8 using HCl
- Add 20ml distilled water to make up the final volume of 100ml

10% Sodium Dodecyl Sulphate (SDS) – 500ml

- Weigh out 50g SDS and add 500ml distilled water

10% Ammonium Persulphate (APS) - 1000µl

- Weigh out 0.1g APS into an eppendorf tube and add 1000µl distilled water

10% Acrylamide separating gel

- Distilled water – 3.85ml
- 1.5M Tris- HCl (pH 8.8) – 2.5ml
- 10% SDS - 100µl
- Acrylamide – 2.5ml
- 10% APS - 50µl
- Temed - 5µl

12% Acrylamide separating gel

- Distilled water – 3.35ml
- 1.5M Tris- HCl (pH 8.8) – 2.5ml
- 10% SDS - 100µl
- Acrylamide – 3.0ml
- 10% APS - 50µl
- Temed - 5µl

4% Acrylamide stacking gel

- Distilled water – 6.1ml
- 0.5M Tris- HCl (pH 6.8) – 2.5ml
- 10% SDS - 100µl
- Acrylamide – 1.0ml
- 10% APS - 100µl
- Temed - 20µl

Running Buffer -1L

- Weigh out 3.03g Tris, 1.44g Glycine and 1g SDS into a beaker
- Add 500ml distilled water and stir until dissolved
- Fill up to 1L mark with distilled water

10X TBS – 5L

- Weigh out 121g Tris and 80g NaCl into a 5L beaker
- Add 2.5L distilled water and stir until dissolved
- Adjust to pH 7.6 using HCl and then fill up to 5L with distilled water
- For use in Western blotting, take 1L measuring cylinder and add 100ml 10x TBS and dilute with 900ml distilled water
- To make TBS-T – add 1ml Tween-20 to 1L diluted solution of TBS

RIPA buffer – 100ml

Add the reagents in the following order. Protect the solution from light and prepare while stirring on ice.

- Tris-HCl pH 7.4 (790 mg Tris + 900 mg NaCl) (50 mM)
- 10 ml of 10% NP-40
- 2.5 ml Na-deoxycholate (0.25%)
- 1 ml of 100 mM EDTA pH 7.4 (1 mM)
- 100 µl of 1 mg/ml Leupeptin (1 µg/ml)
- 80 µl of 5 mg/ml SBT1 (4 µg/ml)
- 100 µl of 1M Benzamadine (1 mM)
- 500 µl of 200 mM NaF (1 mM) Toxic!
- 500 ul of 200 mM Na_3VO_4 (1 mM)
- Mix briefly.
- Allow to incubate until the cells are ready to treat and assay.
- Add 1 ml of Triton X-100. Viscous!
- Aliquot into practical amounts to avoid freeze thawing